Impact of Pt Loading on Proton Exchange Membrane Hydrogen Fuel Cells Performance

by

Pérez Maronda, Xavier

A thesis submitted in partial fulfillment of the requirements for the degree of

Renewable Energy Master degree

Department of Mechanical Engineering

University of Alberta

Abstract

With increasing use of renewable energies, such as photovoltaic, wind, biomass, thermosolar, geologic, appeared the challenge of the storage. If it is talking about the mobile devises, it is easy to see that it is necessary store this energy to use it later. In the case of the vehicles the need is obvious to change the oil engine to electric engine, but this happens in all mobile devices. The polymer electrolyte fuel cells (PEFC) convert hydrogen and oxygen to electricity. The energy is store as hydrogen gas and the waste is water. Nowadays, there are lots of companies studying the viability of these systems. The future of these batteries pass through the good relation between the performance and the price. A significant fraction of the PEMFC cost is focused on the electrodes, exactly in the catalyst used. This catalyst is platinum and it has an important cost comparative with the other parts of the fuel cell [1].

The present thesis studies the effect of Pt loading in the electrode of proton exchange membrane hydrogen fuel cells (PEMFCs). Gasteiger, Panels and Yan study showed that the anode Pt loading doesn't significantly affect the performance of hydrogen fuel cells [2]. However, in the present study different experiments with catalyst-coated membranes (CCM)[1] corroborated what it was known before about the cathode loading. But in the case of the anode loading, it was proved that there is an optimum loading which gives the best performance. This results will reduce the costs of the PEMFC at least in the anode side.

[1] **CCM:** is the assembly of the membrane with the both anode and cathode.

Wind and other clean, renewable energy will help end our reliance on fossil fuels and combat the severe threat that climate change poses to humans and wildlife alike.

– Frances Beineckes.

Acknowledgements

I would like to thank my supervisor, Dr. Marc Secanell for promoting the exchange program between the Polytechnic University of Catalonia and the University of Alberta, and providing me the opportunity to do this experimental project in hydrogen fuel cells in his laboratory. His motivation and energy at work is inspiration for everyone. He gave me confidence and enthusiasm to do this project. I am proud to know him because this is what I want, I want to find the job that makes me feel very happy working in that theme.

I also want to thank my colleges for their support during my research. They provided me everything I needed and explained to me everything I needed. Also, they were a very good lab-mates out of the laboratory. I enjoyed my visit both inside and outside the laboratory. They are a professional team and great people. I am very happy to have been in this team and work in hydrogen fuel cells. I tried to learn as much as possible about PEMFC and about how work. This laboratory is a great place to do the research.

Finally, I would like to thank my family, in special to my girlfriend, because they were very supportive of all my project from the beginning until the end. When you go to live in the other side of the world, it is never easy and if they would have not supported me, I don't know if I would have come and live this experience.

Contents

List of Tables

List of Figures

Chapter 1

Introduction

1.1 Motivation

Energy consumption continues to increase yearly despite the sustainability targets set up in most countries in the world. To avoid that, the UN made some agreements in the lasts decades. In 1997, the Kyoto Protocol was adopted to reduce the GHG in the atmosphere, after that the Paris Agreement tried to further set targets to reduce the climatic change. As a result, the power installed from renewable energy sources is rising and the energy consumption per citizen is falling down every year [3]. Unfortunately, fossil fuels are still the majority of the energy sources. It means that the climatic change is continuing, every day there are more GHG in the atmosphere and the average temperature of the world continues to rise.

New energy supply, environmental and sustainable policies are needed. Without changing, the emissions of carbon dioxide will be more than double by 2050 and the fossil energy demand will be higher than the supply [3]. Nowadays, hydrogen and fuel cell technologies need to be more developed and to reach this development the help of the governments is necessary. Hydrogen fuel cells have gathered huge attention because its zero GHG emission, high efficiency, fast start up time and low operating temperatures [4]. Hydrogen can connect different energy sectors and energy transmission and distribution networks. In the transport sector, they could be one of the main solutions to reduce carbon emissions. Also they can contribute to decarbonization of the industry and the building sector, and integrate very high shares of renewable energy into the energy system [3]. Others renewable energy sources, like solar or wind, can not work all day, they need a energy source which some times doesn't exist. Frequently there is no wind and the wind generators can not produce electricity, or in

the solar case, the solar panels can not work during the night. Contrariwise, there is some parts of the day where the electricity production is higher than the electricity consumption, in this case is when it is good to take advantage of that and stored this overproduction of electricity.This hybrids systems allow use the overproduction electricity when the generators are not working.

Hydrogen can be produced from a lot of primary and secondary sources, such as renewable sources such as solar or wind, biomass, and also from other fossil fuels. Even though hydrogen has no carbon and the waste of the electricity production process is water, its production can produce carbon emissions and because of that the source of its production is important. Nowadays, almost 96% of the hydrogen is produced from fossil fuels [5].
Hydrogen fuel cells use an electrochemical process to produce electricity from a chemical reaction. Fuel cells are similar to batteries, but, ideally, they don't reduce its power output as long as fuel and oxidant supply is provided. The hydrogen fuel cell uses hydrogen and oxygen as fuels. Hydrogen gas enters into the anode side of the *Proton Exchange Membrane Fuel Cell* (PEMFC) and oxygen, as a oxidant, enters into the cathode side as pure oxygen or air. After the electrochemical process, which will be explained in *Hydrogen Fuel Cell Background* 1.2, the fuel cell produce electricity and, as a waste, water and heat. The typical overall efficiency for PEMFC is 50% [6]. Hydrogen can be generated from electricity and water and re-transformed to electricity with the cost of 70% of the input electricity. In addition, hydrogen can be storage in a large quantities for long periods [3].

Focusing in the electricity sector, its increasing represent 40% of the total rising in final consumption to 2040. This share growth is the same that oil growth in the last twenty-five years. The forecast from nowadays and till 2040, the global investment in renewable power plants will increase in front of the investments in fossil fuel power plants. The Figure 1.1 shows the global average investment in power plants till 2040 according to the International Energy Agency.

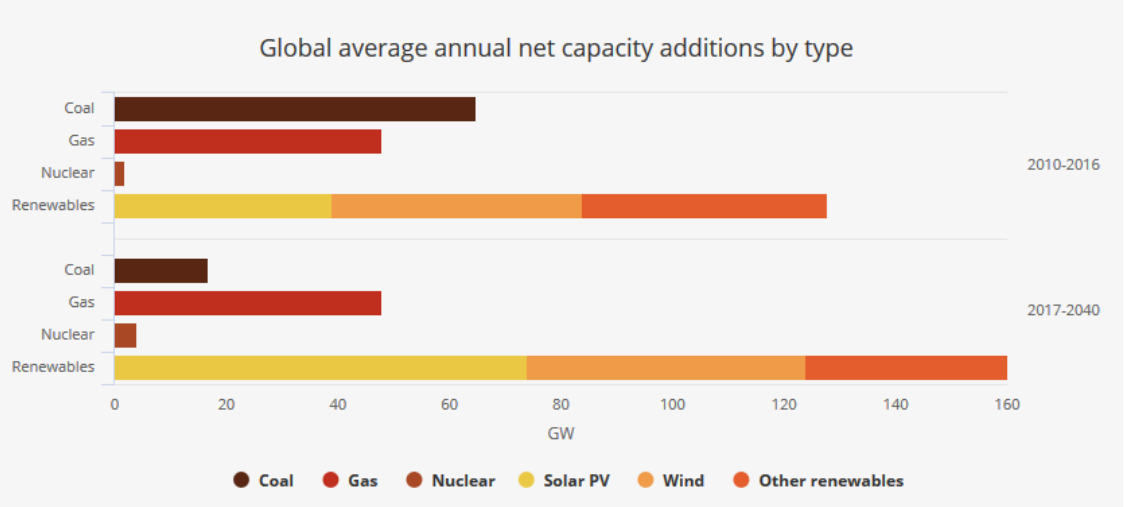

Figure 1.1: Global average investment in power plants (Source: World Energy Outlook 2017. International Energy Agency.)

Talking about hybrids systems, hydrogen can be used as a battery replacing lithium-batteries, which are the most used currently. Lithium is an alkaline metal and quite abundant in the earth. Nowadays, Lithium batteries have a high specific energy, high efficiency and long life [7]. From some years, mobile devices have been made with lithium batteries. The problem is that Lithium batteries contain hazardous materials such as lithium metal and flammable solvents. These batteries are dangerous because can lead to exothermic activities, and fires coming from primary lithium and lithium-ion batteries are relatively frequent [8]. This batteries also use cobalt in the lithium alloy. Cobalt comes basically from the *Congo Democratic Republic* and then is processed in China to produce the elements for the batteries. China accounts for one third of the global lithium-ion batteries production capacity [9]. The high energy density, the very little maintenance, the lower self-discharge rate, the quick charging, the small size and the low weight compared with other batteries, have made the lithium-ion battery the most used in the energy storage market with a production of the order of billions of units per year [7].

Hydrogen is not an energy source, it is an abundant molecular component that can be used as a fuel for end-use conversion processes. It means that hydrogen can produce different kinds of energy but it needs energy to get it from the environment. Almost all the hydrogen production is using in the refineries and chemical industries or refinery products [3]. In the last ten years the hydrogen fuel cells technology was extended because the car sector, however, the first hydrogen fuel cell was developed in the 60s. Toyota, Hyundai and

Honda are some of the car manufacturers that have announced their plans and research on PEMFC vehicles [3]. Even the benefits of the hydrogen fuel cell application, it is unavoidable to compare them with the internal combustion engine, even more on the transport sector. There are some car models running with FCEV (*Fuel Cell Electric Vehicle*) and the plan is to increase the amount of FCEV on the road in the following years [3]. The cars can be fuelled with a gaseous hydrogen and they can run between 500 and 650 km without refuelling. This hydrogen create the electricity to run the electric engine. There is an inconvenient, which is the price of the vehicle still higher that the currently cars. Refuelling stations are a critical elements in the fuel supply chain for hydrogen fuel cells, for the successful development of this market, it is needed a minimum network to wake up the consumer interest

There are some aspects that determine the success of the PEMFC and probably the most important is the price. The price has to be competitive to win the position to others alternatives. In the PEMFC the prices is focus in the electrodes, which are the responsible of the chemical reaction that change the flow of the gases to electricity. The reaction that transform the oxygen and hydrogen into water and electricity happens in the electrode. This part of the fuel cell is the key component of the PEMFC because contains the catalyst, which is the responsable of between the 34% and 45% of the cost of the fuel cell [1] [4]. This catalyst favours the chemical reaction [10] and to avoid to consume big amount of the catalyst layer is very important the fabrication process [1].

There are six types of FC. The most common because of his simplicity is the **proton exchange membrane (PEM)** fuel cell which chemistry will be discussed in section 1.2. PEM use a solid polymer electrolyte that allows the protons to pass through it. This kind of fuel cell can work at low temperatures, use pure hydrogen as a gas fuel and use *Platinum* as a catalyst. Although the platinum is an expensive material, the amount of platinum used in the electrodes is low. Its applications are mainly in vehicles and mobile applications, back-up power and co-generation. As it has been told before, hydrogen is not an easy available fuel and the use of others fuels could solve this issue. One of these alternative is the methanol which can be used directly in the PEM. These cells are called **direct methanol fuel cells (DMFC)** but the problem is their low efficiency. Another type of fuel cell use alkaline electrolyte, but the problem is that it needs pure oxygen and pure hydrogen to work because if carbon dioxide comes into the alkaline environment, carbonates are formed and block the hydrogen and oxygen flow. This *alkaline fuel cells (AFC)* have been used in space vehicles in

the past. One commercial fuel cell is the **phosphoric acid fuel cell (PAFC)** which reach good reaction rate levels with porous electrodes, platinum catalyst and high temperatures (over $200°C$). Also, reforming natural gas solve the problem of the hydrogen. The only cons are the costs, the complexity and the size. The **solid oxide fuel cell (SOFC)** has a good reaction rate level and the incoming gases is natural gas which can be used directly (or can be reformed inside). The problem of this fuel cell is that it works between 600 and $1000°C$, the internal materials are expensive and the gases need to be pre-heated. Also at high temperature works the **molten carbonate fuel cell (MCFC)** and also reach good reaction rate level. It can use methane or syngas from coal directly. It uses a cheap catalyst (nickel). The problem of the MCFC is the electrolyte, a corrosive blend of lithium, potassium and sodium carbonates are used as a electrolyte.

Then, taking in account the efficiency, the low working temperature, the size, and the costs, PEMFC is the most available fuel cell. PEMFCs are more efficient than combustion engines or turbines. This means that small systems can be as efficient as large one. Also, the simplicity (no moving parts), the useful life of the tools and the completely quite working, makes fuel cell a good device. Another positive aspect is the zero emission during the operation. As a disadvantage, the obtainment of hydrogen could produce CO_2 which is a GHG and this obtaining also could be difficult and some process needs a lot of energy.

1.2 Hydrogen Fuel Cell Background

Before discussing the results of this thesis, it is necessary to provide a background of the technology. The chemistry process behind the hydrogen fuel cells is the electrolysis of the water. In this process hydrogen and oxygen can be separated using an electric current inside of water.

In a fuel cell, hydrogen and oxygen are oxidized and reduced, respectively, in order to create an electric current.

Anode:

$$H_2 \rightarrow 2H^+ + 2e^- \tag{1.1}$$

Cathode:

$$1/2O_2 + 2e^- + 2H^+ \rightarrow H_2O \tag{1.2}$$

Overall:

$$2H_2 + O_2 \rightarrow 2H_2O \tag{1.3}$$

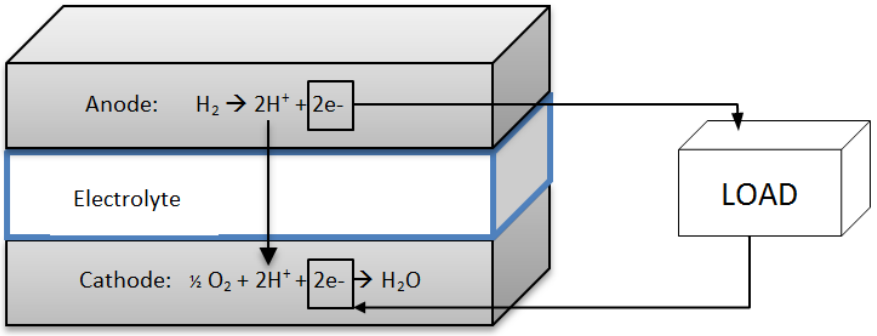

Figure 1.2: Drawing of Cathode-Electrolyte-Anode construction.

Figure 1.2 shows what is happening between the anode and cathode with the help of the electrolyte. In the anode side, hydrogen is divided in two protons and two electrons. The electrons pass through the load generating the current. In the cathode side, the Oxygen is combined with two protons coming from the electrolyte and with the electrons coming from the load to generate water as a waste. Certain polymers can be made to contain mobile H^+ ions. These polymers make a *Proton Exchange Membrane* or *Polymer Electrolyte Membrane (PEM)*. Obviously, the electrolyte must only allow H^+ ions pass through it, and not the electrons. The protons are transported in the water embedded inside the membrane and the electrons can not pass through the membrane because the electric insulate property.

To start the reactions, some activation energy is necessary and the probability to produce this energy is very low. This makes the reactions very slow. There are three methods that can be used to increase the reaction rates:

1. Use of catalyst
2. Raising the temperature
3. Increase the electrode area

The use of catalysts and raising the temperature increase the reaction rate in any chemical reaction. However, the rate of the reaction is proportional to the surface area because fuel

cell reactions take place at the surface of the catalyst. As it is shown in the Figure 1.2, H_2 is divided in electrons and H^+ in the anode side, and at the same time, this H^+ is combined with O_2 and electrons to create water in the cathode side. These two reactions need an activation energy to make it because the probability that the overall reaction happens is very low. The electrode area is very important because the reaction rate is proportional to its area. For this reason when it is talk about the current of the fuel cell, normally, it is talk about current per cm^2 Pt. As it will be showed more ahead, the voltage of a fuel cell is quite small so, it will be necessary to stack many cells to produce enough voltage. The bipolar plate has two main functions: make the connections between the cathode of one cell and the anode of the other cell, and also feed the cell with oxygen for the cathode and hydrogen for the anode. The bipolar plate can have different shapes of channels such as parallel, serpentine, parallel serpentine, grid or long parallel [11]. In the case of the parallel channels, water produced could block one of the channels in the inlet gases and the gas will move through the others channels leaving a region of the electrode unsupplied.

Energy balance

To study the transformation of the energy in a hydrogen fuel cell, the following inputs and the outputs need to be considered as in the Figure 1.3.

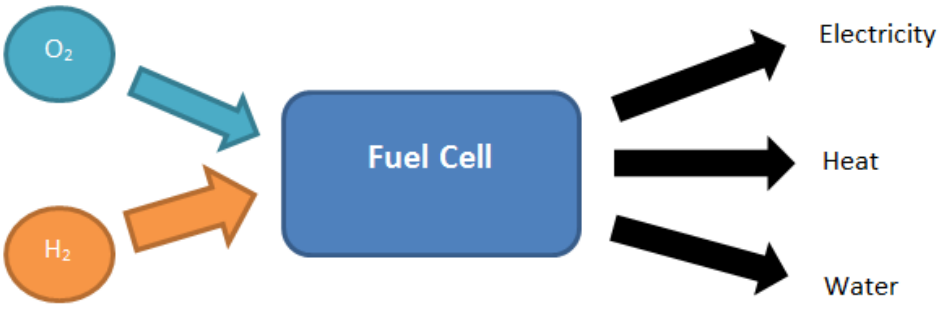

Figure 1.3: Process diagram

The energy outputs of this balance can easily be calculated by $P = VI$ and $E = VI\Delta t$, but it is not so easy the calculation with the chemical inputs. To calculate the energy of the inputs it is necessary to introduce the *Gibbs free energy*. The Gibbs free energy is used to determine if a reaction is thermodynamically viable or not [11]. The variation of Gibbs free energy (ΔG_f) can be calculated by

$$\Delta G_f = \Delta H - T\Delta S \tag{1.4}$$

where ΔH is the change in enthalpy, ΔS is the change in entropy between the reactants and products, and T is the temperature. When is used ΔG_f, the f indicate that a compound is formed from its element. So, in a fuel cell, the change in the Gibbs free energy of formation is given by the expression (1.5).

$$\Delta G_f = G_f(products) - G_f(reactants) \tag{1.5}$$

To simplify the calculations, specific the molar energy is used, which is indicated by a bar over the letter ($\bar{g_f}$). For example, the Gibbs free energy of formation of 2 moles of H_2O following the equation (1.3).

$$\Delta \bar{g_f} = 2(\bar{g_f})_{H_2O} - 2(\bar{g}_f)_{H_2} - (\bar{g}_f)_{O_2} \tag{1.6}$$

For the hydrogen fuel cell reaction, $2N_A$ electrons pass through the electric circuit for 1 consumed mole. Using Faraday's law for electrolysis, the corresponding charge is

$$-2N_A e^- = -2F \tag{1.7}$$

where F is the Faraday constant [1]. Then, the electrical work is

$$Electrical work done = charge * V = -2FV \tag{1.8}$$

Finally,

$$\Delta \bar{g}_f = -2FV_r \tag{1.9}$$

where V_r is the reversible voltage or open circuit voltage (OCV).

Efficiency

To calculate the theoretical efficiency of a fuel cell, one option could be to compare the electrical energy produced with the **calorific value** [2].

$$\eta_{max} = \frac{\Delta \bar{g_f}}{\Delta \bar{h_f}} \tag{1.10}$$

[1] **Faraday constant:** is the amount of electric loading in a mole of electrons. $F = 96485.33$ [C/mole].
[2] **Calorific value:** is the amount of energy released on the combustion of this material or fuel.

Dividing numerator and denominator by 2F,

$$\eta = \frac{V_c}{1.48} \tag{1.11}$$

Because not all the fuel is reacted, it has to add a coefficient to correct this fuel unreacted, $\mu_f = \frac{reactedmassfuel}{inputmassfuel}$. Finally,

$$\eta = \mu_f \frac{V_c}{1.48} \tag{1.12}$$

The fuel cell

The cell voltage of an operating fuel cell is not the same than theoretical value at open circuit. Even the open circuit voltage is less than the theoretical value. The Figure 1.4 is the common graph to represent electrochemical performance in the PEMFC. Is composed by cell voltage to current density. This normalized currents density makes easier to compare different fuel cells with different sizes.

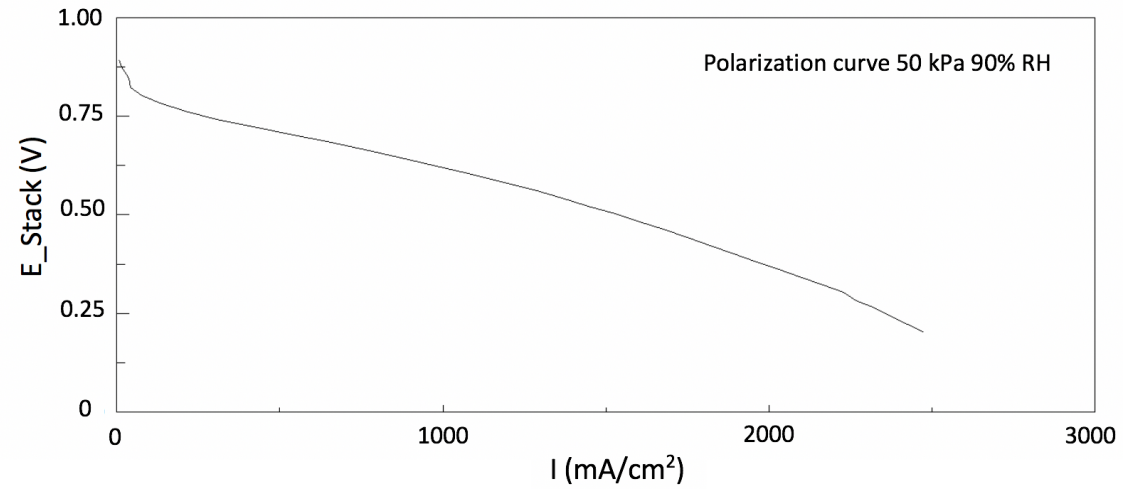

Figure 1.4: Example of polarization curve

There are 4 causes for the dropping voltage:

- **Activation losses:** due to the slowness of the reaction on the surface of the electrodes.
- **Fuel cross over and internal current:** these losses come from the fuel diffusion and electron flow through the electrolyte.
- **Ohmic losses:** due to the resistance of the electrodes, various interconnections and the resistance to the ions flow through the electrolyte.

- **Mass transport losses:** these losses come from the concentration of the reactants at the surface of the electrodes.

The electrolyte

In the core of the proton electrolyte fuel cell there is a polymer membrane electrolyte composed by Nafion which is a material that have good chemical resistance and give a mechanical strong property to the membrane. In addition, allow the absorption of large quantities of water and, when the membrane is well hydrated, allow the flow of the H^+ ions through it. This membrane can be less than 50μm.

The electrode

The anode and cathode electrodes are essentially the same and they are compose by Nafion and Platinum, which is the best catalyst. This catalyst made the proton exchange membrane fuel cells expensive at the beginning when it used 30 mg/cm^2, nowadays, the amount of catalyst has been reduced to 0.1 mg/cm^2, which accounts for 55% of the total PEMFC cost [10]. Platinum catalyst is formed into very small particles on the surface of the carbon powder. The platinum is highly a spread out allowing a high portion of the surface area keep in contact with the reactants. There are two methods to build the electrode:

1. **Gas diffusion electrode:** the blend of carbon powder and catalyst is fixed to a porous and conductive material called *gas diffusion layer* which provide basic mechanical structures and diffuse the gas onto catalyst. Then, each electrode is fixed to the membrane electrolyte. As a result, the obtained assembly is the *membrane electrode assembly (MEA).*

2. **Catalyst coated membrane (CCM):** this method consist on depositing the platinum on carbon catalyst on the electrolyte membrane directly using rolling, or spaying, or printing process. When the CCM is done, the GDL is added. The GDL works only as electrical connection between carbon-supported catalyst and the current collector. Another functionality of the GDL is carring out the water produced from the electrolyte surface (hydrophobic properties).

In both methods the carbon-supported catalyst are joined to the electrolyte on one side, and on gas diffusion layer on the other side. The impregnation of the electrode with the

electrolyte is done by the spread out of the electrolyte over the catalyst and makes *the three phase contact* between the reactant gas, electrolyte and catalyst surface.

1.3 Experimental background

1.3.1 Polarization Curves

The performance of the fuel cell is characterized by fuel cell voltage-current density graph shown in Figure 1.5. When an external load is connected to the fuel cell, a net current flows through the load. As it has been said in section 1.2, this current is proportional to the active area of the electrodes. As the cell voltage becomes smaller, the density current becomes higher. The factors that determinate the cell voltage-current density relationship can be understood as irreversible losses. There is an initial source of losses in the fuel cell performance coming from the fuel crossover, internal short and parasitic oxidations [6].

The activation losses are the difference between the measured electrode potential and the theoretical electrode potential. The activation losses can be reduced increasing the cell temperature, using more effective catalyst, increasing the roughness of the electrode, increasing the reactant concentration and increasing the pressure.

The crossover is due to the hydrogen passing through the electrolyte and reacting directly with oxygen on the cathode without generated current on the cell. The hydrogen crossover generate the internal waste of electrons in the opposite direction through the electrolyte called internal currents. Internal currents and crossover losses are reduced in high temperatures cells.

The ohmic losses are the losses due to the electrical resistance in the electrodes and the resistance of the flow of the ions passing through the electrolyte. To reduce the internal resistance, an electrode with the highest possible conductivity could be used. Optimize the design choosing components as less resistance as possible, and using the electrolyte as thin as possible. Would also reduce the resistance.

When the oxygen supplied in the cathode electrode reacts during operation, its concentration will be reduced in the electrode and as a result there will be a the reduction in the voltage. The same situation happens in the anode electrode with the hydrogen. Increase the pressure of the gasses could be a good solution to reduce the mass transport losses.

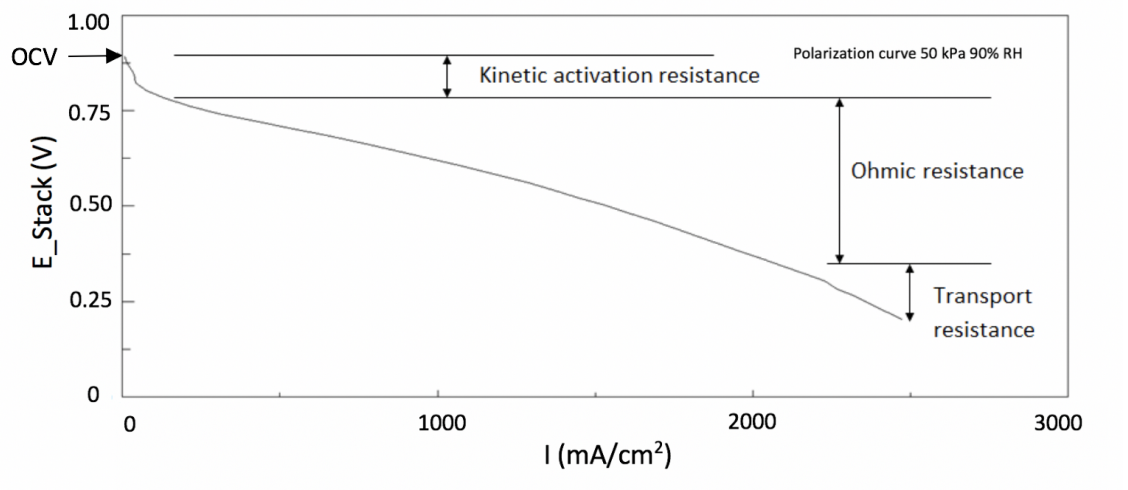

Figure 1.5: Losses of polarization curve

1.3.2 Cyclic Voltammetry

The main objective of cyclic voltammetry is to characterize the electrochemical surface area (*ECSA*) in the electrode and hydrogen crossover. To experimentally determine the fuel crossover, the O_2 or air is changed for inert gas in the working electrode, in this specific case N_2. For the study of the anode side, the anode is chosen as the working electrode, and the cathode is used as a counter electrode with H_2 gas. So, anode is purged with N_2 as a working electrode and cathode is fed with H_2 as a counter electrode. A potential is scanned from 0 to 1.2 V and coming back to 0 V ten times with a rate of 40 mV/s. This scan is done at $30°C$. This experiment is called linear sweep voltammetry (LSV). The output of working electrode current *vs.* working electrode potential is used to calculate the hydrogen crossover from Faraday's law,

$$\frac{i}{2F} = -\frac{dn_{H_2}}{dt} = -\dot{n}_{H_2} \tag{1.13}$$

where F is the Faraday's constant (96485 C/mol), i the current density, n is the moles number and t is the time elapsed in seconds [11].

The eletrochemical activity depends on the reactants, conducting materials and active catalyst. To determine the ECSA from the cyclic voltammetry analysis, the electrode is cycling over a voltage range. The electrode potencial is the number of reactive surface that can be obtained from the total charge for monolayer adsoprtion or desorption. The hydrogen

adsorption (or desorption) reaction (HAD) is characterized by

$$Pt + H^+ + e^- \leftrightarrow Pt - H_{ads} \tag{1.14}$$

The proton reduction to absorbed H_{ads} during the reverse potential sweep occurs between 0.4 V and 0.05 V. An example of that can be observed in the 1.6.

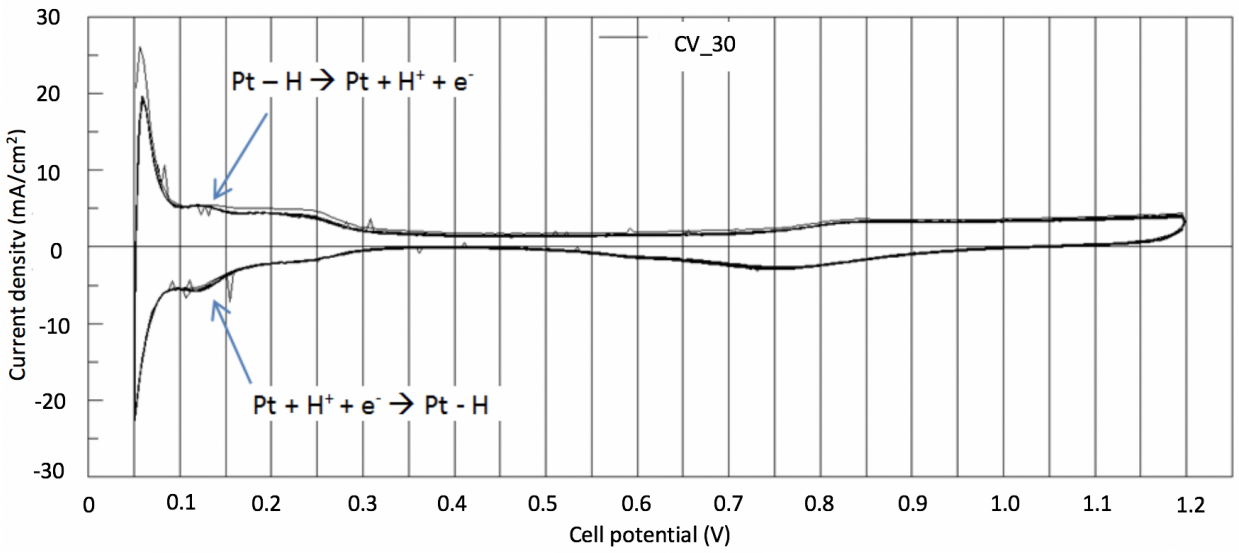

Figure 1.6: Example of cyclic Voltametry

The reaction consist on the deposition of protons on the electrode surface. The electromechanical surface area is calculated from the charge density, $ECSA(cm^2Pt/gPt) = \frac{q}{\Gamma L}$, where $\Gamma = 210\mu C/cm^2$ Pt (Gloaguen 1977, Kinoshita 1977) [6], L is the Pt content in the electrode and q is the hydrogen adsorption charge calculated from the integral of the area. During the cyclic voltammetry experiment,the potential of the working electrode is swept first in the anodic direction and later in the cathodic direction. The ratio of ECSA to specific area of Pt, is the fraction of catalyst that is electrochemicaly available to react. So, higher ECSA means better catalyst.

1.3.3 Cell resistance

The cell resistance is calculated directly from the polarization curves by the test station using the current interrupt method. Current interruption take in consideration a fuel cell where the concentration overpotencial is negligible and the voltage drop is due to ohmic losses and activation losses. When the current is suddenly cut off, it takes some time to disperse the

charge layer but the ohmic losses reduce immediately to zero [11]. The current interrupt method show rapidly indicators of internal losses in the working fuel cells.

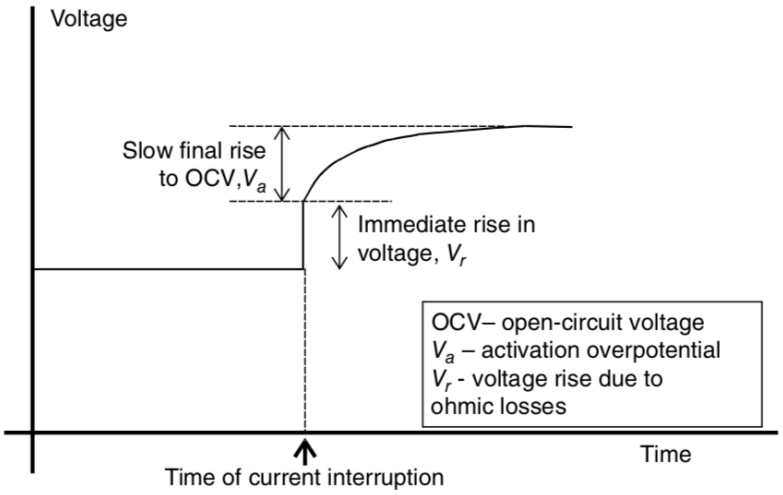

Figure 1.7: Scheme of current interrupt test. (Source: Fuel Cell Systems Explained 2nd Edition)

As a result of current interrupt, the Figure 1.7 shows an example of cell resistance of a fuel cell at 90% of relative humidity.

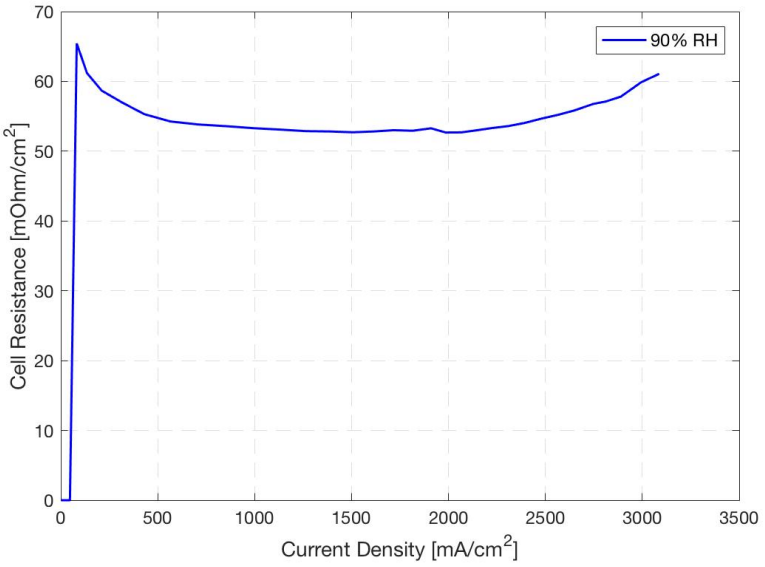

Figure 1.8: Cell resistance 90% relative humidity

1.4 Literature Review

1.4.1 Previous studies

The research of the voltage performance of the MEAs were significant over the last three decades. Due to the innovation in the cell voltage and the significant reduction in MEA platinum loadings, allowed to pass from 0.60 V to 1.0 A/cm^2 [2] until 3.0 A/cm^2 of nowadays. Gasteiger, Panels and Yan [2] experiments with catalyst-coated membranes with H_2/O_2 and H_2/air demonstrated that the catalyst loading could be reduced to 0.05 mg_{Pt}/cm^2 in the anode electrode and to 0.2 mg_{Pt}/cm^2 in the cathode electrode without significant losses. This work demonstrated the trade-off between Pt-catalyst loading and cell voltage. Qi and Kaufman reported the optimal Pt loading to be dependent on the type of Pt/C catalyst due to changes in the catalyst surface area [1]. In the case of 20% Pt/C catalyst, the optimal loading was related in 0.2 $\pm$ 0.05 mg/cm^2 and 0.35 $\pm$ 0.05 mg/cm^2 in the case of 40% [12]. The performance increase substantially from 0.05 mg/cm^2 to 0.2 mg/cm^2 but after that loading, the performance is constant [13]. Similar trends are observed in other literature on low catalyst loadings [14][15].

1.5 Objectives

The present thesis studies the Pt loading effect, in anode side and cathode side, on the catalyst of hydrogen fuel cell. After all the experiments, the thesis will demonstrate the connection between the Pt loading and the fuel cell voltage. The large research on the development of low-temperature PEMFC allowed a high increase in the voltage of the MEA. This gains was consequence of thinner membranes which produced high cell voltages at current densities over 1A/cm^2 [2]. This improvements in the cell voltage, allowed the reduction of Pt loading in the catalyst cheapening the cost of the fuel cell. Also, the thinner electrodes reached by inkjet printed techniques reduced the transport resistance at the reaction site. The results of these literature are deeply discussed [16] [15] [17] [1]. There are a lot of studies which try to study if the performance of the fuel cell is affected by the Pt loading in the electrode. Qi and Kaufman [12] report optimal Pt loading values depending on Pt/C catalyst. The fuel cell performance increase from 0.05 mg/cm^2 to 0.2 mg/cm^2 and it is minimal after this amount of loading. This research started from the article of General Motors [2] where it is affirmed that in the anode side and working with H_2/Air, the loading of Pt can be reduced

until 0.05 mg_{Pt}/cm^2 without significant losses and the Pt loading of the cathode side can be reduced until 0.2 mg_{Pt}/cm^2. These experiments were done in different conditions which we are working nowadays. They used to use current densities of 1 A/cm^2 and today the current densities can reach 3 A/cm^2 with 0.1 mg_{Pt}/cm^2 in the cathode side.
Other differences with their article were: a) the active area, which was 50 cm^2 in their experiments and 5 cm^2 in this study, and b) the bipolar plate, where they used 2 and 3 parallel serpentine channels and in this study single serpentine channel bipolar plates were used.
Because of the gap in the previous studies of the anode side high current density, it was proposed to perform some experiments to prove that changing the Pt loading in the anode electrode, didn't change the performance significantly as Gasteiger, Panels and Yan said [2] .

This study wants to be the beginning of the new studies about the performance at current loadings. The chosen loadings are lower than 0.1 mg/cm^2 and the current densities reach 3.0 A/cm^2 at high relative humidities.

Chapter 2

Experimental procedures

This chapter describes the procedure and operation of the experimental process. It will be described the manufacturing process, all testing procedures and the experimental samples.

2.1 Manufacturing the catalyst coated membranes

The CCM were manufactured using inkjet printing method with a catalyst ink containing 40%wt Pt/C, 30%wt Nafion (5% Liquion Nafion-solution), a blend of IPA and PG as solvents. A detailed description of the process is given by Shukla, Stanier, Saha, Stumper and Secanell [1]. The CCMs tested are 5 cm^2. Different samples coming from different CCMs were printed for this study with various catalyst loadings. In the Table 2.1 all CCMs printed are given.

Table 2.1: Printed CCMs

	Cathode	Anode
First Printing		
CCM 1	0.10 mg/cm^2	0.10 mg/cm^2
CCM 2	0.10 mg/cm^2	0.07 mg/cm^2
CCM 3	0.10 mg/cm^2	0.03 mg/cm^2
CCM 4	0.10 mg/cm^2	0.05 mg/cm^2
Second Printing		
CCM 1B	0.10 mg/cm^2	0.10 mg/cm^2
CCM 2B	0.10 mg/cm^2	0.08 mg/cm^2
CCM 3B	0.10 mg/cm^2	0.06 mg/cm^2
CCM 4B	0.10 mg/cm^2	0.06 mg/cm^2

2.2 MEAs assembly

The components of a single fuel cell consist on membrane electrode assembly (MEA), gaskets, flow channels, current collectors and end plates. Once the CCM is dry, it is laminated between lamination foil of 3 mil inch. Previously, it is necessary to remove a square in the middle of the laminate sheet to hold the electrodes free. In the same step, the holes for the assembly are mark and punch with the corresponding stamping press. The Figure 2.1 show the result of the laminated CCM. It is very important to mark the anode and cathode side of the CCM if the loadings are different.

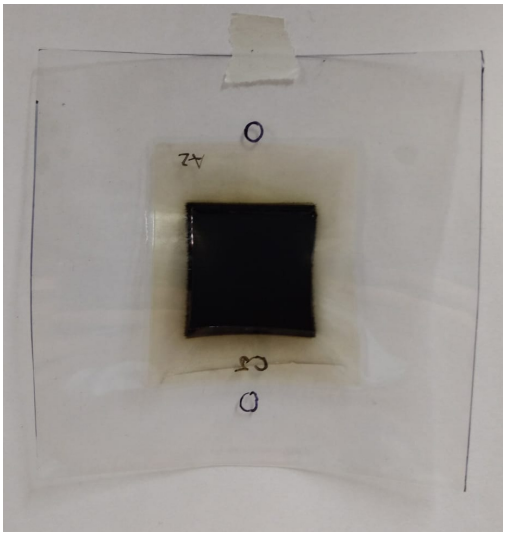

Figure 2.1: CCM lamination

Once the lamination is done, the gaskets should be cut, as the lamination sheets, with the square center window of 5 cm^2. The correct gaskets should be chosen depending on the gas diffusion layer (GDL), the lamination, PEM and electrode thickness as it is shown in the Figure 2.2. The thickness of the electrodes and the PEM were measured with a micrometer. The selected GDL was the Sigracet 29 BC made with carbon fiber paper substrates. Finally, the chosen gaskets were 0.006 inch thick rigid PTFE coated fiberglass.

The chosen GDL is cut with a knife in a 5 cm^2 square. This GDL square is aligned in the GDL hole with the darkest part, which is the microporous layer (MPL), facing to the CCM. Using sandwiching method, the CCM, with the laminate sheets, the GDL and the gaskets were assembled with a serpentine channel bipolar plate, current collectors and end plates. Before start the test in the testing station, a pressure paper is used in order to check the correct pressure and the correct assembly of the MEA. This pressure paper is assembled

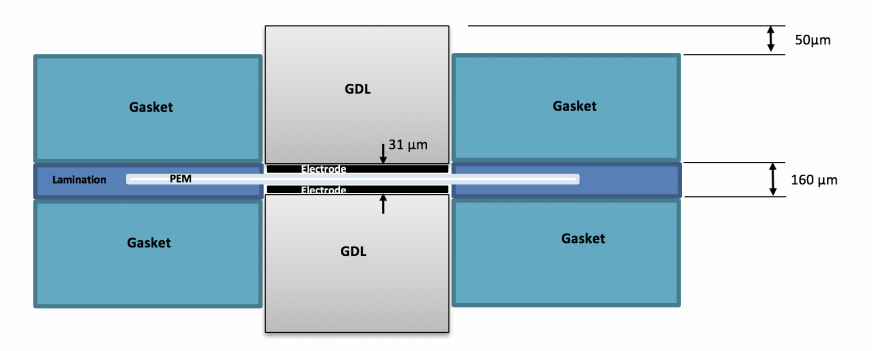

Figure 2.2: Scheme of the assembly

between the GDL and the bipolar plate and then the fuel cell is closed. Once the cell is closed with the correct pressure, 55 inch-pounds in this case, it will be opened again to check the correct assembly. This procedure was done in each assembly during the experimental procedure. The Figure 2.3 shows an example of a test result of well assembled cell.

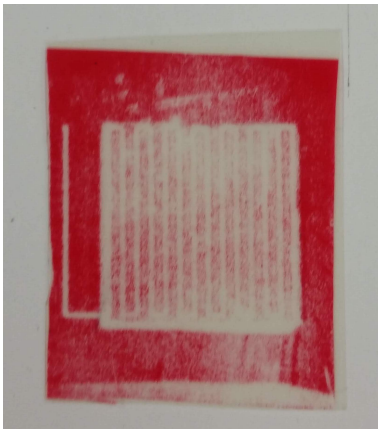

(a) Pressure test

Figure 2.3: Pressure test

It is easy to see the different serpentine channels of the bipolar plate in the Figure 2.3. The final assembly of the fuel cell is shown in the Figure 2.4.

2.2.1 Electrochemical testing

To compare the CCMs, 3 different tests were performed which were already explained in the section 1.3. Now it will be showed each setup.

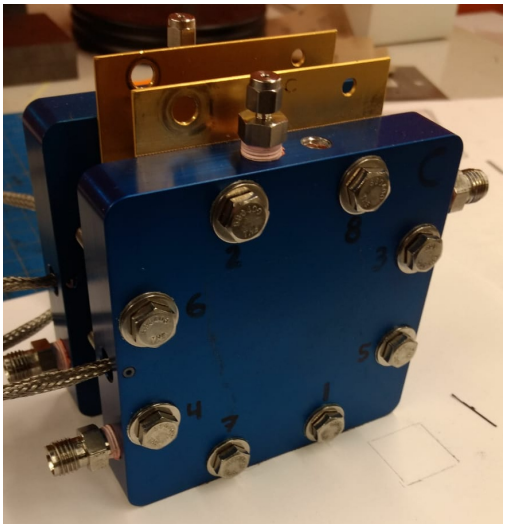

Figure 2.4: FuelCell

Conditioning

The conditioning objective is the membrane hydrated in order to perform effectively. The full conditioning takes 16 hours and it is done after the assembly and before the experiments. The energy system design laboratory (ESDLab) has developed his own conditioning protocol which includes a combination of constant current and potential cycling at 80°C and 80% relative humidity.

Polarization curves

For this experiment, hydrogen is used in the anode side and air in the cathode side. The experiment was run three times for each sample with different relative humidities (50%, 70% and 90%). All of them with 80°C cell temperature, 2/6 stoichiometry and 50 kPa backpressure.

Cyclic voltammetry

Cyclic voltametry is performed with hydrogen and nitrogen. The studied side is were the nitrogen goes and in the other side it has to be run with hydrogen. It means that in the anode study, the hydrogen pass through the cathode and the nitrogen through the anode. The temperature of the cell in is $30°C$.

2.3 Samples

The CCMs in Table 2.1 are tested twice, once as given in the table and once again with anode and cathode reversed in order to study both anode and cathode loading. In the case of CCM1 and CCM1B, the experiment will be done once due to the same loading of the CCMs. Also, in the case of the anode study and with the propose to have more data, more samples were used. These samples are the labelled with the letters LK and LU. The tables 2.2 and 2.3 summarizes all the samples used in the anode study and the cathode study.

Table 2.2: Anode Samples

Anode Study		Anode loading (mg/cm^2)	Cathode loading (mg/cm^2)	Anode Layers
Sample 01	CCM 1	0.095	0.106	13
Sample 02	CCM 2	0.072	0.106	11
Sample 03	CCM 3	0.028	0.106	3
Sample 04	CCM 4	0.050	0.106	7
Sample 05	CCM 3B	0.028	0.106	3
Sample 06	CCM 4B	0.050	0.106	7
Sample 07	CCM 2B	0.072	0.106	10
Sample 08	CCM 1B	0.106	0.106	12
Sample LK1	CCM LK1	0.095	0.095	-
Sample LK2	CCM LK2	0.067	0.095	-
Sample LK3	CCM LK3	0.028	0.095	-
Sample LK4	CCM LK4	0.056	0.106	-
Sample LU	CCM LU	0.050	0.095	-

Table 2.3: Cathode Samples

Cathode Study		Anode loading (mg/cm^2)	Cathode loading (mg/cm^2)	Cathode Layers
Sample 01	CCM 1	0.106	0.095	13
Sample 02B	CCM 2	0.106	0.072	11
Sample 03B	CCM 3	0.106	0.028	3
Sample 04B	CCM 4	0.106	0.050	7
Sample 05B	CCM 3B	0.106	0.028	3
Sample 06B	CCM 4B	0.106	0.050	7
Sample 07B	CCM 2B	0.106	0.072	10
Sample 08	CCM 1B	0.106	0.106	12

Chapter 3

Results and discussion

3.1 Previous results

The Figure 3.1 with 50% RH, shows that the best performance resulted is the sample LK2 which has $0.07 mg_{Pt}/cm^2$, however, all the curves are very similar and this graph is not enough to take strong conclusions. Is in the 70% relative humidity 3.2 where the perform of each CCM is different. In the other way that it could suppose from the previous articles [2], the worst result is the polarization curves with higher Pt loading (sample LK1). It is easy to see that the kinetic activation resistance are still very similar in all the curves but in the case of the sample LK1 is in the ohmic losses where it takes the difference. In the higher relative humidity, Figure 3.3 the results are completely unexpected. The performance between the sample LK2 and sample LK4 are very similar while the sample LK1 and sample LK3 have worst results. After these results the question was if there is an optimum loading where the performance of the fuel cell is optimum. If it was in this way, the found of this optimum would bring saves of money and better performance. To continue this hypothesis it was study both electrodes with different loadings. As the objective is always minimize the platinum loading to reduce costs, the samples started in 0.1 mg_{Pt}/cm^2 and were falling down as the previous LK's samples. In the next section it will be follow the experiments explained in previous part 1.3, were printed 4 CCM's twice with different loadings and then they were tested to obtain the necessary data.

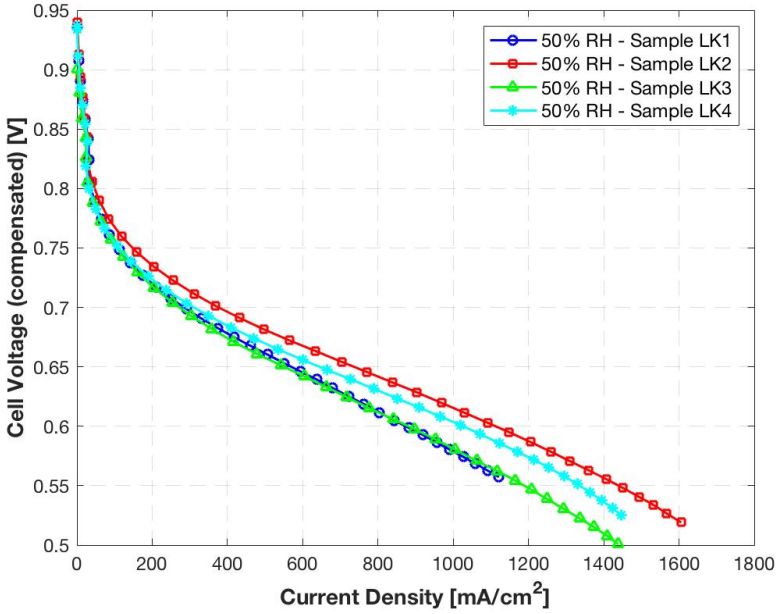

Figure 3.1: Samples LK 50% Relative Humidity

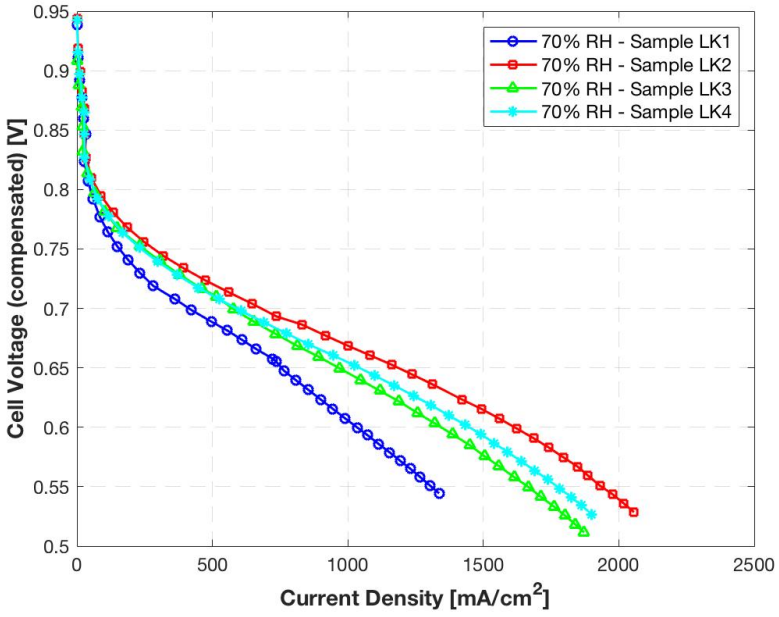

Figure 3.2: Samples LK 70% Relative Humidity

3.2 ECSA characterization by cyclic voltammetry

First, the electrodes were characterized by cyclic voltammetry to make sure ECSA increased with loading. The electrochemical surface area of all the samples is shown in Figure 3.4 and Table 3.1. This study was separated in two different groups the samples with variable

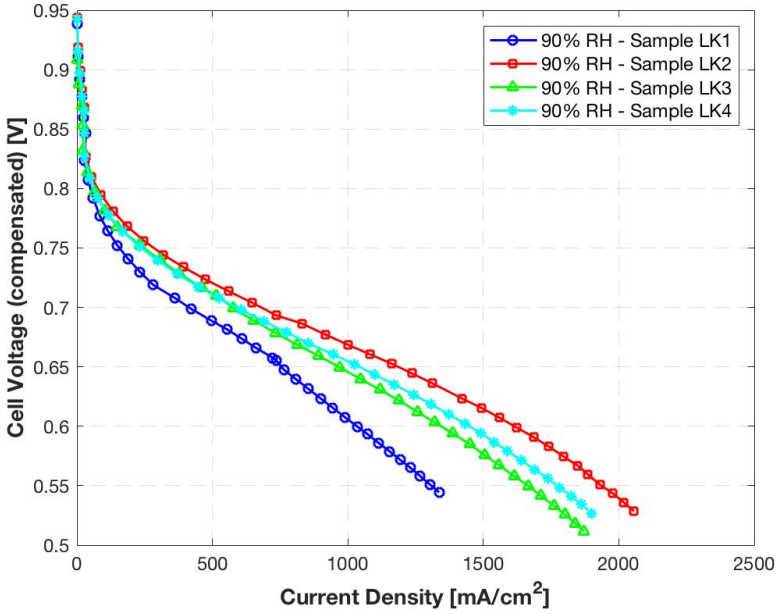

Figure 3.3: Samples LK 90% Relative Humidity

loading electrode study and fixed loading electrode study. This was because the experiment of cyclic voltametry was done for all the samples and when the experiment run in the fixed loading side, all the results are, obviously, exactly the same.

More interesting is the study of the electrochemical surface area for the variable loadings.

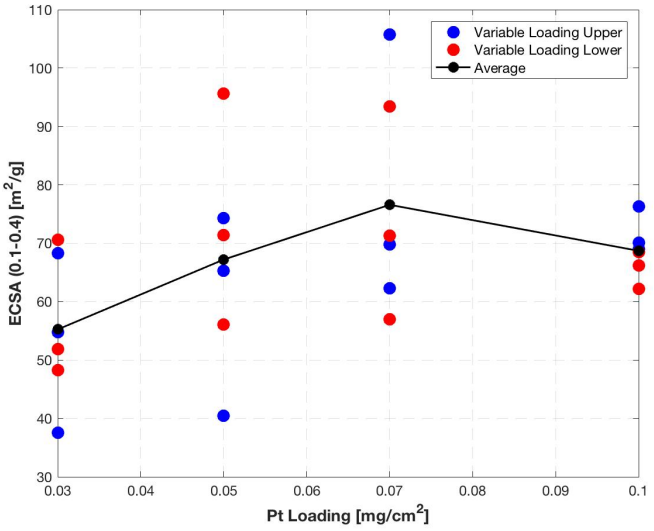

Figure 3.4: ECSA - Variable loadings

From the result of the electrochemical surface area of the samples shown in the Table 3.1

Table 3.1: Sumary of ECSA of all the samples

Variable loading electrode study			ECSA(m^2/g) Catalyst layer	m^2 Pt/ cm^2 Limit 0.1 - 0.4	Cross over (mA/cm^2)
Sample	Loading(mg/cm^2)	Area			
Sample 01	0.1	Upper	70.11	0.0070	0.89
		Lower	62.20	0.0062	0.89
Sample 08	0.1	Upper	76.26	0.0076	1.07
		Lower	66.17	0.0066	1.07
Sample LK1	0.1	Upper	68.97	0.0690	0.55
		Lower	68.53	0.0069	0.55
Sample 02	0.07	Upper	62.32	0.0044	0.94
		Lower	57.10	0.0040	0.94
Sample 07	0.07	Upper	105.76	0.0074	0.57
		Lower	93.40	0.0065	0.57
Sample LK2	0.07	Upper	69.76	0.0049	0.55
		Lower	71.29	0.0050	0.55
Sample 04	0.05	Upper	40.47	0.0020	1.74
		Lower	95.65	0.0048	1.74
Sample 06	0.05	Upper	65.27	0.0033	0.78
		Lower	56.08	0.0028	0.78
Sample LK4	0.05	Upper	74.33	0.0037	0.00
		Lower	71.43	0.0035	0.00
Sample 03	0.03	Upper	54.79	0.0016	0.75
		Lower	48.30	0.0015	0.75
Sample 05	0.03	Upper	37.56	0.0011	0.22
		Lower	51.89	0.0016	0.22
Sample LK3	0.03	Upper	68.32	0.0020	0.53
		Lower	70.6	0.0021	0.53

it is easy to see the big difference between the upper ECSA and lower ECSA of the sample CCM 04 and the distance between the results of the CCM 04 and CCM 04B in the Figure 3.4. Before continue, the sample CCM 04 will be discarded because its ECSA results. Figure 3.4 shows the ECSA of all the samples, for upper and lower area. With these results, it is not easy to make any conclusion, but as in the previous experiments, the average shows the good performance in the samples with 0.05 mg/cm^2, 0.07 mg/cm^2 and 0.1 mg/cm^2, all around 70 m^2/g.

Figure 3.4 shows that ECSA appears to be similar at different loadings which contradicts the Shukla's results [1] where is said that ECSA decrease when the Pt loading increase.

3.3 Pt loading effect in the anode side

As it was said in the section 3.1 of the current thesis, the results of the LK's samples are different that it could expect taking into account the Gasteiger H. A, Panels J. E, Yan S. G results [2]. The CCM's performance with 0.1 mg/cm^2 anode loadings are not the best and it seems that there is an optimum loading. After the testing of the first CCMs, the samples with lower loading have better performance than the sample with higher loading. Figure 3.5 shows similar trends of the performance of the Sample 02, Sample 03 and Sample 04 at 50% RH. Sample 01 follows the trend at kinetic region and increase the ohmic losses and mass transport losses. This same performance of the Sample 01 is repeated for the 70% and 90% RH. Figure 3.6 shows that the performance of the Sample 01 and Sample 02 are very similar with high kinetic losses in the Sample 01. Finally, in Figure 3.7 the mass transport losses of the Sample 02 make fall down suddenly the cell voltage reaching the polarization curve of the Sample 01 below 0.4 V. If the Sample 04 is discard, as in the previous section, the best performance is the performance of the Sample 03.

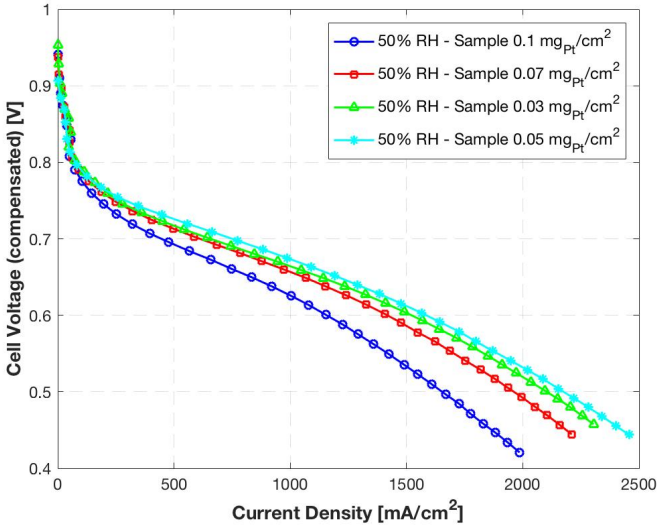

Figure 3.5: First Samples comparative 50%RH. Anode side.

Surprisingly, the second results were different than de firsts ones. The performance of 50% RH polarization curves are very similar for all loadings (see Figure B.4). Figure 3.8 shows the better performance of Sample 07 in the kinetic and ohmic region, but it falls down suddenly due to the mass transport losses. Exactly the opposite trend follows the Sample 05, where it has the worst performance in the kinetic and ohmic regions but it has the lowest

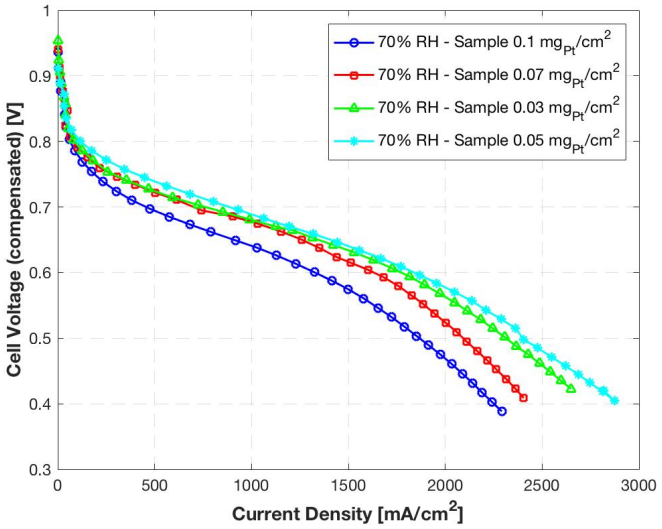

Figure 3.6: First Samples comparative 70%RH. Anode side.

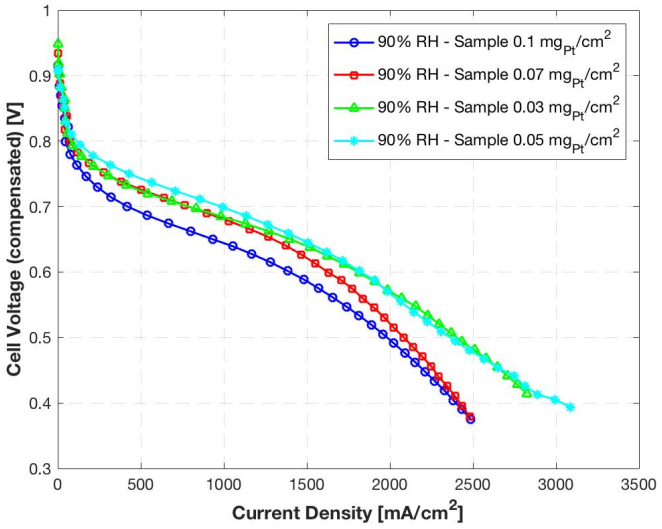

Figure 3.7: First Samples comparative 90%RH. Anode side.

mass losses. The performance are similar until 1500 mA/cm^2 in the highest relative humidity and the Sample 05 has the lowest mass transport again, like in the 70% RH graph 3.8.

It is difficult to draw any conclusion with these different results of the first and second printing. But, the mass transport losses are lower in the lower loading for both printings.

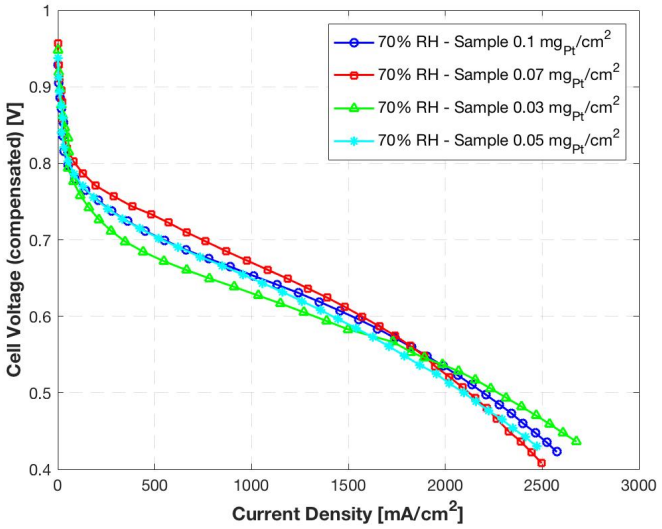

Figure 3.8: Second Samples comparative 70%RH. Anode side.

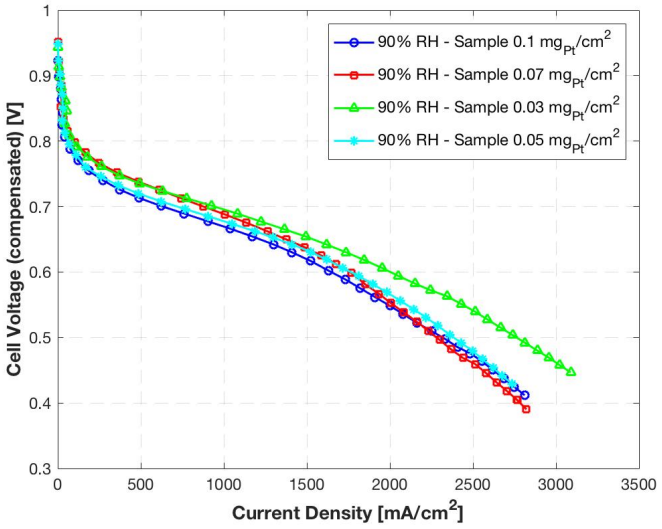

Figure 3.9: Second Samples comparative 90%RH. Anode side.

To discard errors with the assembly in the second printing, the graph of cell resistance *vs.* current density is shown in Figures 3.10, 3.11 and 3.12 for the first printing and in Figures 3.13, 3.14 and 3.15 for the second printing. As it can be observed, the cell resistance is very similar in both printings for each curve and relatives humidities. For 50% relative humidity, the cell resistance is around 100 mOhm/cm^2 (see Figure B.13), around 80 mOhm/cm^2 for 70% RH (see Figure B.14) and around 60 mOhm/cm^2 for 90%RH (see Figure B.15).

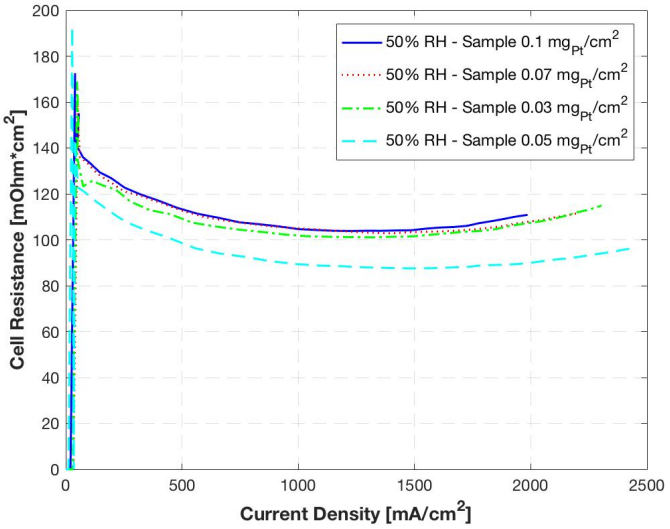

Figure 3.10: Cell resistance 50% RH. First printing. Anode side.

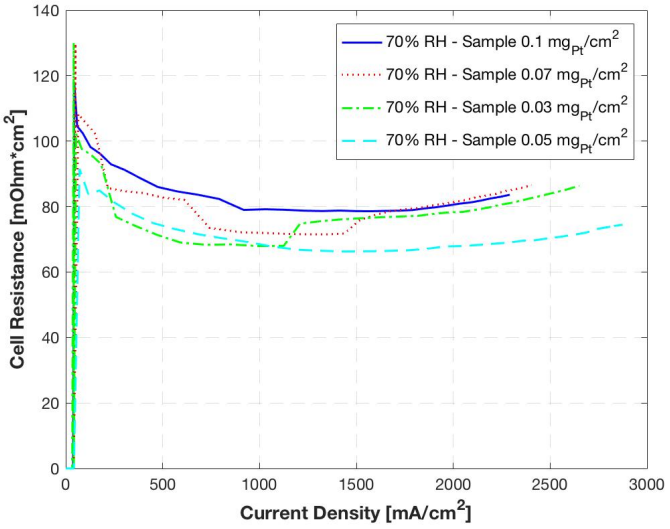

Figure 3.11: Cell resistance 70% RH. First printing. Anode side.

In the way to discuss more data, Figures 3.16, 3.17 and 3.18 show the cell voltage for each Pt loading for 1 A/cm^2, 1.5 A/cm^2 and 2 A/cm^2 for the first printing. All the graphs have similar trends where, the worst voltage for all density current is associated to 0.1 mg/cm^2 (Sample 01), and the best voltage correspond to the 0.05 mg/cm^2 (Sample 04).

Taking in account that the Sample 04 was discarded, the results are not clear. To show more information and to discuss the voltage for each loading, it was plot all the samples in one graph for each relative humidity.

In the case of 50% RH (Figure 3.19, the average is very flat in 1 mA/cm^2. In this current

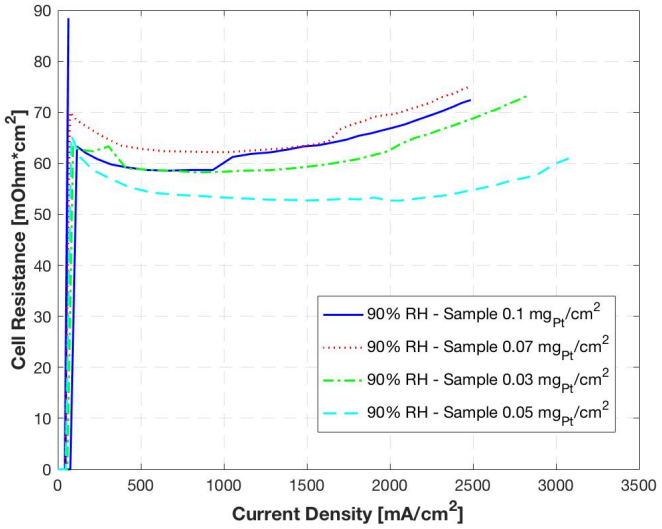

Figure 3.12: Cell resistance 90% RH. First printing. Anode side.

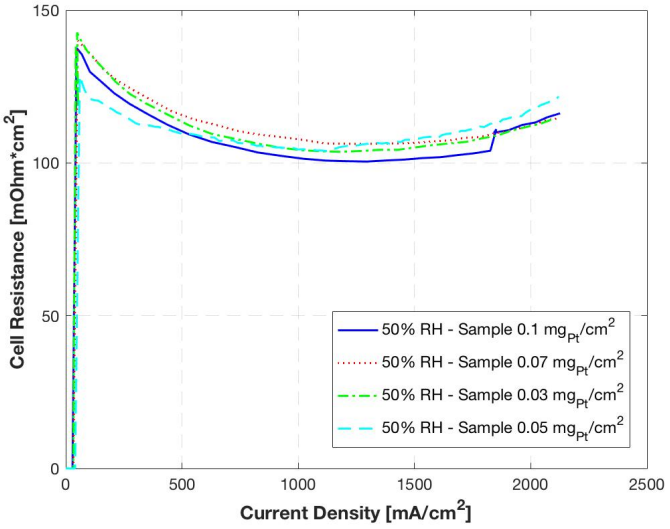

Figure 3.13: Cell resistance 50% RH. Second printing. Anode side.

density there are data for all the samples (first printing, second printing and LK printing). In the 1,5 mA/cm^2 and 2 mA/cm^2 current densities, there are only the data of first and second printing. This was because the LK printing didn't get this current density values. For the 1,5 mA/cm^2 and 2 mA/cm^2, the difference between 0.03, 0.05 and 0.07 $mgPt/cm^2$ is 0.05 V in the highest value of the average. In all current densities, the worst performance is given by the 0.1 $mgPt/cm^2$. Figure 3.20 shows again the stable voltage in around 1 mA/cm^2 and int this case, also the constant current density in the loading below 0.1 mA/cm^2. Also, in this graph there are only the first printing and second printing data in the highest current

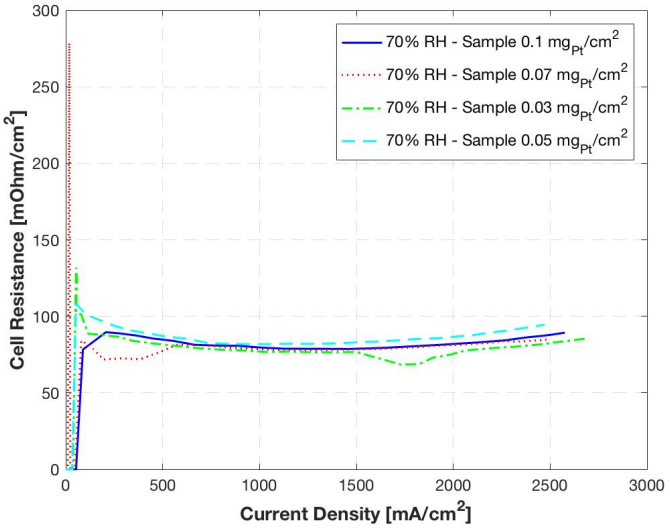

Figure 3.14: Cell resistance 70% RH. Second printing. Anode side.

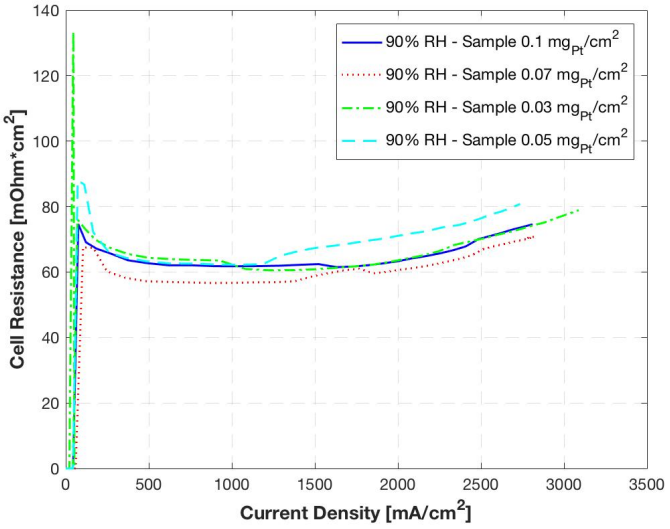

Figure 3.15: Cell resistance 90% RH. Second printing. Anode side.

densities. Again, the average of the cell voltage is less than 0.05 V in the worst case for 0.03, 0.05 and 0.07 $mgPt/cm^2$ and the worst performance is shown by the 0.1 $mgPt/cm^2$. For the 90% RH 3.21, the performance is similar than the others 2 graphs. The average cell voltage show an stability and this stability fall down in the highest Pt loading for all current densities.

After these results, the comparative was done between the same loadings. In the comparative between all 0.1 mg_{Pt}/cm^2 samples (see Figures B.16, B.17 and B.18), the highest difference is in the mass transport losses and the kinetic and ohmic losses are very similar. In

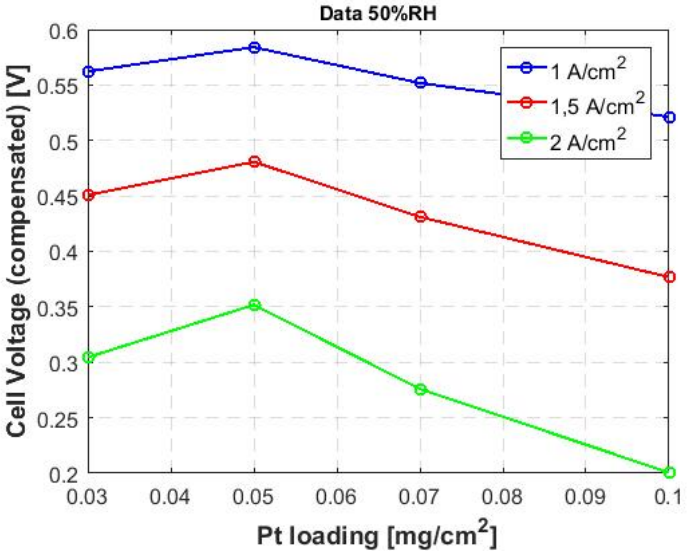

Figure 3.16: Cell Voltage - Pt Loading 50% RH. First printing. Anode side.

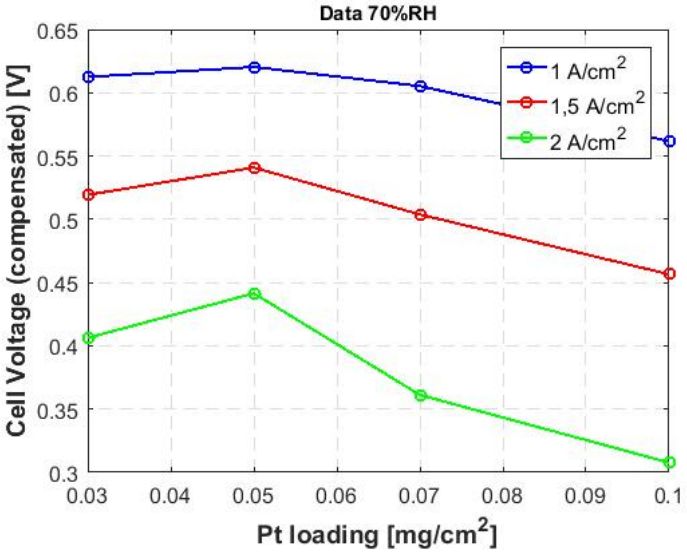

Figure 3.17: Cell Voltage - Pt Loading 70% RH. First printing. Anode side.

the case of 0.07 mg_{Pt}/cm^2 the samples, the performance of the polarization curve is similar for all relative humidities (see Figures B.19, B.20 and B.21). These similar results make more believable the performance of 0.07 mg_{Pt}/cm^2 samples. The results are different in the case of the comparison of 0.05 mg_{Pt}/cm^2 samples. The Figure 3.22 shows the polarization curves performance at 50% RH for 0.05 mg_{Pt}/cm^2 samples. The kinetic losses are similar in the case of Sample 04 and Sample 06, and better than the Sample LK4. The Ohmic losses and the mass transport losses seem very similar at three samples.

The Figure 3.23 shows the lower kinetic losses in the Sample 04 and the similar perfor-

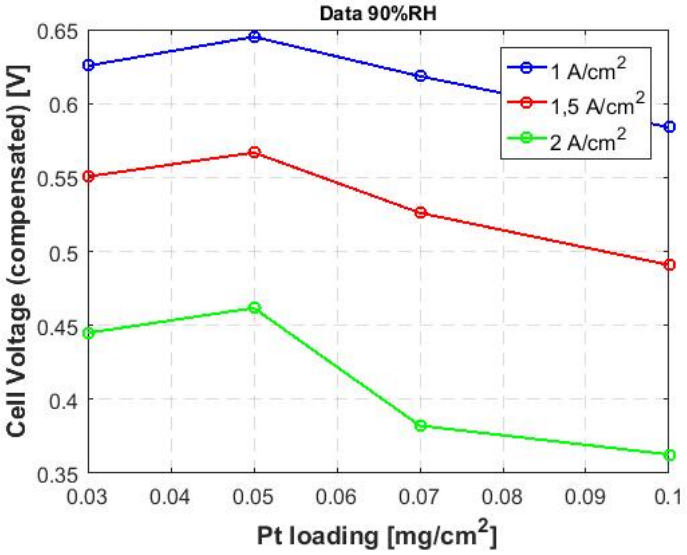

Figure 3.18: Cell Voltage - Pt Loading 90% RH. First printing. Anode side.

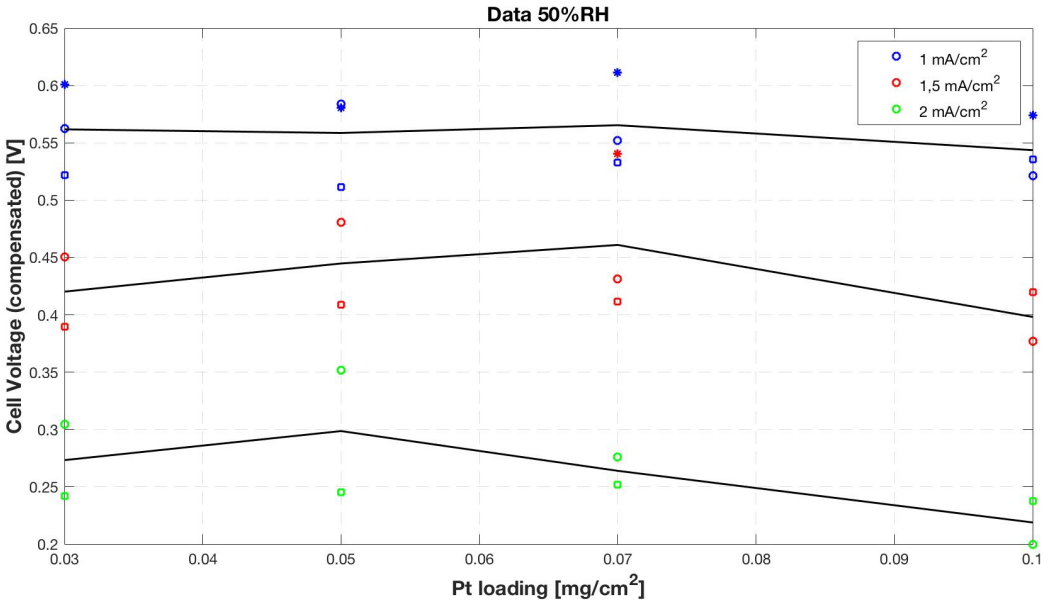

Figure 3.19: Cell Voltage - Pt Loading 50% RH. All the samples with the average

mance in the Ohmic and mass transport region with all samples. At high relative humidity, all the polarization curves are very similar in all regions, except on mass transport region of Sample LK4.

Something similar than 0.05 mg_{Pt}/cm^2 samples happens in the 0.03 mg_{Pt}/cm^2 samples. In the 50% RH, the only difference is in the kinetic losses of the Sample 03 which is lower than the others (see the following Figure 3.24).

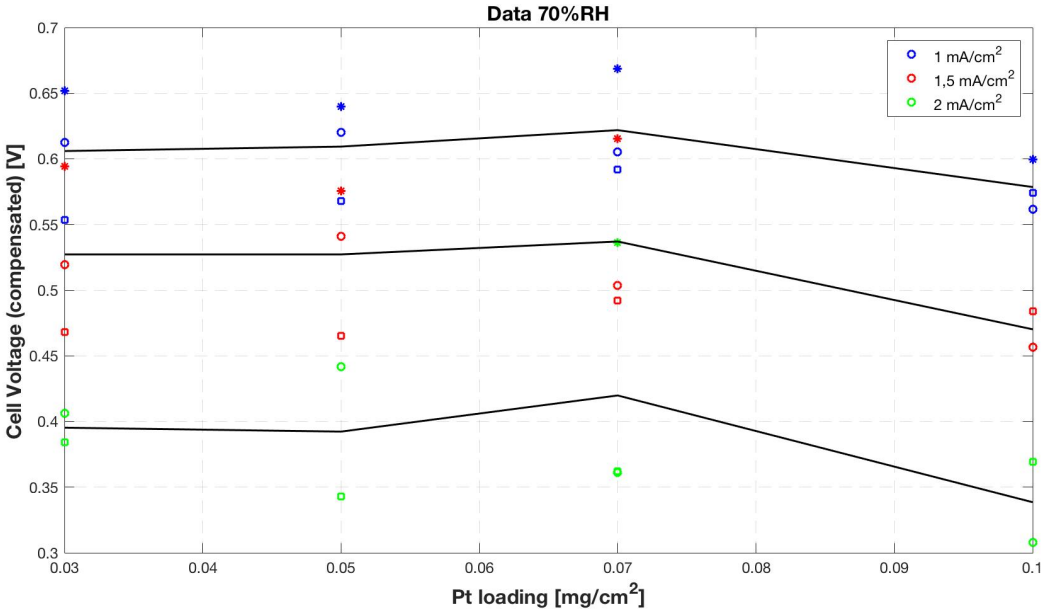

Figure 3.20: Cell Voltage - Pt Loading 70% RH. All the samples with the average

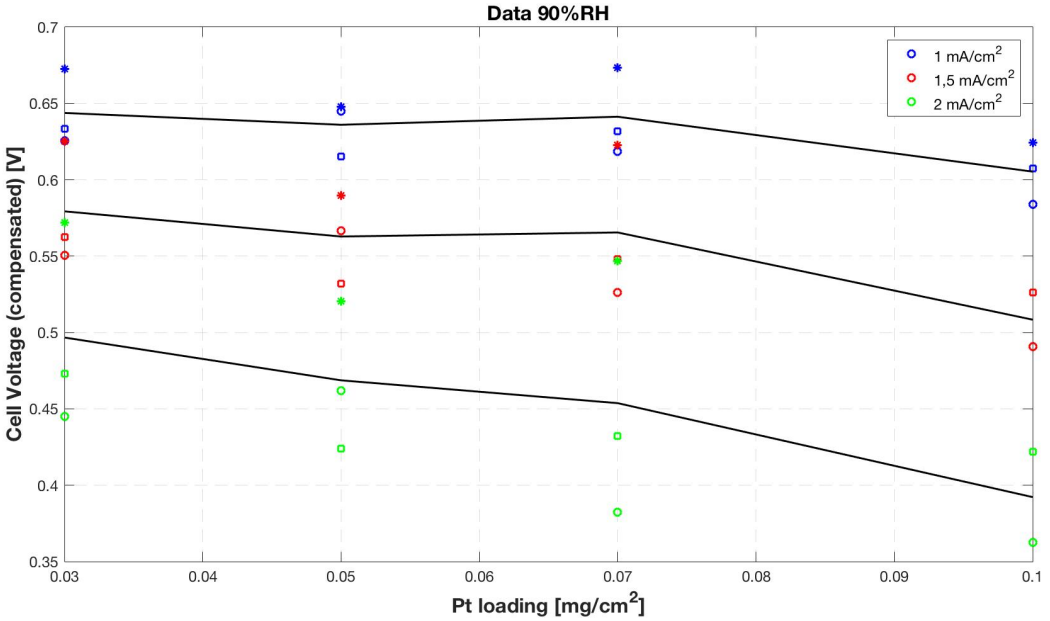

Figure 3.21: Cell Voltage - Pt Loading 90% RH. First printing. All the samples with the average

In the case of the 70% RH, the kinetic losses of the Sample 05 are higher but the mass transport losses are lower than the other samples (see Figure 3.25.

Notice that, the most similar performance, between samples of the same loading for all loadings is at 90% relative humidity.

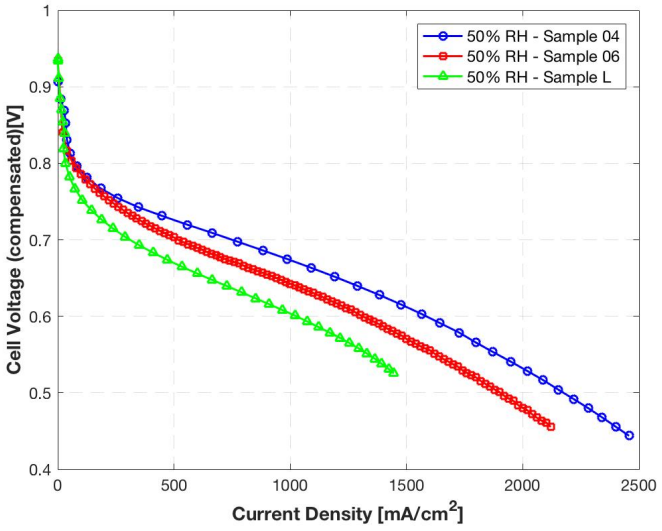

Figure 3.22: 0.05 mg_{Pt}/cm^2 Pt loading comparative samples at 50% RH. Anode side.

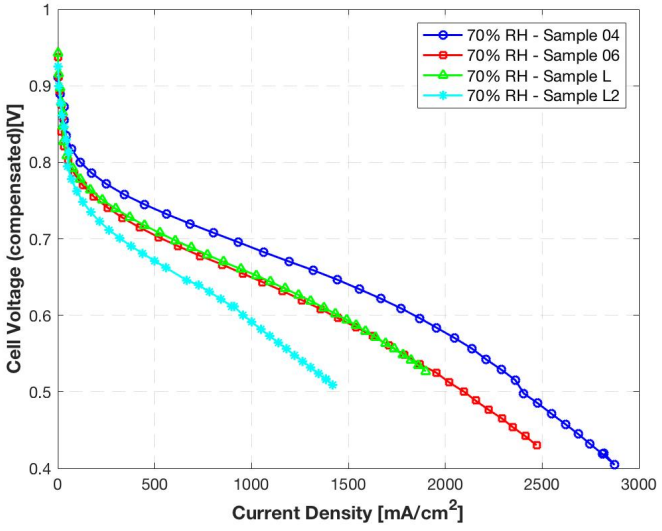

Figure 3.23: 0.05 mg_{Pt}/cm^2 Pt loading comparative samples at 70% RH. Anode side.

Finally, the last comparison in this section is done with the polarization curves average. The objective of this comparison was plot the average fuel cell performance for each relative humidity. In the 50% and 70% RH, all the performance are very similar for each loading (see Figure B.25 and B.26). In the 90% RH, the kinetic losses of the 0.1 mg/cm^2 samples are higher than the others and the mass transport losses of the 0.03 mg/cm^2 samples are lower. These two behaviours are shown in the Figure 3.26.

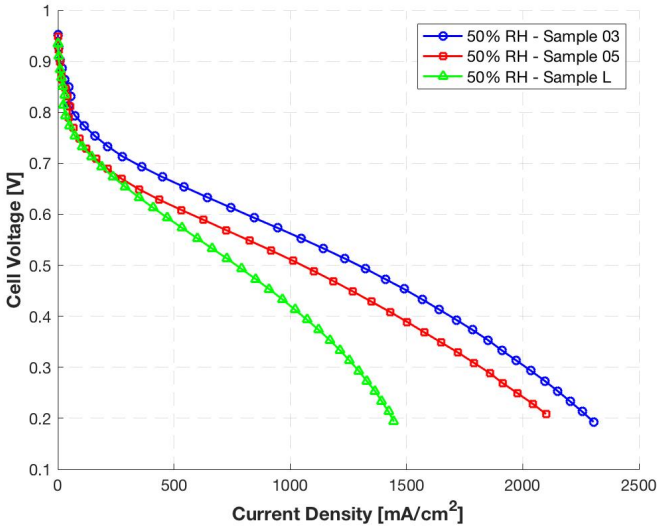

Figure 3.24: 0.03 mg_{Pt}/cm^2 Pt loading comparative samples at 50% RH. Anode side.

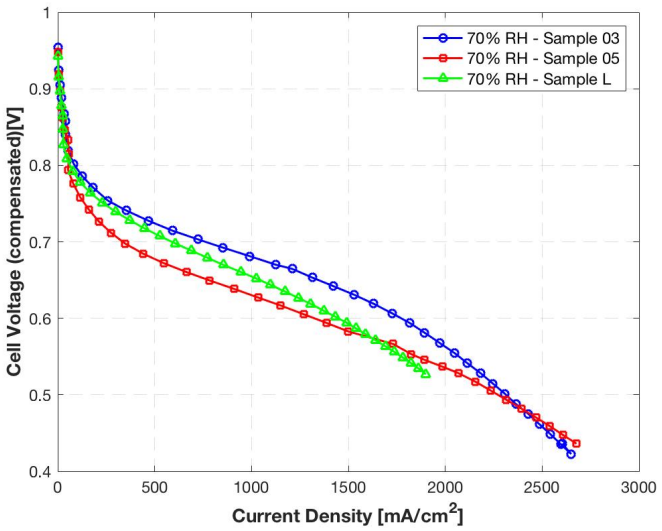

Figure 3.25: 0.03 mg_{Pt}/cm^2 Pt loading comparative samples at 70% RH. Anode side.

With these results, is possible to think that the assembly of the CCM 3 and CCM 4 were better than the others because, in general, the performance is better for all relative humidities. However, in the ECSA study 3.2 Sample 04 was discarded. To determine the influence of the assembly it is necessary to analyse the results of the cell resistance *vs.* current density. Comparing the cell resistance graphs of all samples at 50% RH at the same time, the difference is not obvious as it can be seen in the Figures 3.27.

From this comparison, it can be taken the conclusion that the Sample 03 and Sample

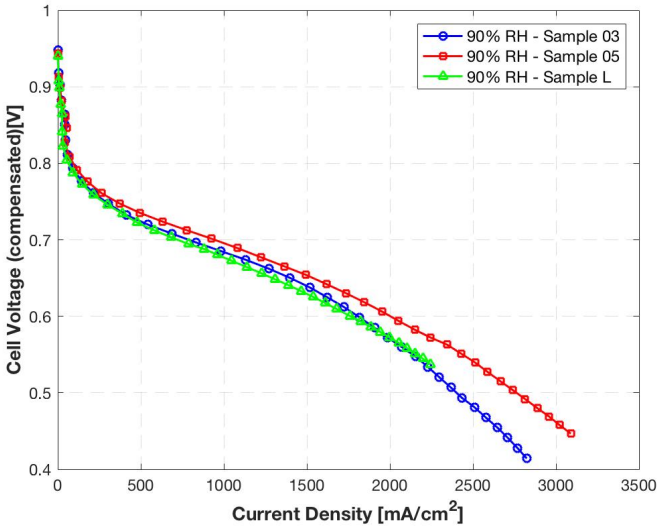

Figure 3.26: 0.03 mg_{Pt}/cm^2 Pt loading comparative samples at 90% RH. Anode side.

04 corresponding to CCM 3 and CCM 4 has the best assembly. However, as Sample 04 is discarded, it will be continuos only with Sample 03. But to take this as a conclusion, is better to compare the next RH. In the Figure 3.11 the performance of the Sample 03 is better with a lower cell resistance. Finally, Figure 3.12 show again the lower cell resistance of the Sample 03.

These results corresponding on the better assembly of the CCM 3 will be discussed in the next chapter (chapter 4).

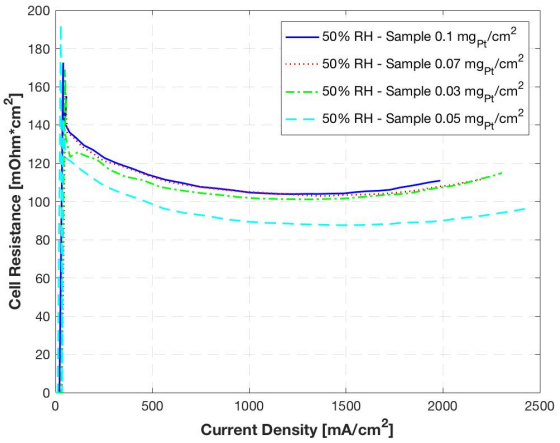

(a) First printing

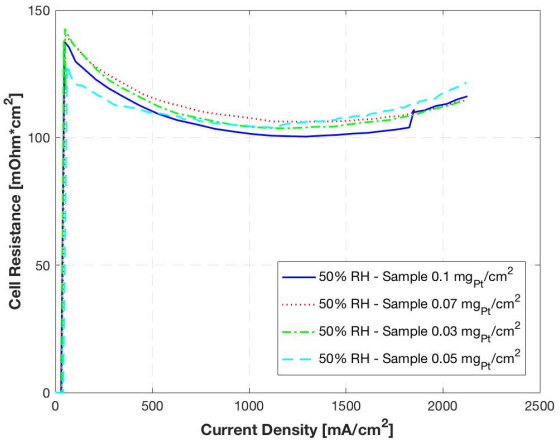

(b) Second printing

Figure 3.27: Cell resistance 50% RH. Anode side.

3.4 Pt loading effect in the cathode side

In the case of the cathode study, the results were the expected. The sample with the highest loading had the best performance and the sample with the lowest loading had the worst performance for all the samples and relative humidities. All the results of these polarization curves are showed in the appendix B.

All the graphs show the worst performance when the loading is reduced. To confirm the correct assembly of these samples, it can be checked the graphs of the cell resistance for each samples and relative humidity.

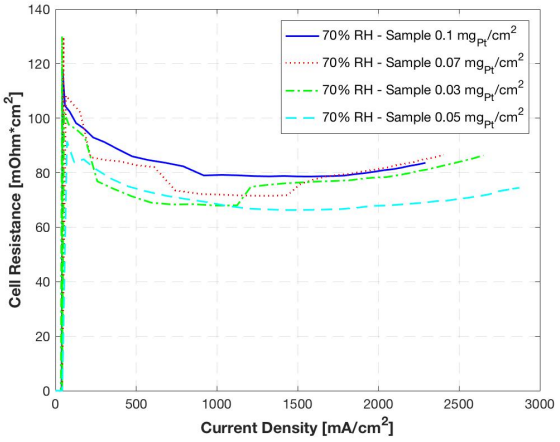

(a) First printing

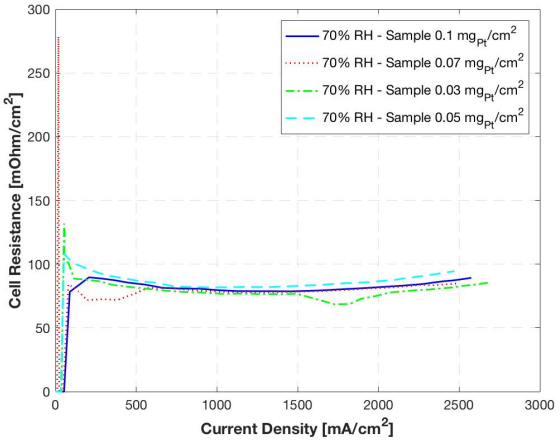

(b) Second printing

Figure 3.28: Cell resistance 70% RH. Anode side.

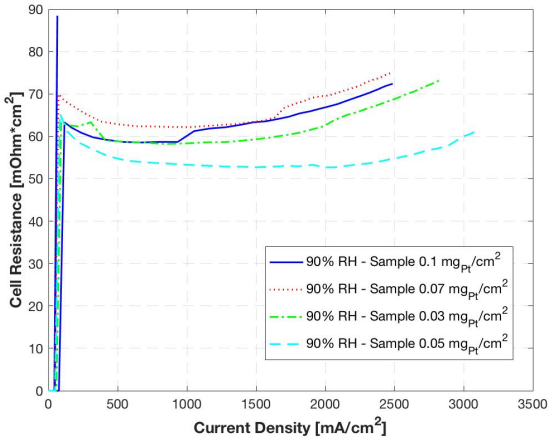

(a) First printing

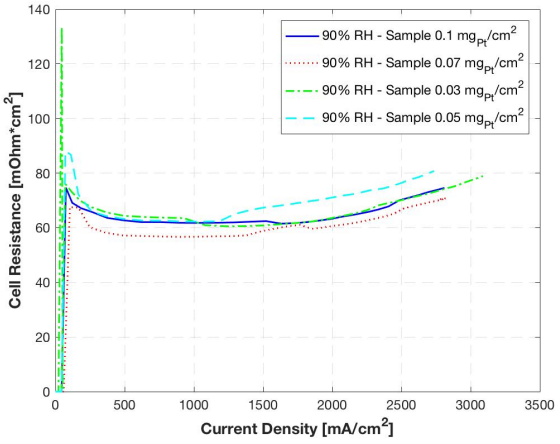

(b) Second printing

Figure 3.29: Cell resistance 90% RH. Anode side.

Chapter 4

Conclusion and future work

From some time ago, the electrode studies in PEMFC were focus in the cathode side. These studies show poor performance of this electrode below 0.1 mg/cm^2 and a small influence in the performance when the anode loading is changed [2]. These results made the studies focus in the cathode electrode because, in theory, had more influence in the performance. The motivation of this study came from the change in the operation variables comparing with these studies. At the beginning, this study focused in the influence of the Pt loading in the anode side because of these reasons. During the fabrication process, the decision was made to study both electrodes, anode and cathode. Before start the experiments, the study included the performance of 4 CCMs and then decide which others CCMs are more interesting to continue the study. This roadmap was planned because the time for the thesis was not too long. In general, all the first printing's results are better than second printing's results and LK's results. As it was commented in the previous chapter 3, the Sample 04 has very good cell resistance performance and better polarization curves. With these results, if I should to choose one of the three sets, I would choose the first printing results because they have better performance comparing with the recent studies and with the other two sets of the present thesis. In my opinion, the first printing was assembled better than the others two because the better polarization curves. From these experiments I learn that the assembly is very important part in the fuel cell experiments. To confirm this initial hypothesis, I would suggest to repeat the same experiments printing new CCMs with these loadings three times as the thesis and then, compare the six sets.

As a conclusion, in the anode study, at higher relative humidities low loadings show better performance. This could be because there is a water crossover (*First hypothesis*). It would be necessary to check this point in futures studies. The kinetic part in the polarization

curves is very similar for all the loading with 0.15 V as a higher difference.

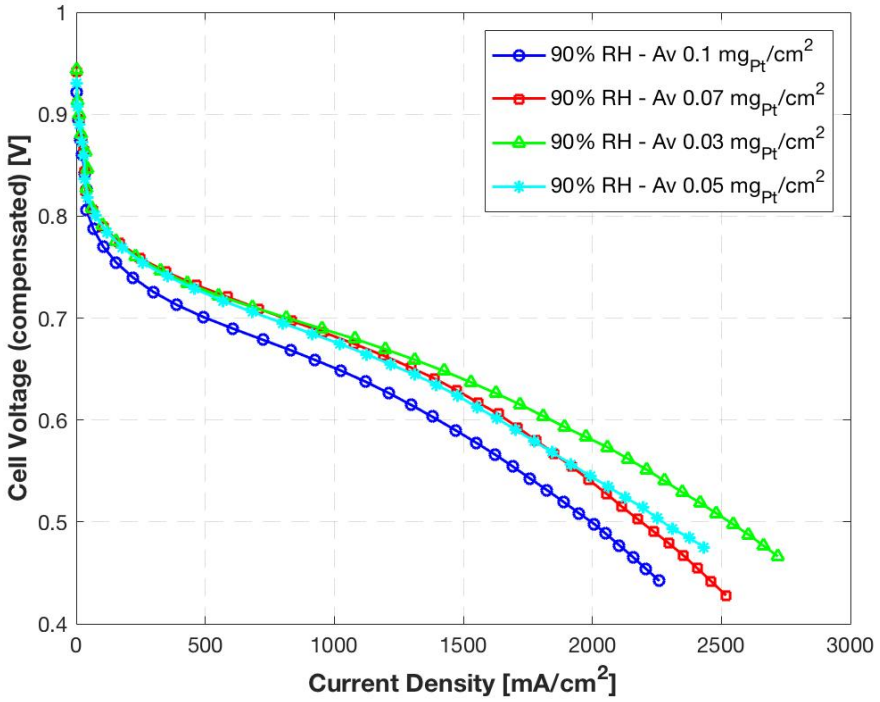

Figure 4.1: Pt loading comparative samples at 90% RH. Anode side.

The conclusion from the cathode study is the same of another previous studies that said that the loading of the cathode electrode can not fall below 0.1 mg/cm^2.

The results of the firsts four CCMs were not the expected results and it was decided to extend the experiments to all the CCMs to take more results. Even this decision, it is obvious that the amount of results is not enough to make finals conclusions and because of that it is necessary to continue with the study with more testings. To make more true the following conclusions or validate it it would be necessary to continue the study with a new roadmap. This new roadmap would consist in:

1. Make the experiments of the polarization curves of the same samples: this is to check the assemblies of the fuel cells and see why the first printing had better performance. If this performance is more or less similar in both printing, the difference could be in the printing.

2. Print 8 more CCMs with 4 loadings: this step would check the printings. The 8 printings should have different loadings than the other printings. To continue the

study it would be better discard the 0.1 mg/cm^2 in the anode and cathode, and choose other loading between 0.3 mg/cm^2 and 0.5 mg/cm^2 or, 0.5 mg/cm^2 and 0.7 mg/cm^2. Also, and in the way to not do extra work, the cathode study wouldn't be done.

3. Make a water crossover study to check the *first hypothesis*.

References

[1] Saha M.S Stumper J Secanell M Shukla S, Stanier D. "Analysis of Inkjet Printed PEFC Electrodes with Varying Platinum Loading". *The Electrochemical Society*, pages 677–687, 2016.

[2] Yan S. G Gasteiger H. A, Panels J. E. "Dependence of PEM fuel cell performance on catalyst loading". *Journal of Power Sources 127*, pages 162–171, 2004.

[3] International Energy Agency. "Hydrogen and Fuel Cells". *Technology roadmap*, page 75, 2015.

[4] Ramaprabhu S Chandran P, Ghosh A. "High-performance Platinum-free oxygen reduction reaction and hydrogen oxidation reaction catalyst in polymer electrolyte membrane fuel cell". *Scientific reports, v8, art 3591*, pages 1–11, 2018.

[5] Dincer I Siddiqui O. "Examination of a new solar-based integrated system for desalination, electricity generation and hydrogen production". *Renewable and sustainable energy reviews*, pages 224–234, 2018.

[6] Fenton J M. Russel Kunz H Cooper K H., Ramani V. *Experimental methods and data analyses for polymer electrolyte fuel cells*. Scribner Associates, Inc., 2009.

[7] Garche J Scrosati B. "Lithium batteries: Status, prospects and future". *Journal of Power Sources, v195, Issue 9*, pages 2419–2430, 2010.

[8] Snee T Lisbona D. "A review of hazards associated with primary lithium and lithium-ion batteries". *Process Safety and Environmental Protection, v89, Issue 6*, pages 434–442, 2011.

[9] Huang K Hu J Li C Gong Y, Yu Y. "Evaluation of lithium-ion batteries through the simultaneous consideration of environmental, economic and electrochemical performance indicators". *Journal of Cleaner Production, v170*, pages 915–923, 2018.

[10] Dauda W.R.W Husainia T Haque M. A Majlana E. H, Rohendib D. "Electrode for proton exchange membrane fuel cells: A review". *Renewable and Sustainable Energy Reviews 89*, pages 117–134, 2018.

[11] Dicks A Larminie J. *Fuel Cell Systems Explained 2nd Edition*. Wiley, 2003.

[12] Kaufman A Qi Z. "Low Pt loading high performance cathodes for PEM fuel cells". *Journal of Power Sources 113*, pages 37–43, 2003.

[13] Gamliel D Ganesan P Popov B Kriston A, Xie T. "Effect of ultra-low Pt loading on mass activity of polymer electrolite membrane fuel cells". *Journal of Power Sources*, pages 243–958, 2013.

[14] Pintauro P Brodt M, Wycisk R. "Nanofiber electrodes with low platinum loading for high power hydrogen/air pem fuel cells". *Journal of the Electrochemical Society*, page 160 (8), 2013.

[15] Gu W Owejan P. J, Owejan E. J. "Impact of Platinum Loading and Catalyst Layer Structure pn PEMFC Performance". *Journal of The Electrochemical Society, 160*, pages 824–833, 2013.

[16] Sinha P Grezler A. T, Caulk D. "The Impact of Platinum Loading on Oxygen Transport Resistance". *Journal of The Electrochemical Society, 159*, pages 831–840, 2012.

[17] Weber Z. A Ikogi Y Yoshida T Nonoyama N, Okazaki S. "Analysis of Oxigen-Transport Diffusion Resistance in Proton-Exchange-Membrane Fuel Cells". *Journal of The Electrochemical Society, 158*, pages 416–423, 2011.

Appendix A

Initial experiment

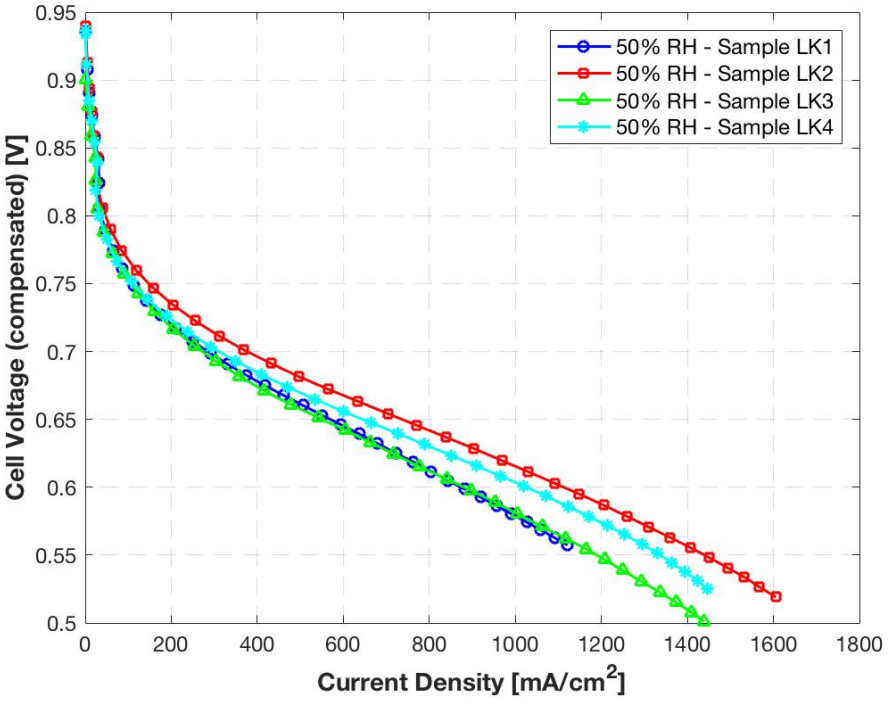

Figure A.1: Samples LK 50% Relative Humidity

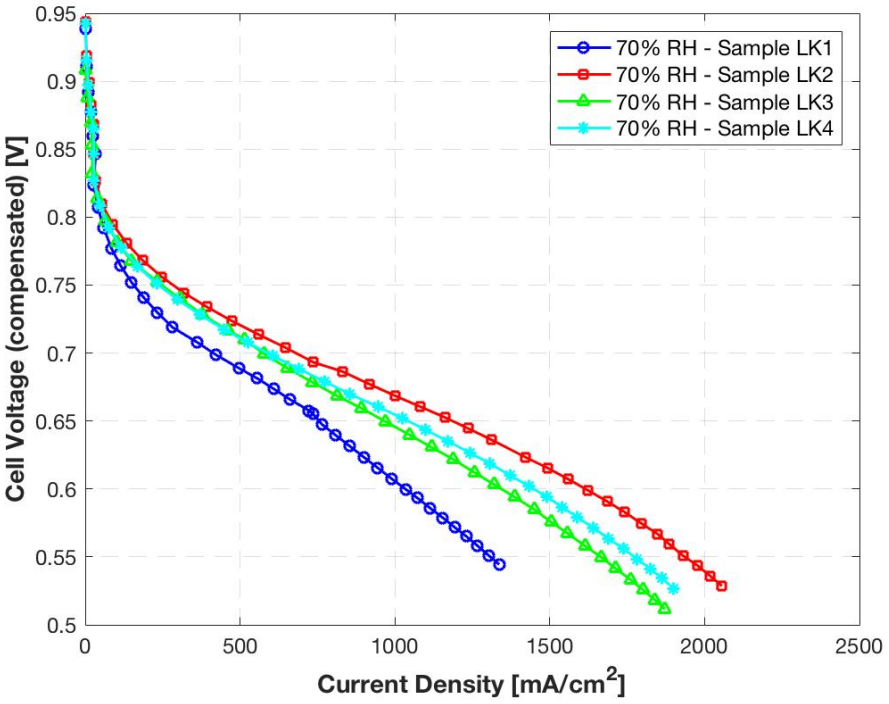

Figure A.2: Samples LK 70% Relative Humidity

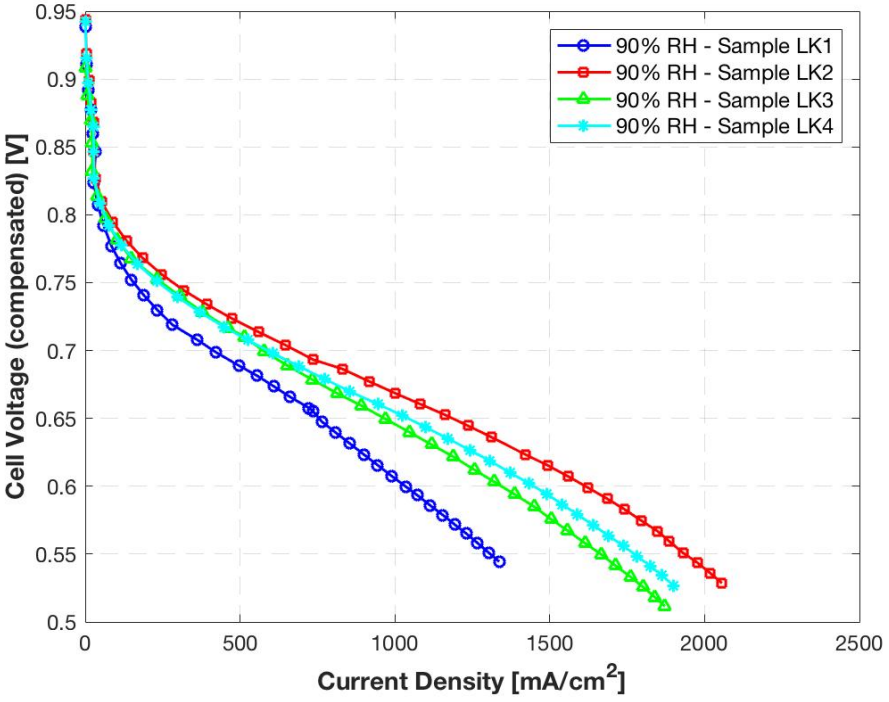

Figure A.3: Samples LK 90% Relative Humidity

Appendix B

Samples results

B.0.1 Pt loading effect in the anode side

Polarization curves first printing

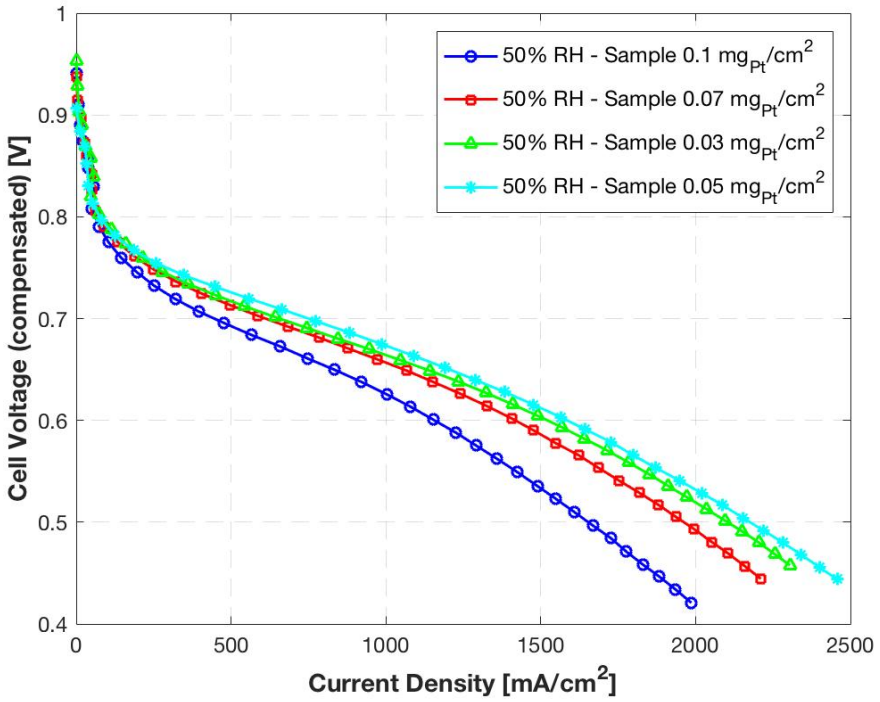

Figure B.1: First Samples comparative 50%RH. Anode side.

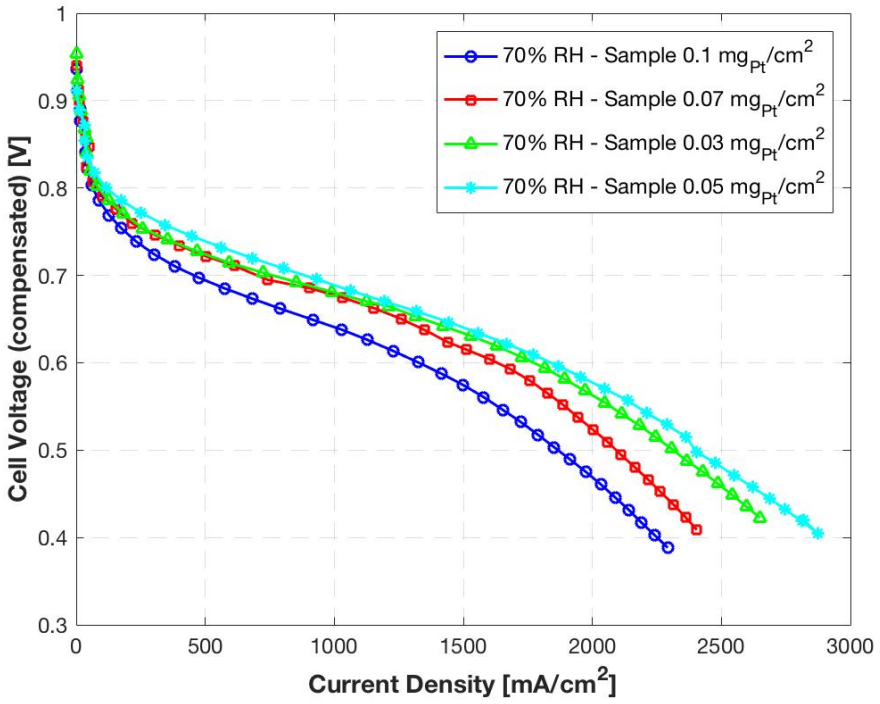

Figure B.2: First Samples comparative 70%RH. Anode side.

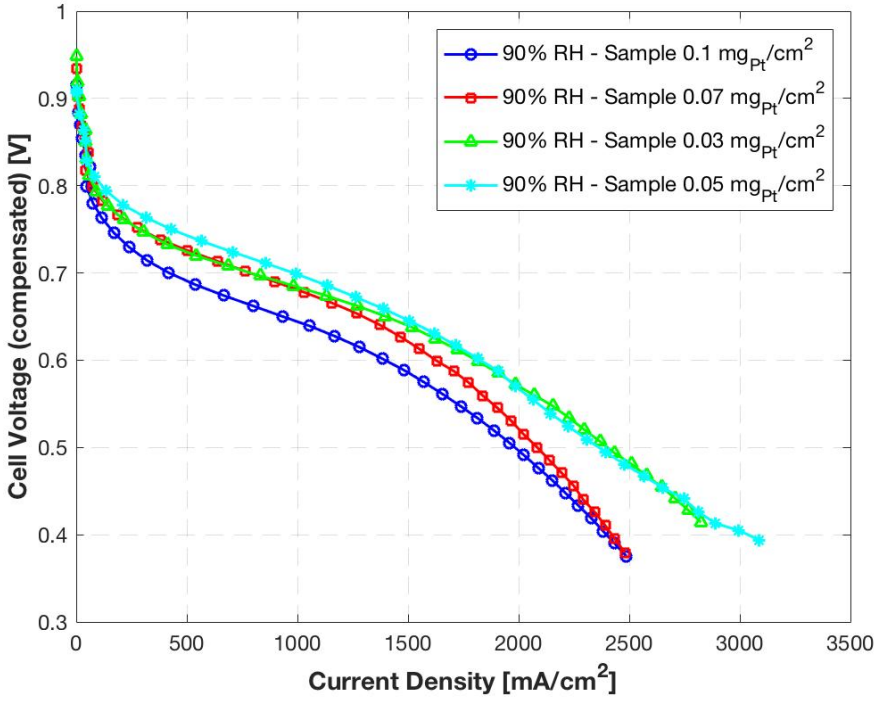

Figure B.3: First Samples comparative 90%RH. Anode side.

Polarization curves second printing

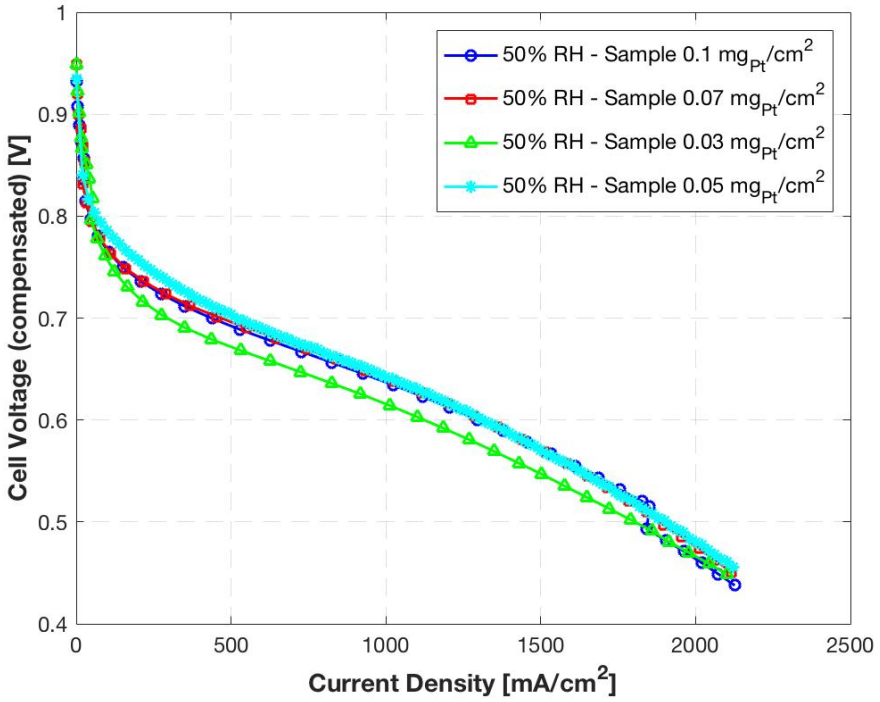

Figure B.4: Second Samples comparative 50%RH. Anode side.

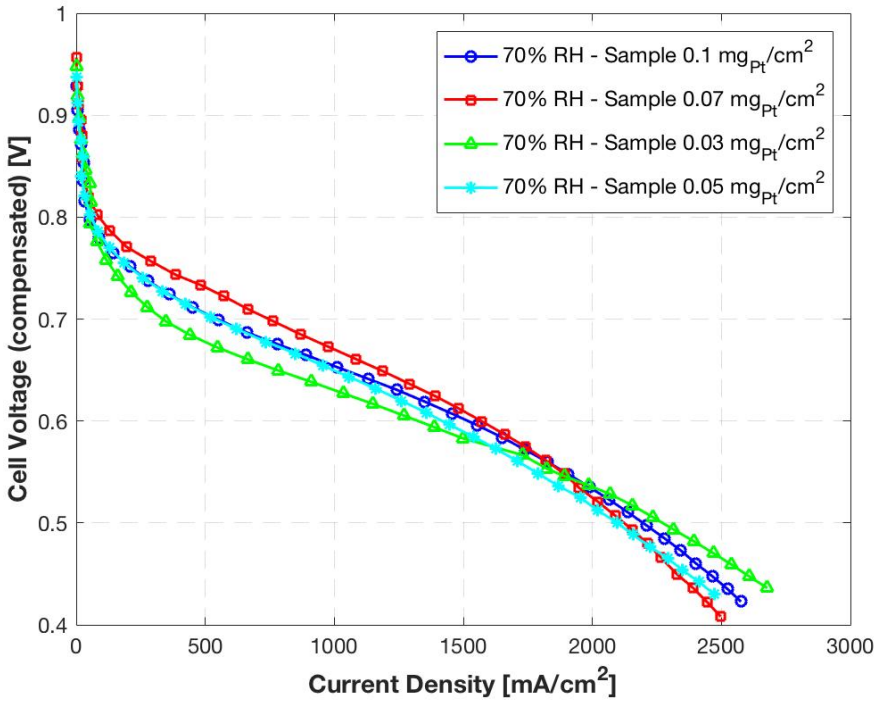

Figure B.5: Second Samples comparative 70%RH. Anode side.

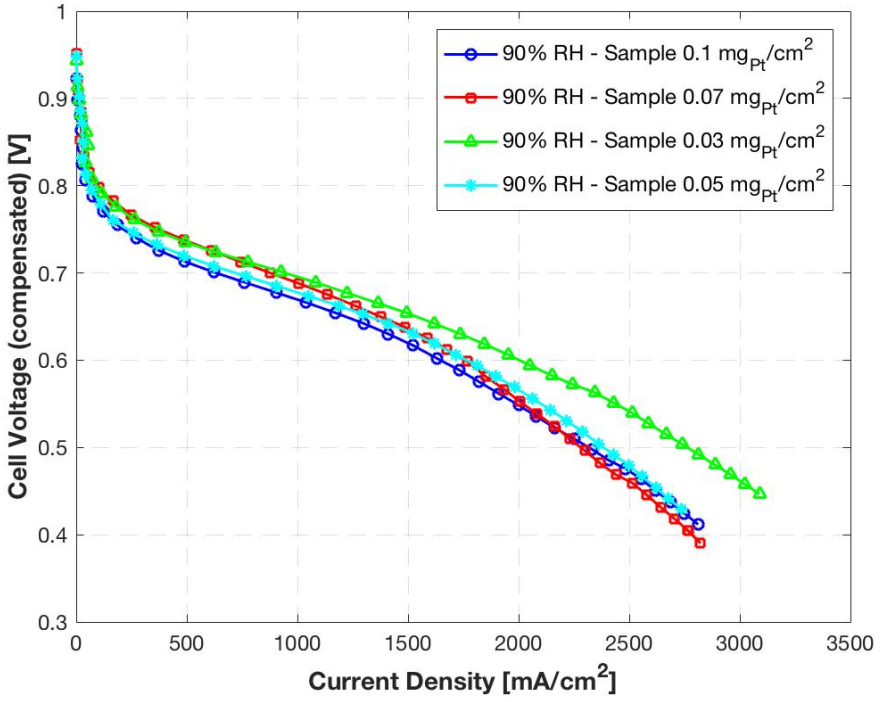

Figure B.6: Second Samples comparative 90%RH. Anode side.

Cell voltage - Pt loading study first printing

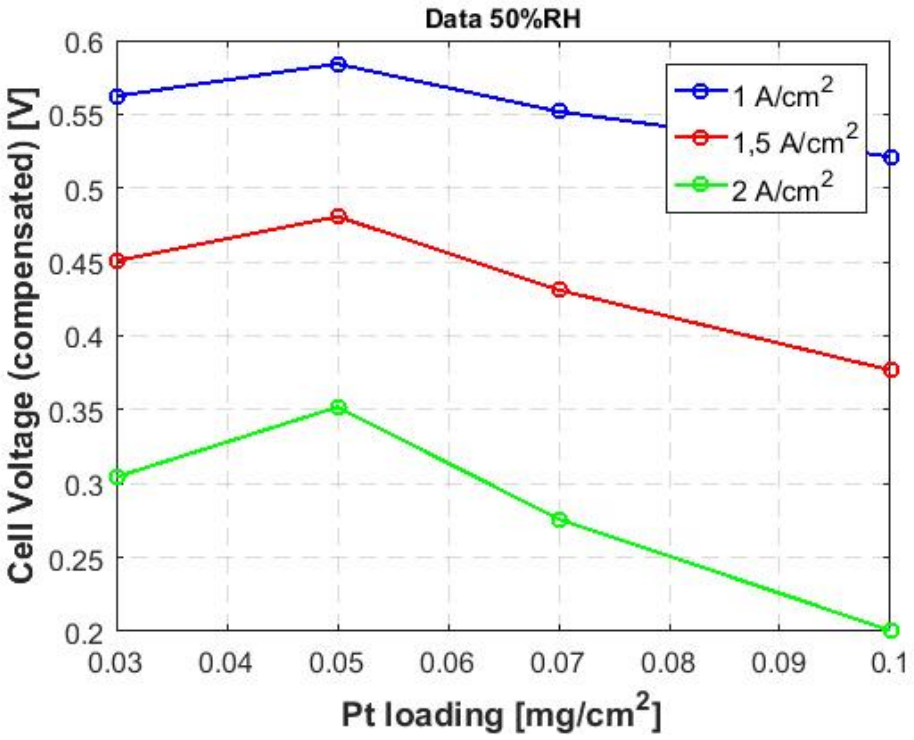

Figure B.7: Cell Voltage - Pt Loading 50% RH. First printing. Anode side.

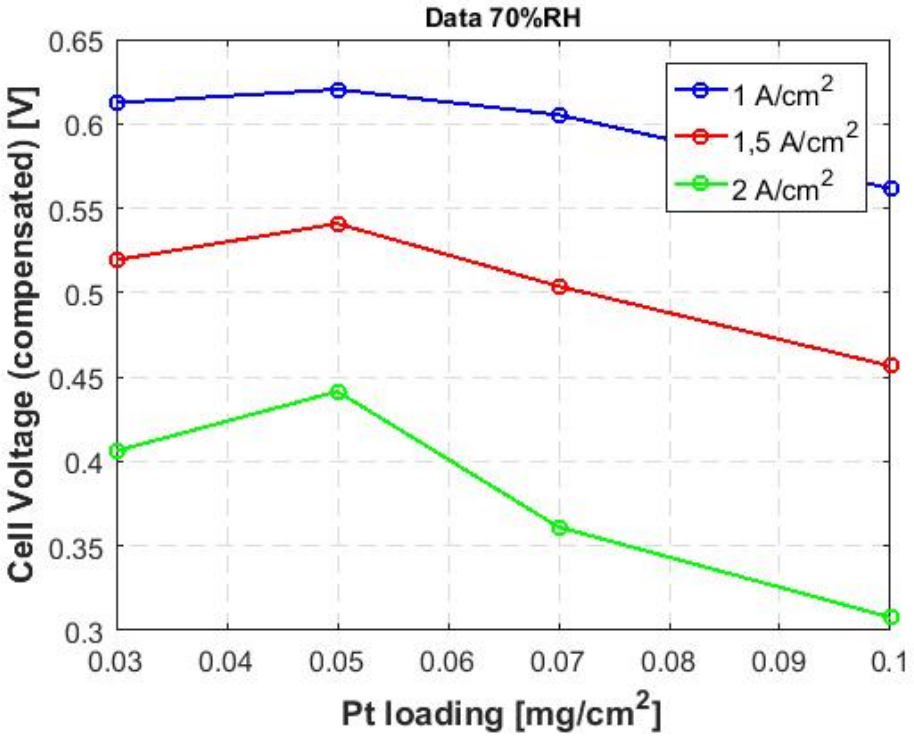

Figure B.8: Cell Voltage - Pt Loading 70% RH. First printing. Anode side.

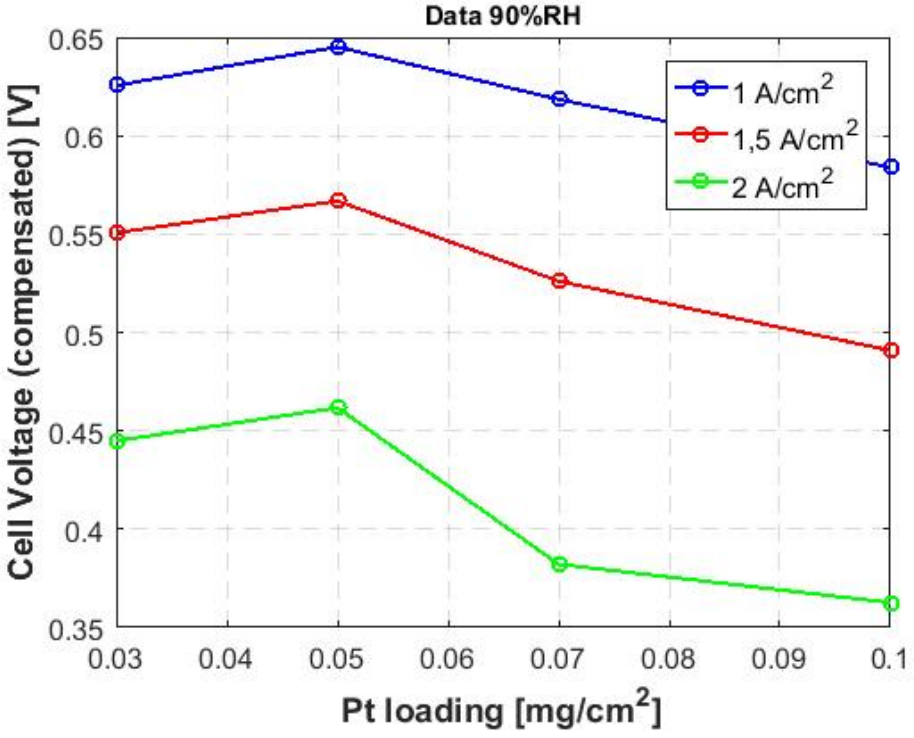

Figure B.9: Cell Voltage - Pt Loading 90% RH. First printing. Anode side.

Cell resistance first printing

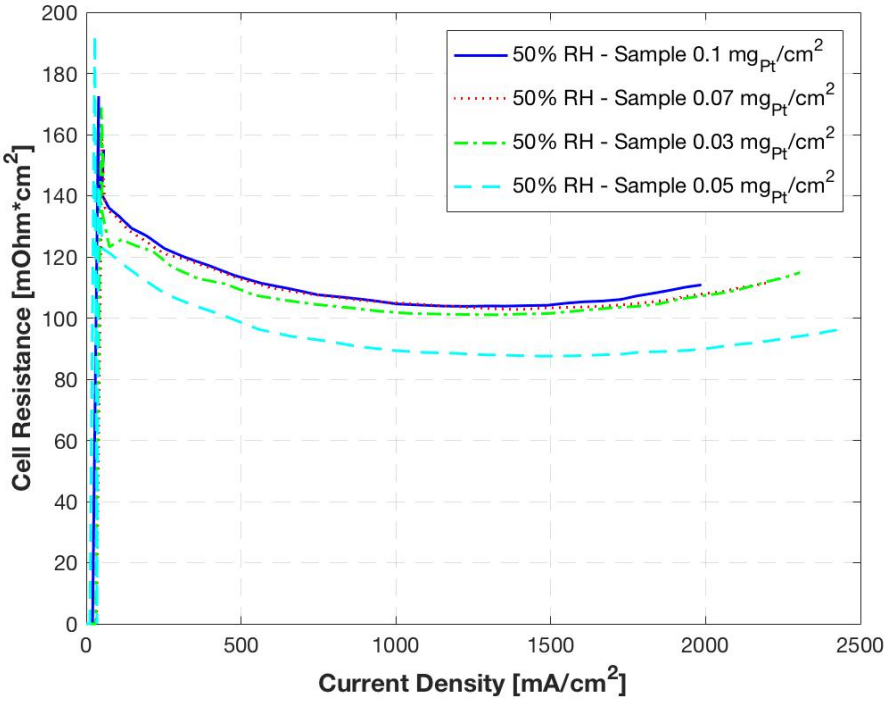

Figure B.10: Cell resistance 50% RH. First printing. Anode side.

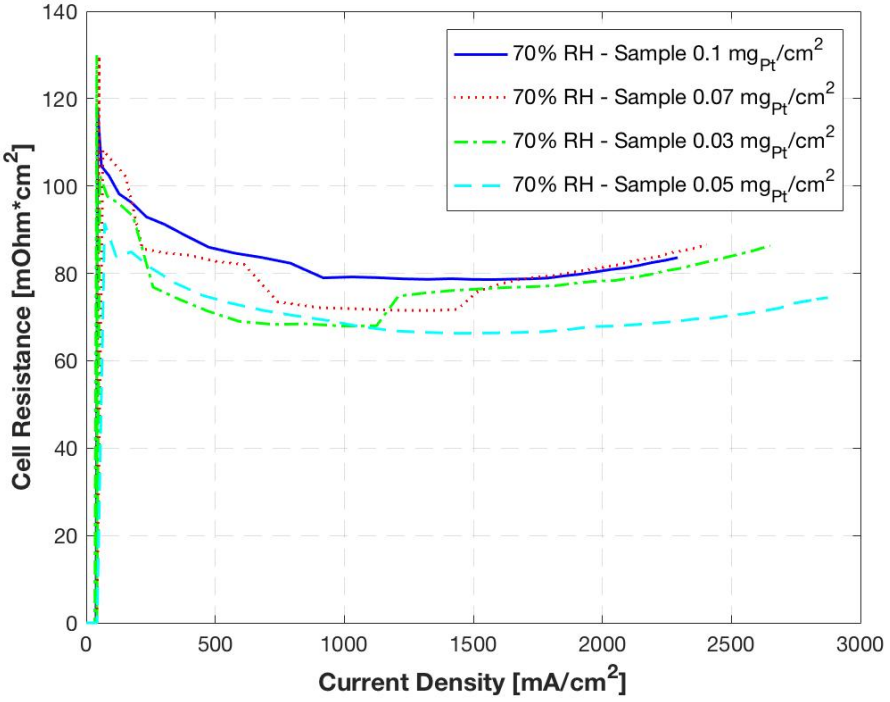

Figure B.11: Cell resistance 70% RH. First printing. Anode side.

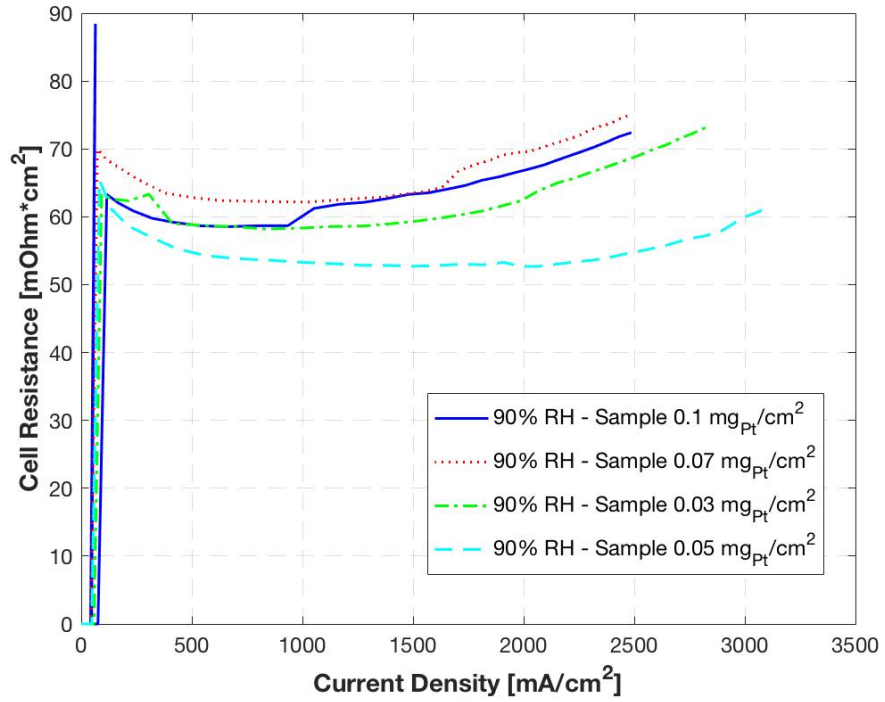

Figure B.12: Cell resistance 90% RH. First printing. Anode side.

Cell resistance second printing

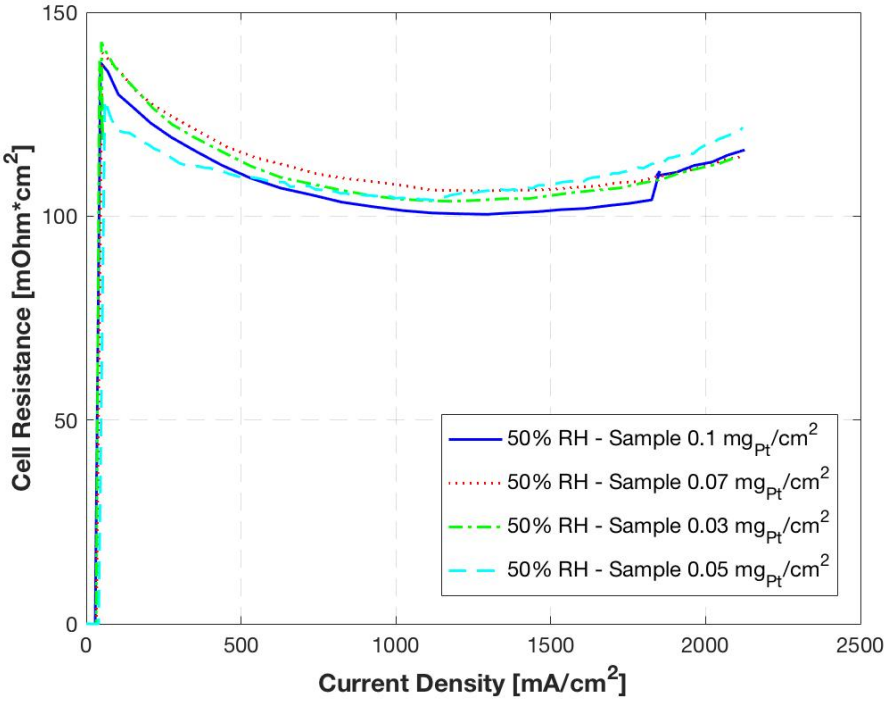

Figure B.13: Cell resistance 50% RH. Second printing. Anode side.

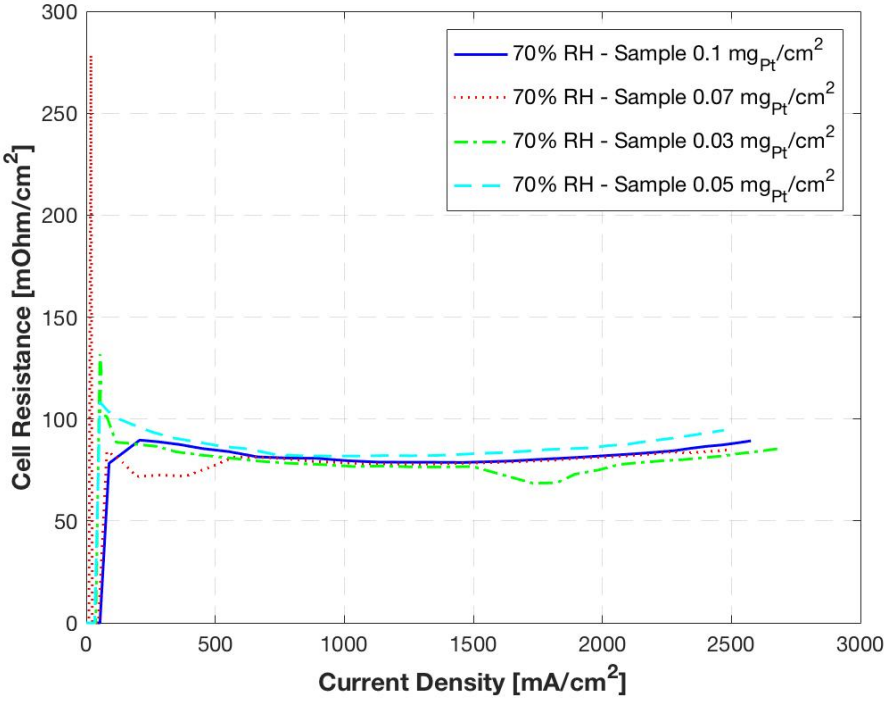

Figure B.14: Cell resistance 70% RH. Second printing. Anode side.

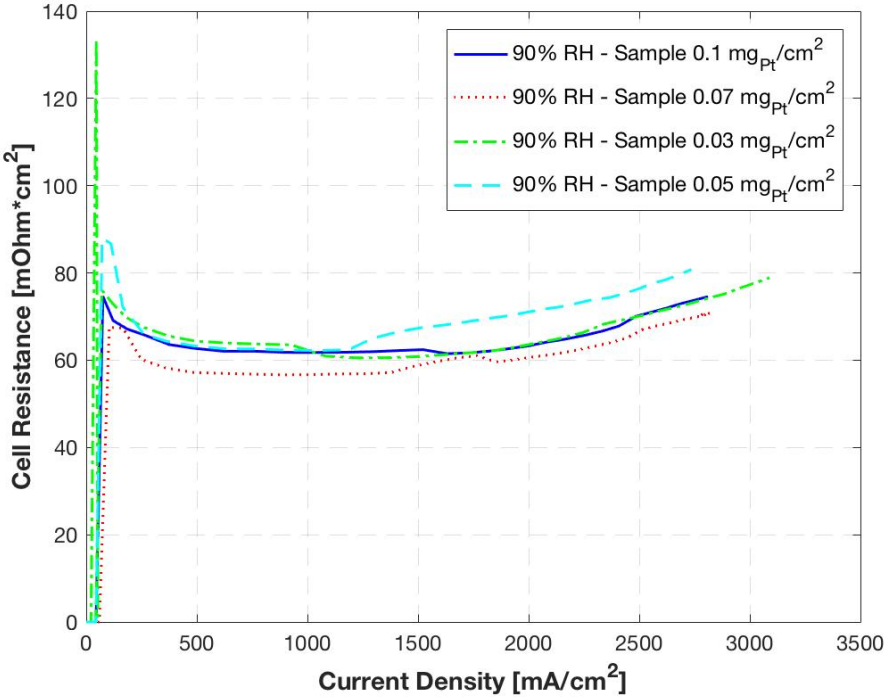

Figure B.15: Cell resistance 90% RH. Second printing. Anode side.

Comparative 0,1 mg

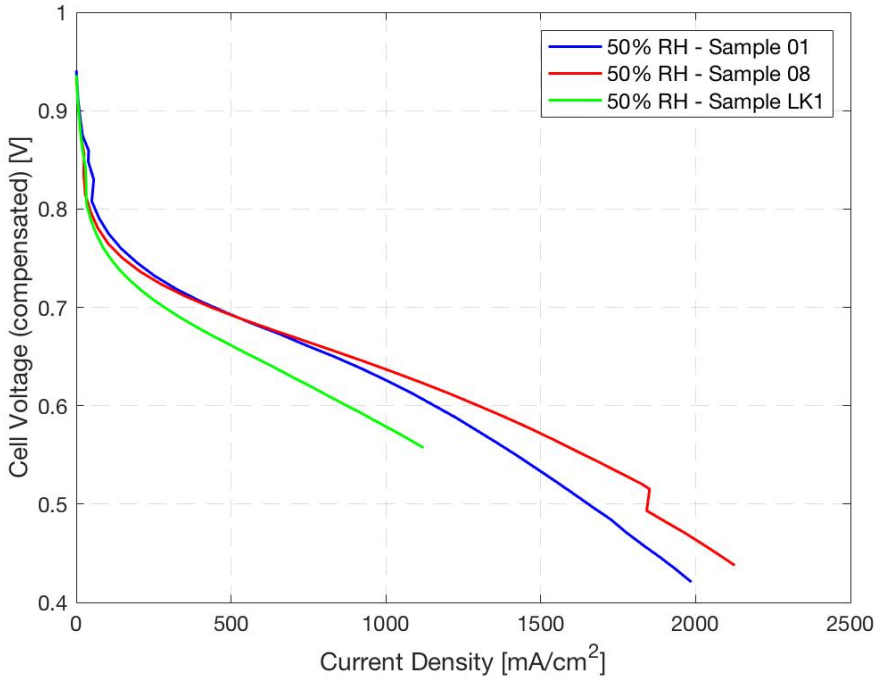

Figure B.16: 0.1 mg_{Pt}/cm^2 Pt loading comparative samples at 50% RH. Anode side.

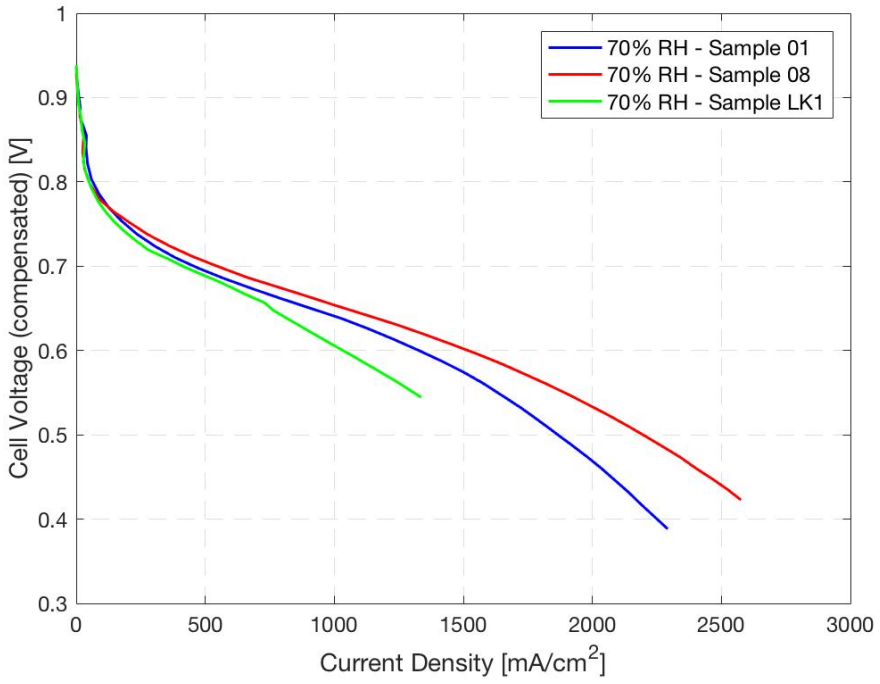

Figure B.17: 0.1 mg_{Pt}/cm^2 Pt loading comparative samples at 70% RH. Anode side.

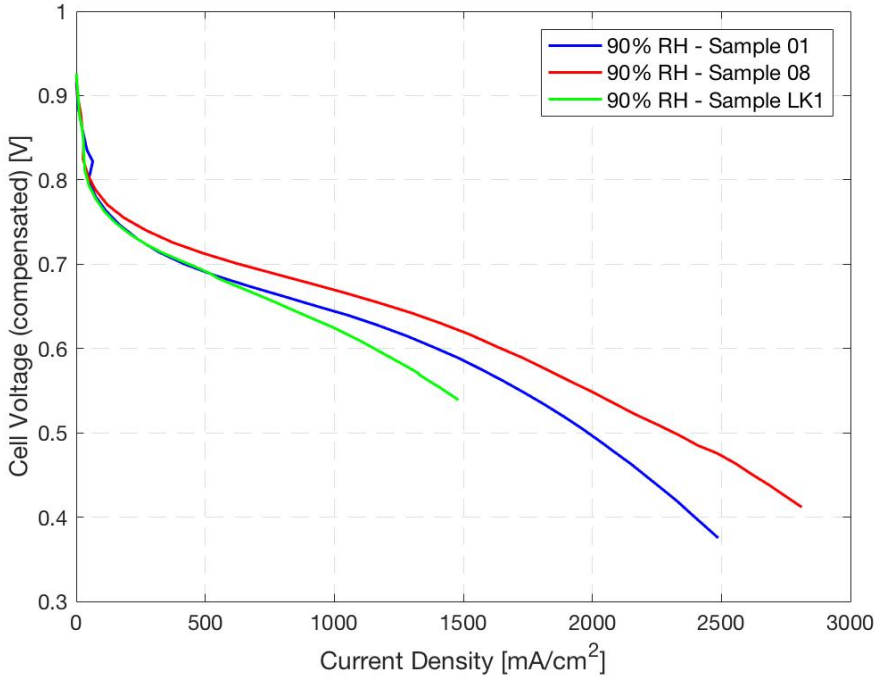

Figure B.18: 0.1 mg_{Pt}/cm^2 Pt loading comparative samples at 90% RH. Anode side.

Comparative 0,07 mg

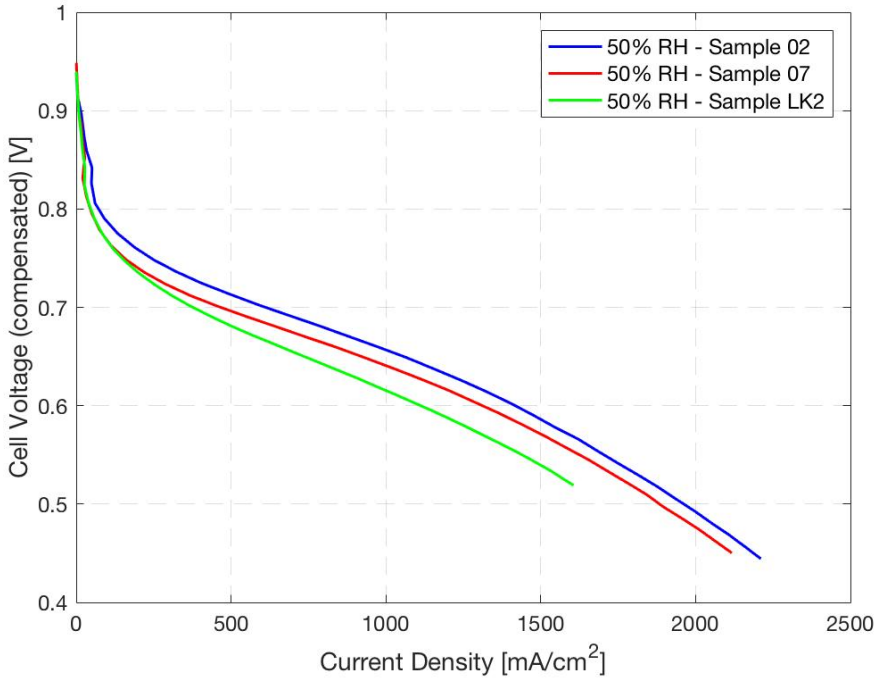

Figure B.19: 0.07 mg_{Pt}/cm^2 Pt loading comparative samples at 50% RH. Anode side.

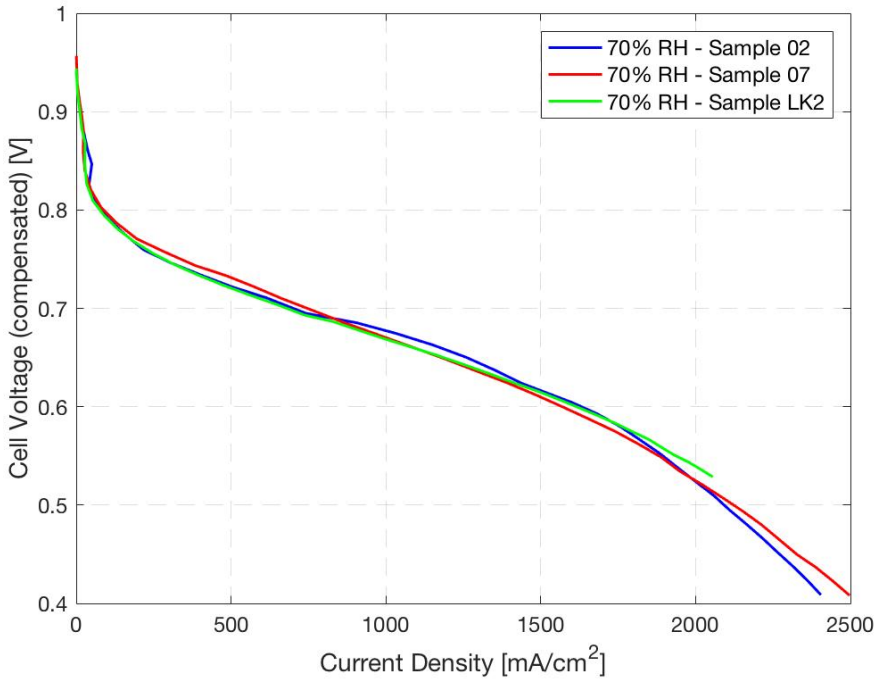

Figure B.20: 0.07 mg_{Pt}/cm^2 Pt loading comparative samples at 70% RH. Anode side.

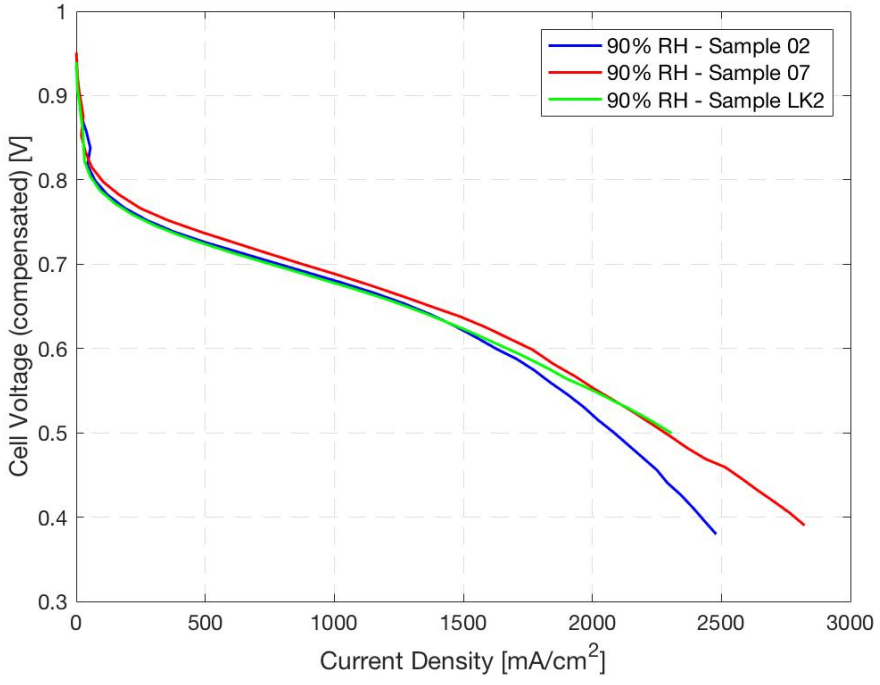

Figure B.21: 0.07 mg_{Pt}/cm^2 Pt loading comparative samples at 90% RH. Anode side.

Comparative 0,05 mg

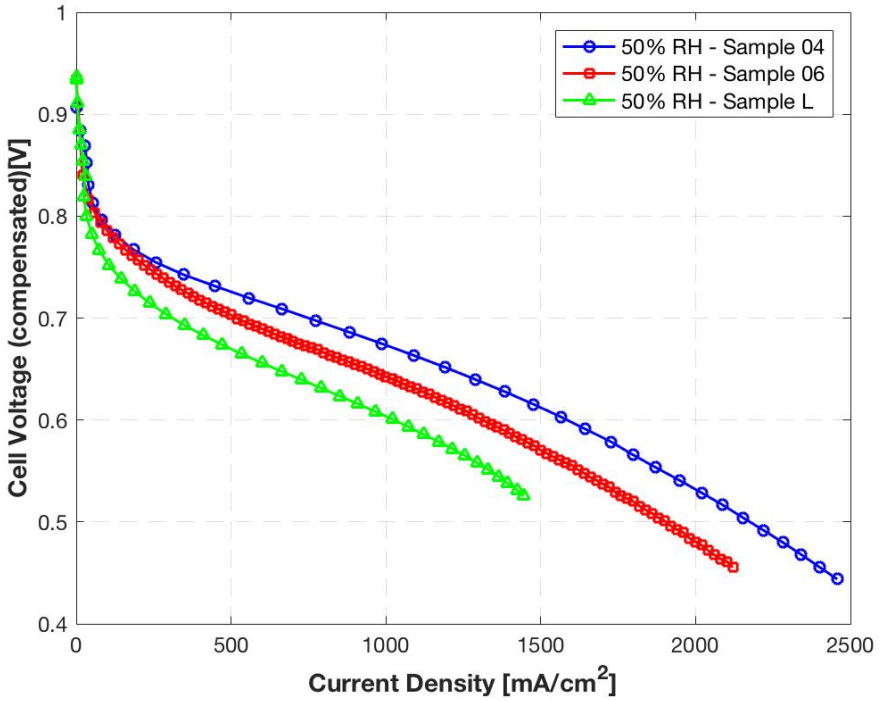

Figure B.22: 0.05 mg_{Pt}/cm^2 Pt loading comparative samples at 50% RH. Anode side.

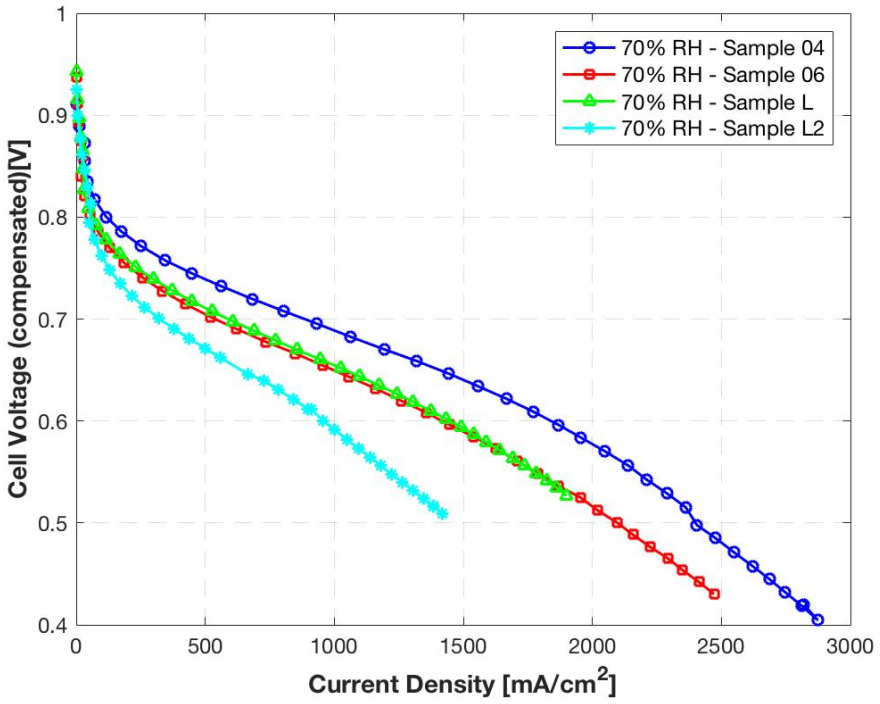

Figure B.23: 0.05 mg_{Pt}/cm^2 Pt loading comparative samples at 70% RH. Anode side.

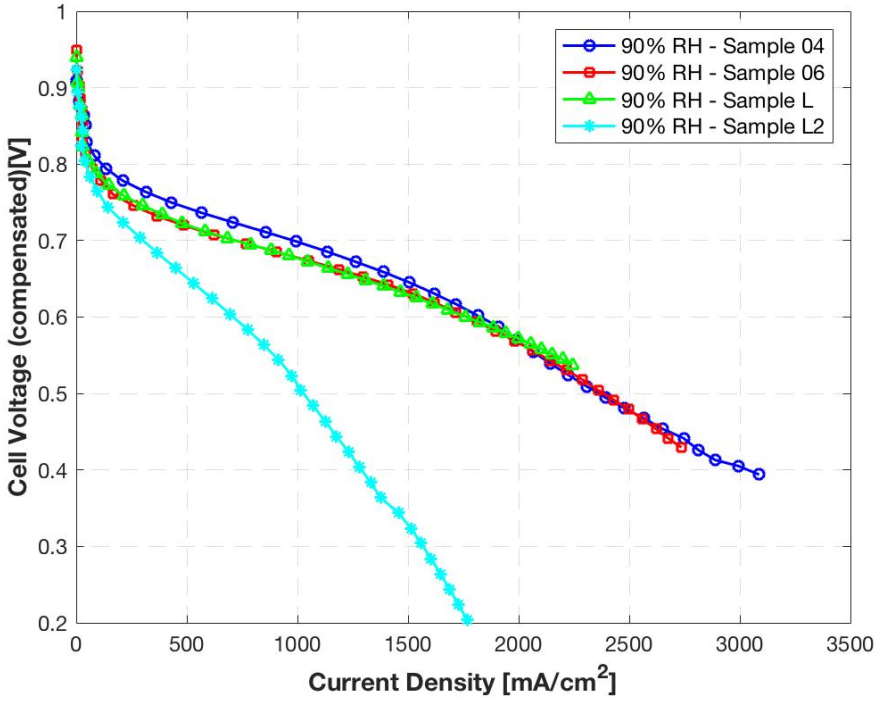

Figure B.24: 0.05 mg_{Pt}/cm^2 Pt loading comparative samples at 90% RH. Anode side.

Comparative 0,03 mg

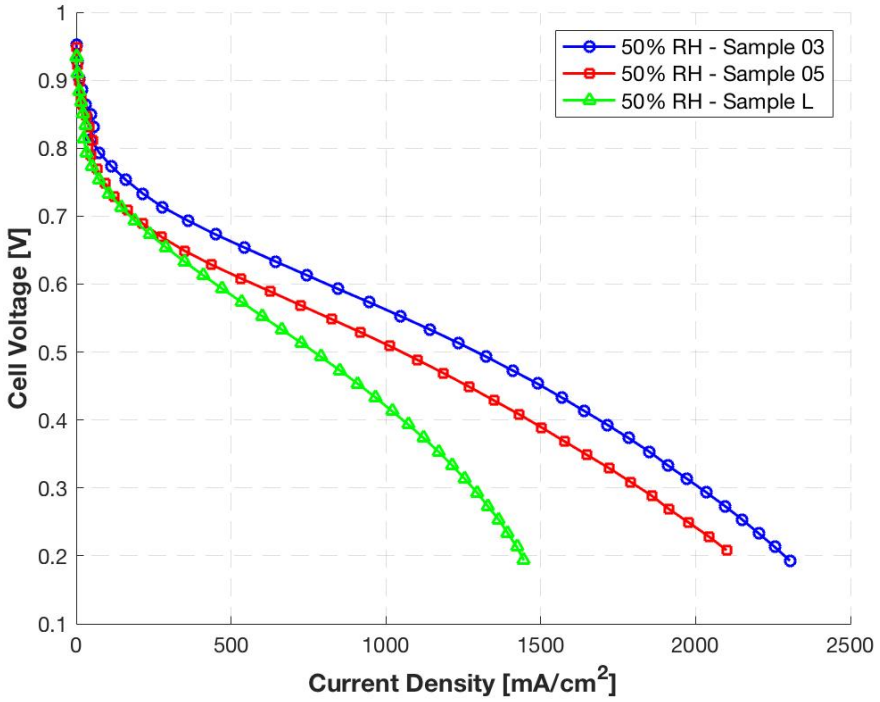

Figure B.25: 0.03 mg_{Pt}/cm^2 Pt loading comparative samples at 50% RH. Anode side.

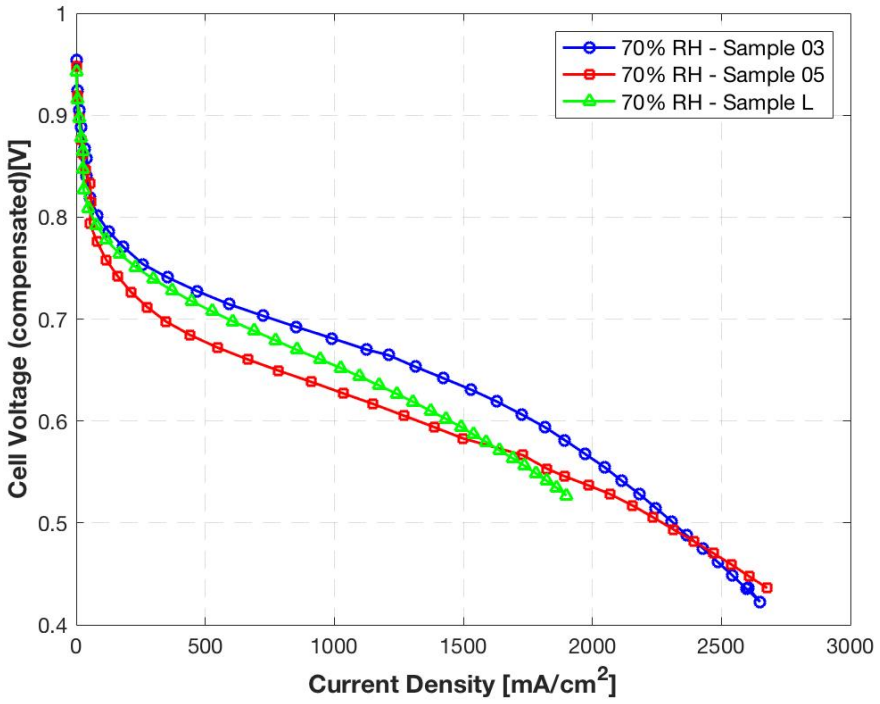

Figure B.26: 0.03 mg_{Pt}/cm^2 Pt loading comparative samples at 70% RH. Anode side.

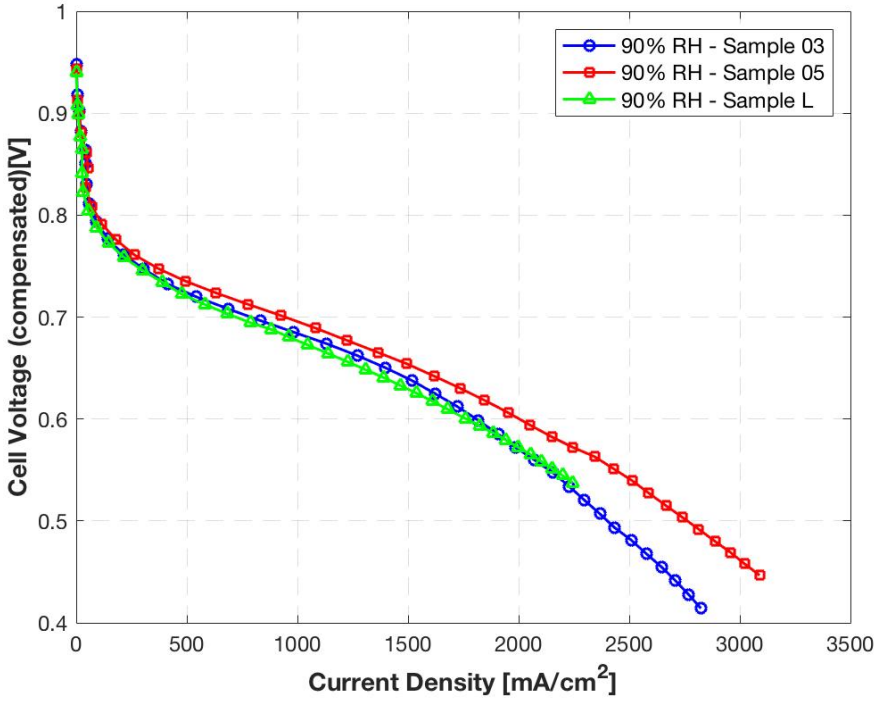

Figure B.27: 0.03 mg_{Pt}/cm^2 Pt loading comparative samples at 90% RH. Anode side.

Average by relative humidity

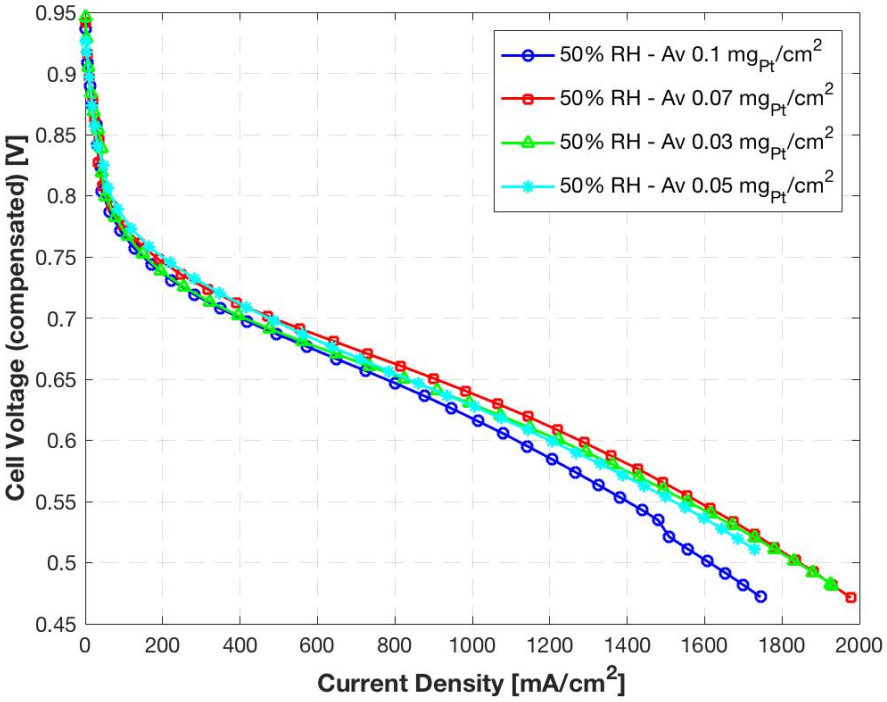

Figure B.28: Pt loading comparative samples at 50% RH. Anode side.

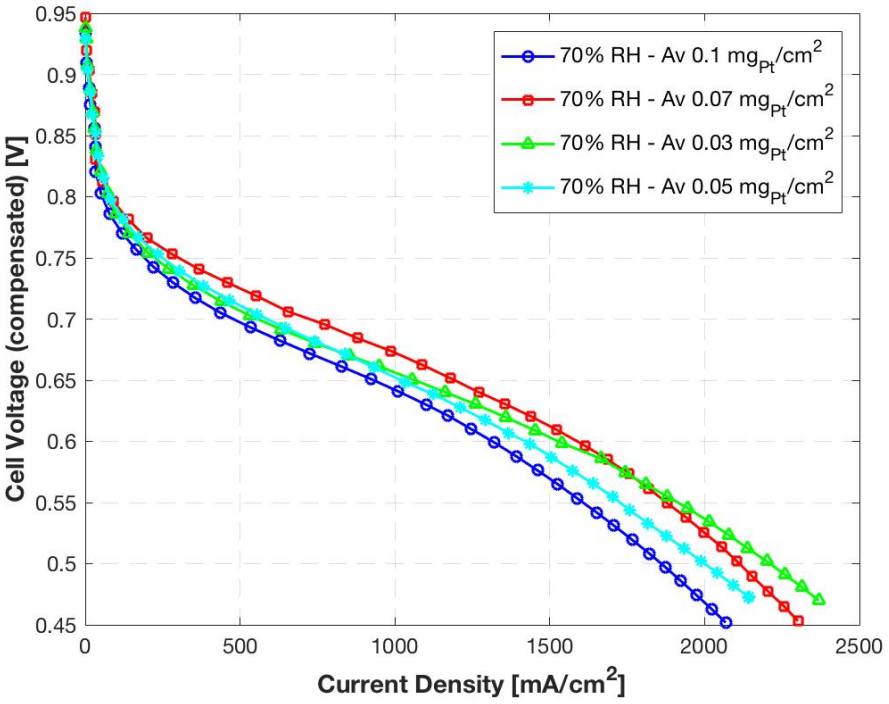

Figure B.29: Pt loading comparative samples at 70% RH. Anode side.

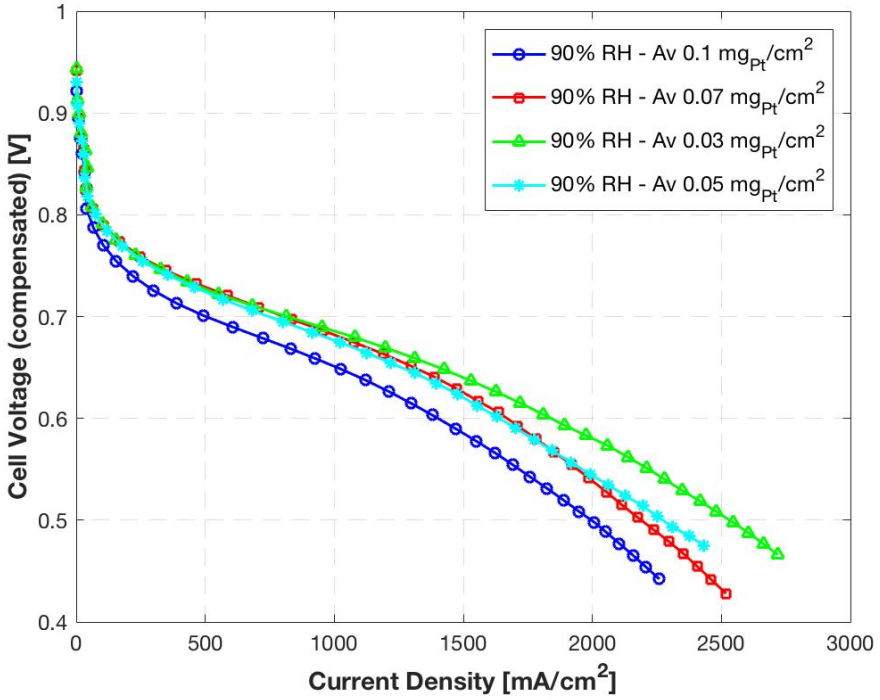

Figure B.30: Pt loading comparative samples at 90% RH. Anode side.

B.0.2 Pt loading effect in the cathode side

Cell voltage - Pt loading study first printing

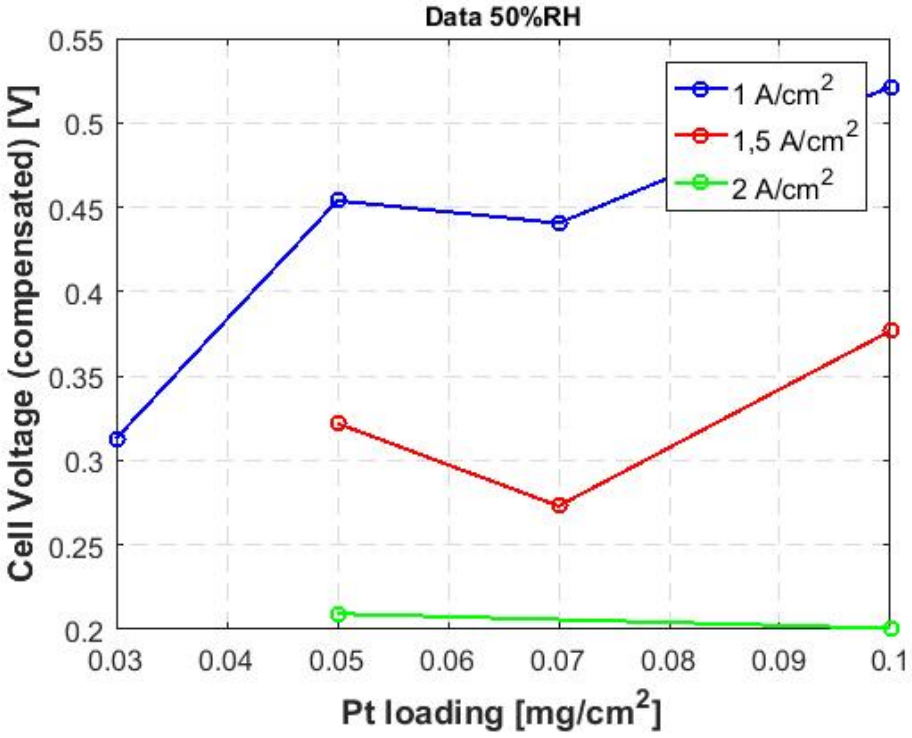

Figure B.31: Cell Voltage - Pt Loading 50% RH. First printing. Cathode side.

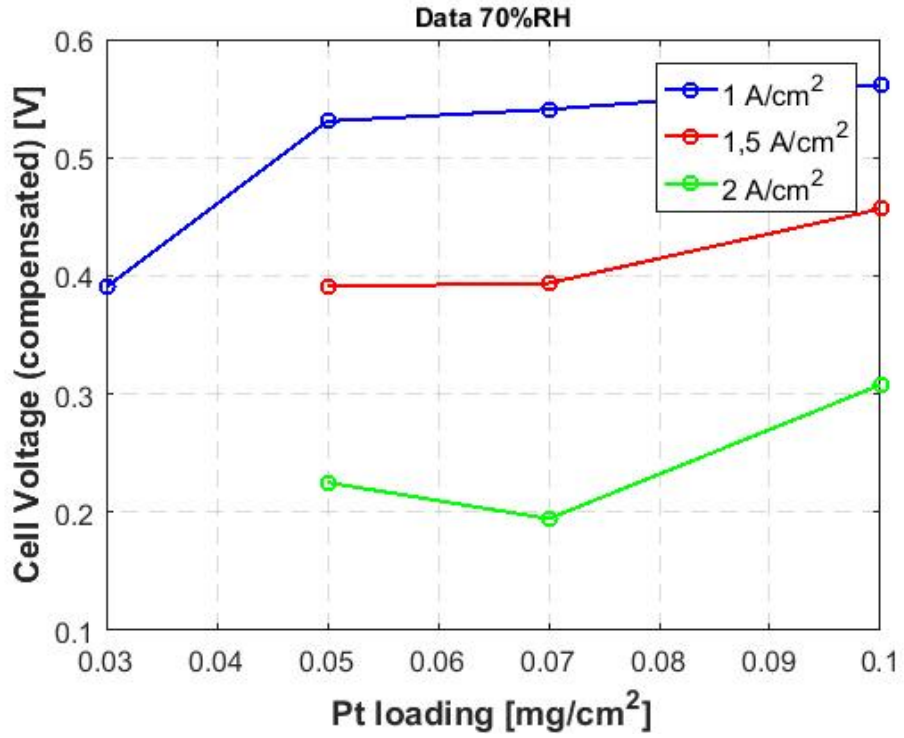

Figure B.32: Cell Voltage - Pt Loading 70% RH. First printing. Cathode side.

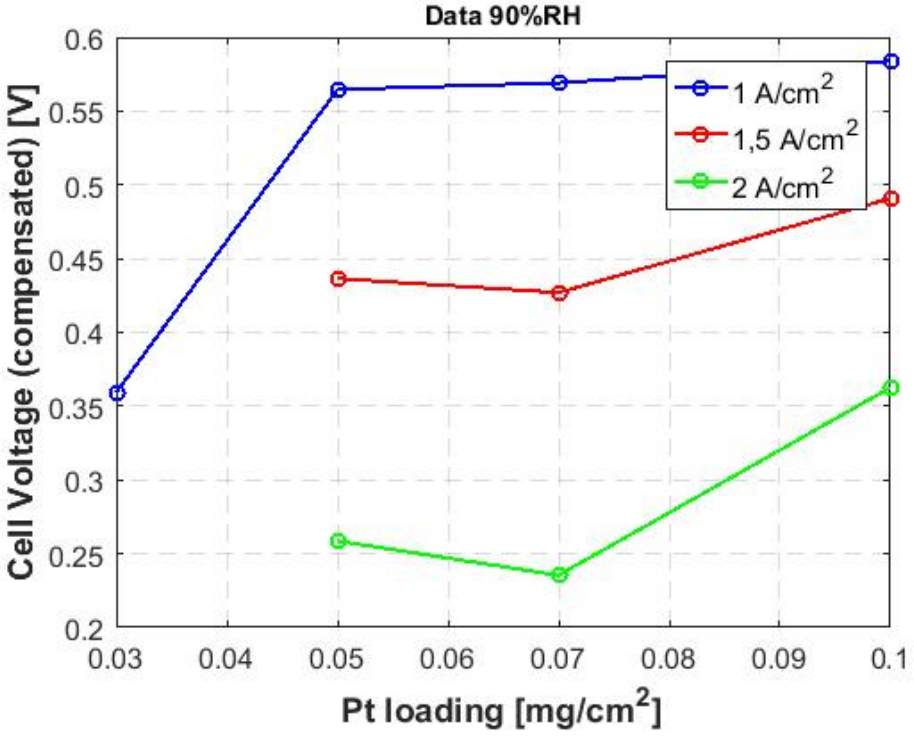

Figure B.33: Cell Voltage - Pt Loading 90% RH. First printing. Cathode side.

Cell resistance first printing

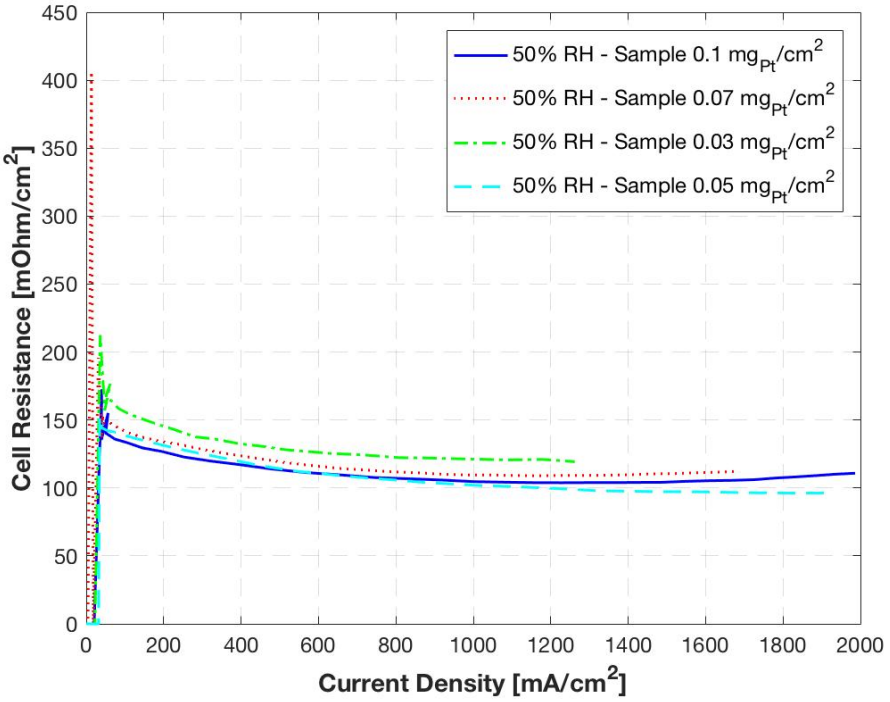

Figure B.34: Cell resistance 50% RH. First printing. Cathode side.

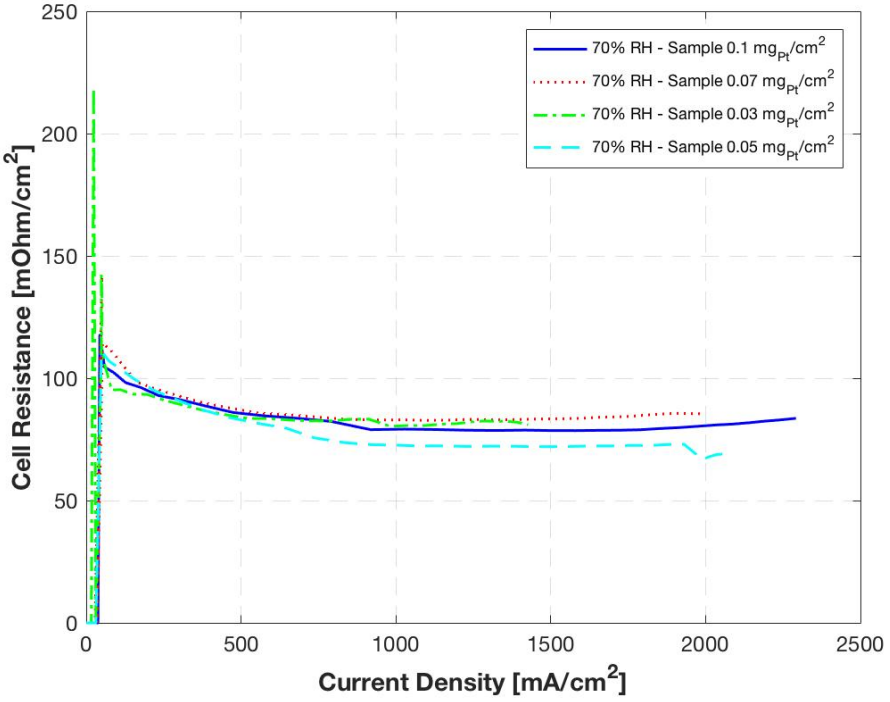

Figure B.35: Cell resistance 70% RH. First printing. Cathode side.

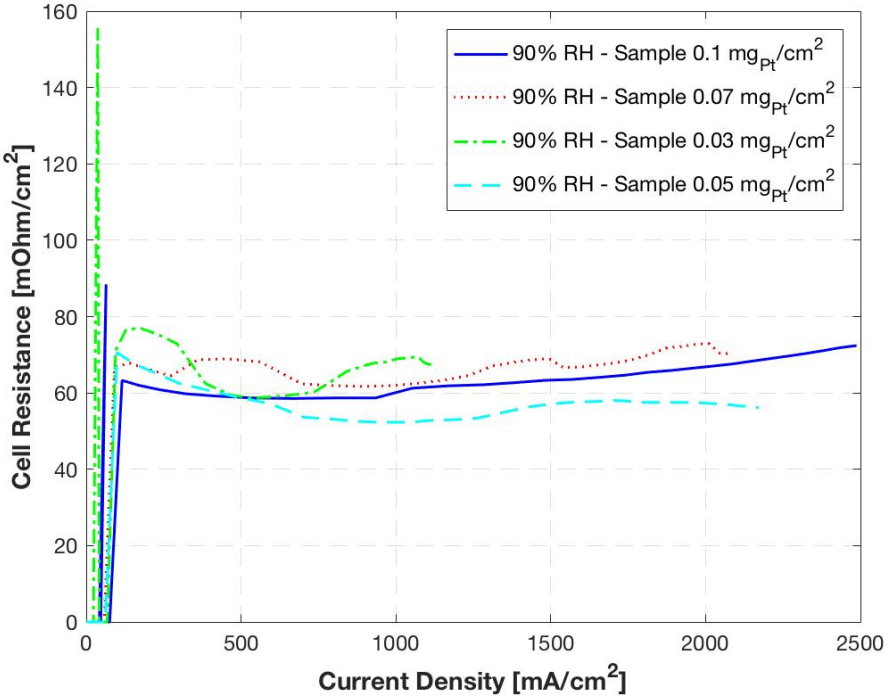

Figure B.36: Cell resistance 90% RH. First printing. Cathode side.

Cell resistance second printing

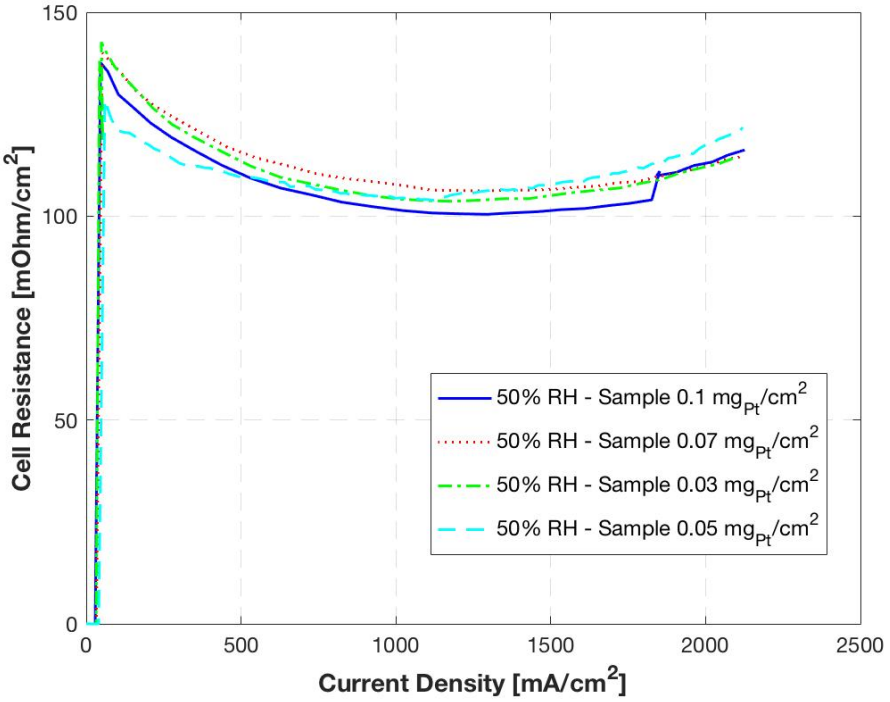

Figure B.37: Cell resistance 50% RH. Second printing. Cathode side.

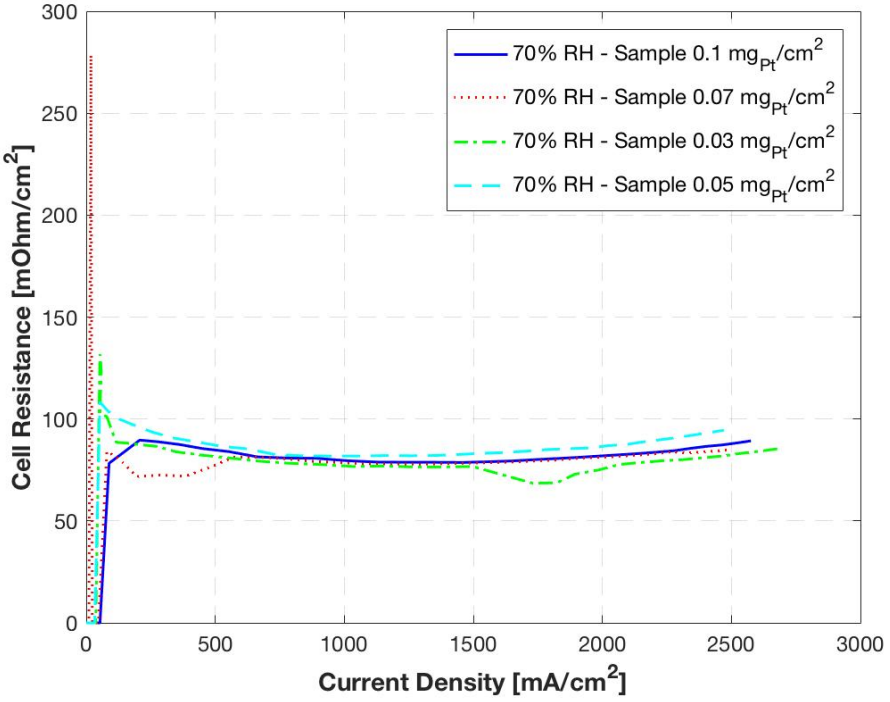

Figure B.38: Cell resistance 70% RH. Second printing. Cathode side.

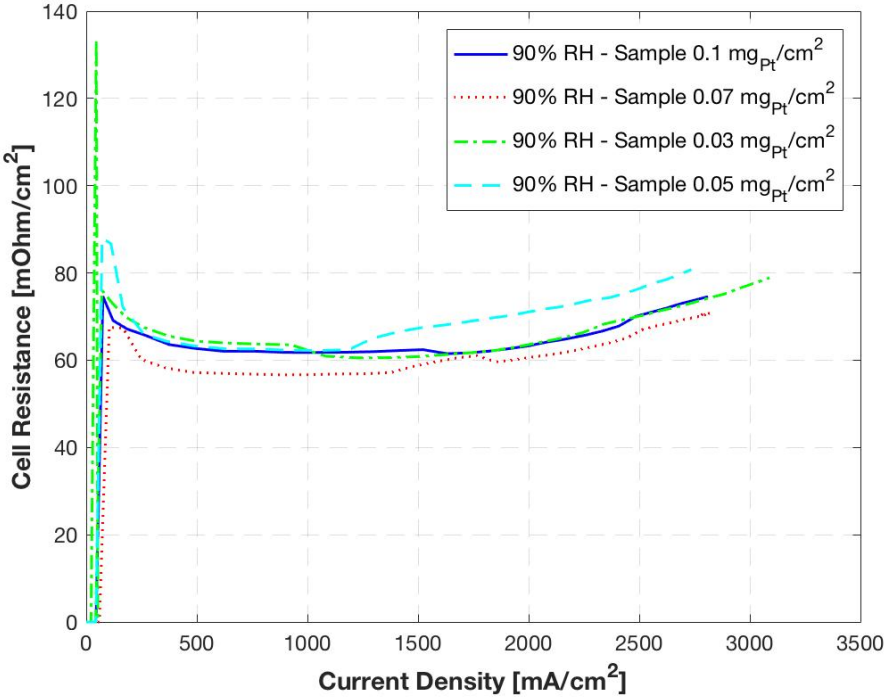

Figure B.39: Cell resistance 90% RH. Second printing. Cathode side.

Comparative 0,1 mg

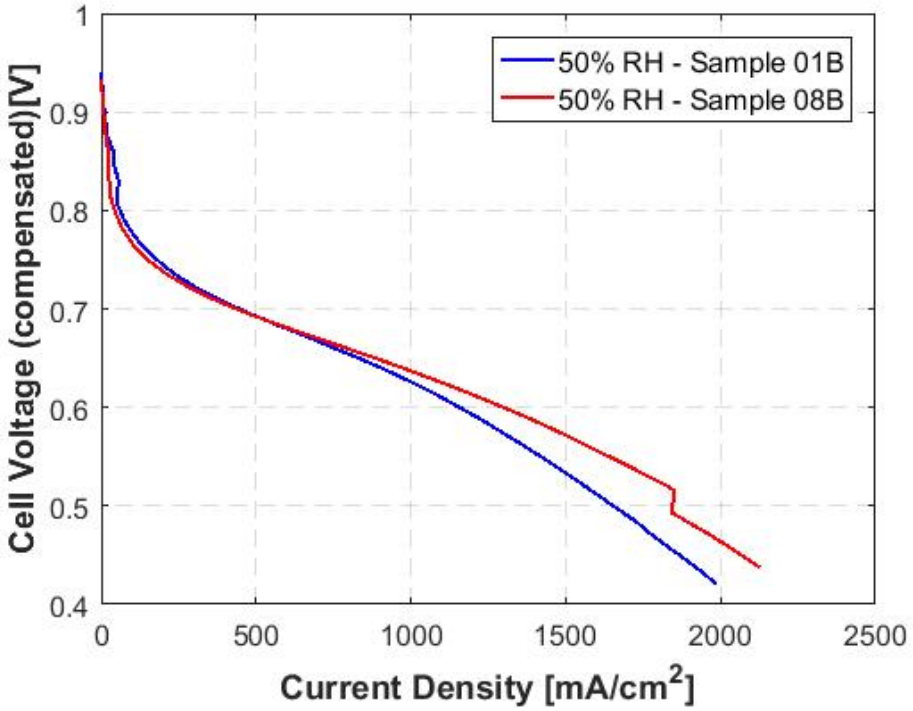

Figure B.40: 0.1 mg_{Pt}/cm^2 Pt loading comparative samples at 50% RH. Cathode side.

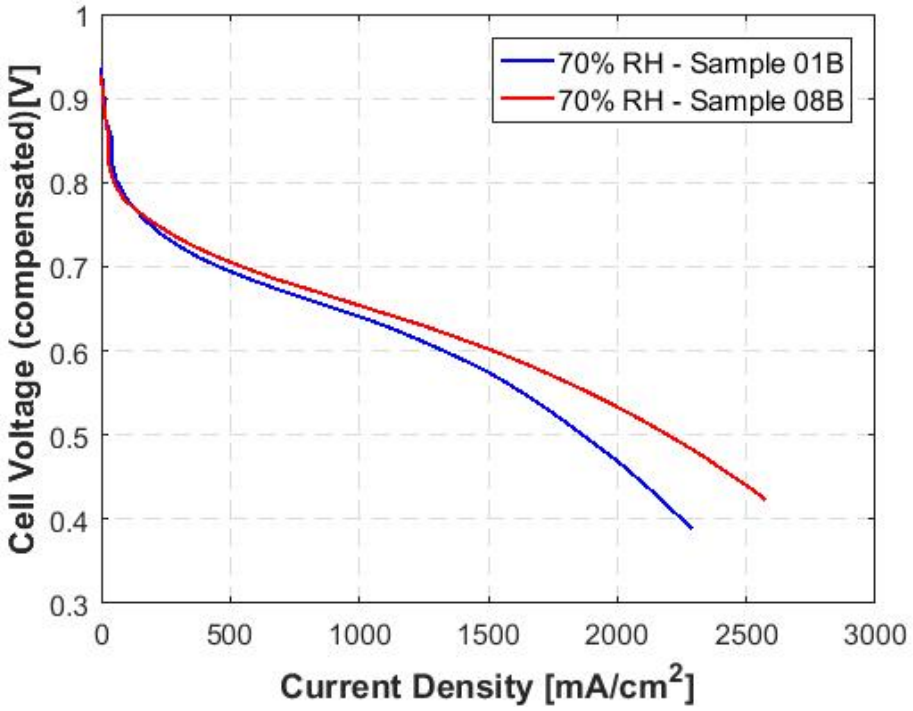

Figure B.41: 0.1 mg_{Pt}/cm^2 Pt loading comparative samples at 70% RH. Cathode side.

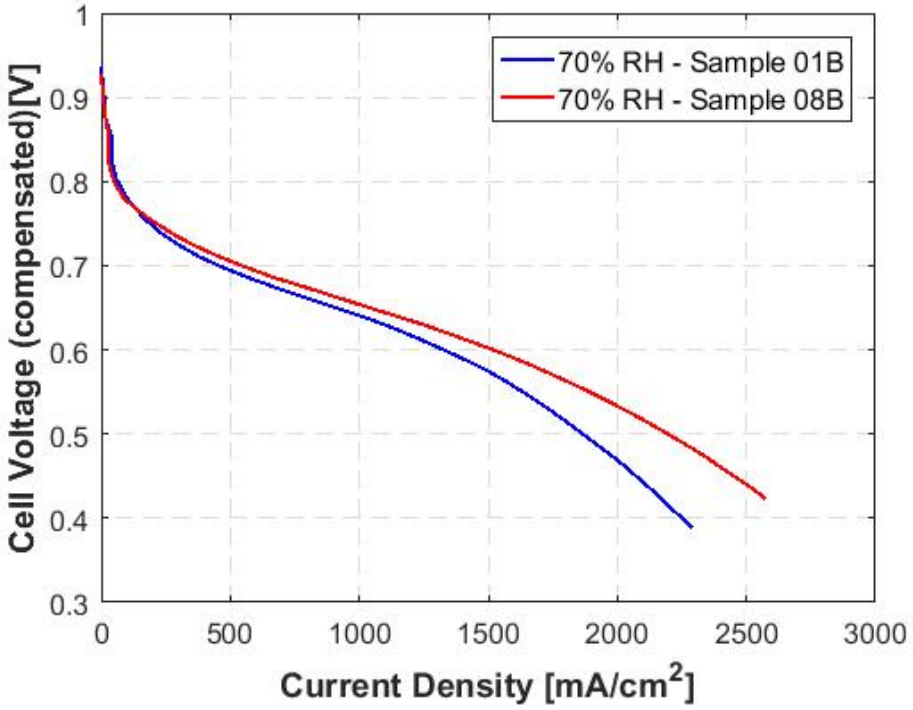

Figure B.42: 0.1 mg_{Pt}/cm^2 Pt loading comparative samples at 70% RH. Cathode side.

Comparative 0,07 mg

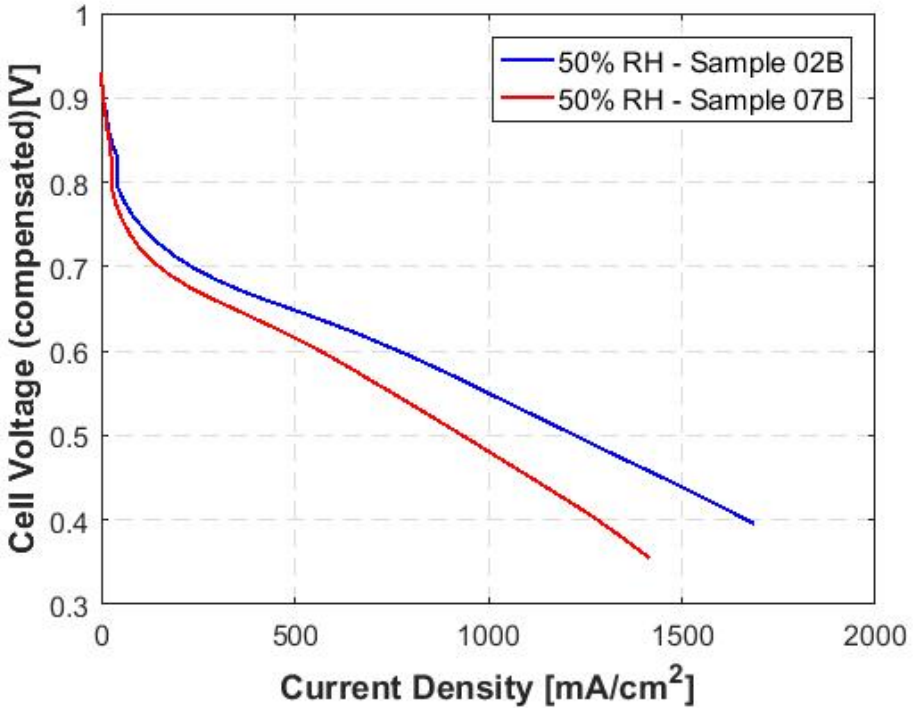

Figure B.43: 0.07 mg_{Pt}/cm^2 Pt loading comparative samples at 50% RH. Cathode side.

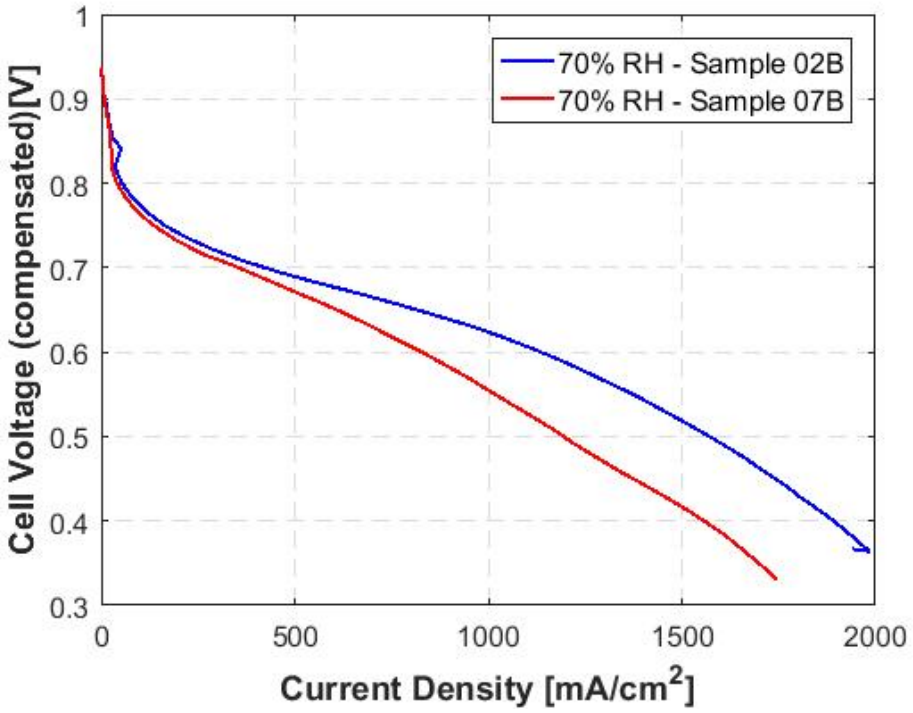

Figure B.44: 0.07 mg_{Pt}/cm^2 Pt loading comparative samples at 70% RH. Cathode side.

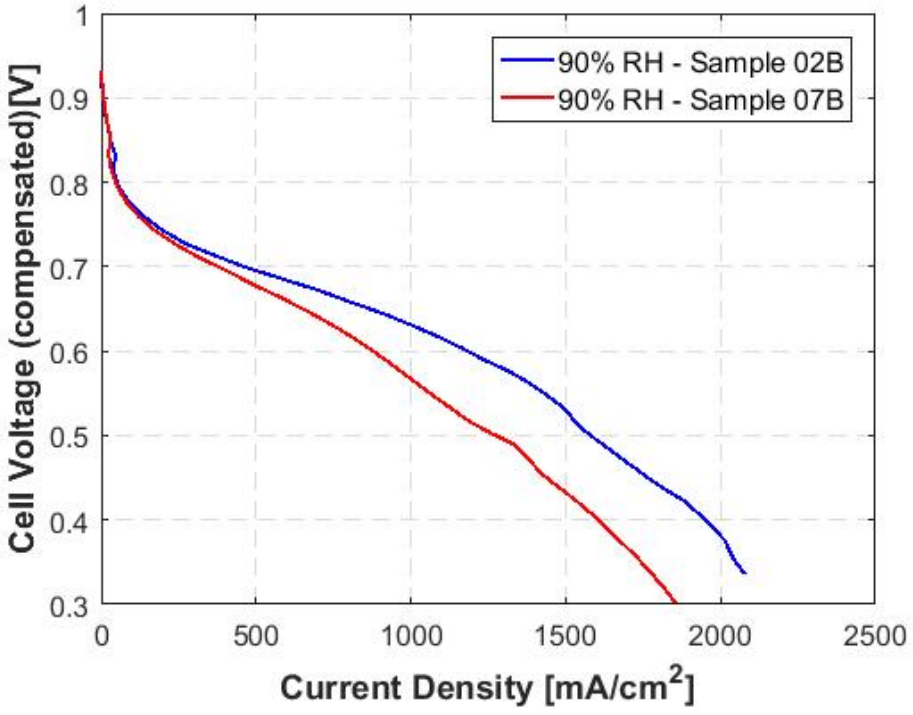

Figure B.45: 0.07 mg_{Pt}/cm^2 Pt loading comparative samples at 90% RH. Cathode side.

Comparative 0,05 mg

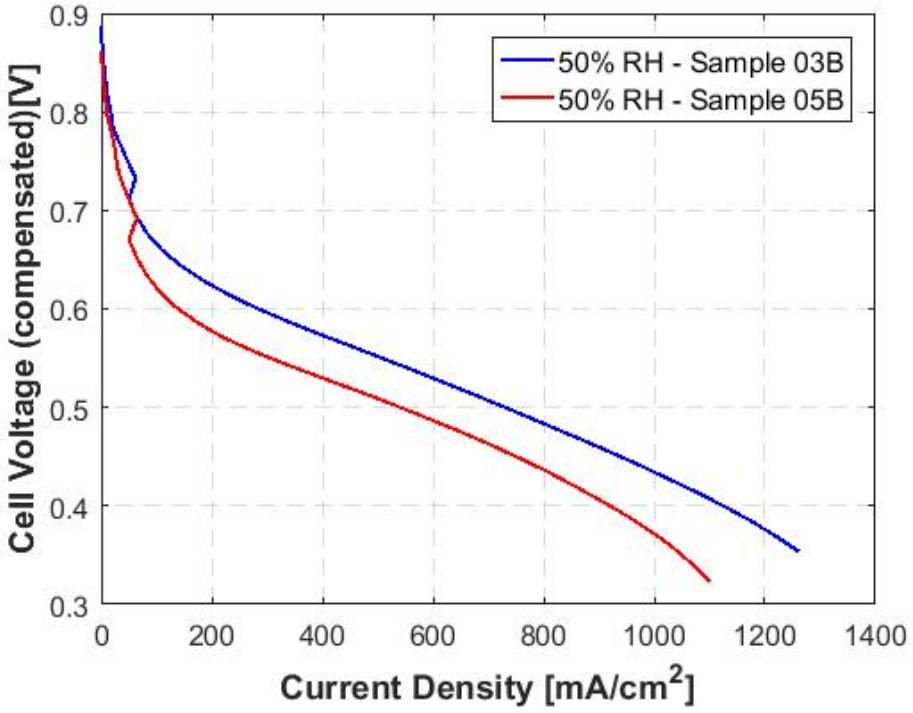

Figure B.46: 0.05 mg_{Pt}/cm^2 Pt loading comparative samples at 50% RH. Cathode side.

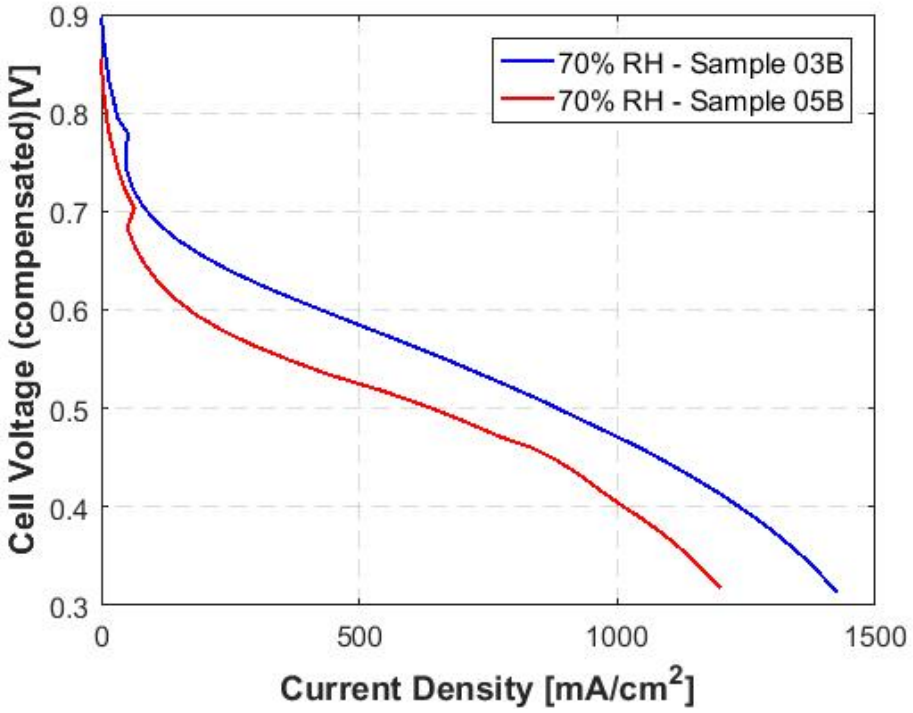

Figure B.47: 0.05 mg_{Pt}/cm^2 Pt loading comparative samples at 70% RH. Cathode side.

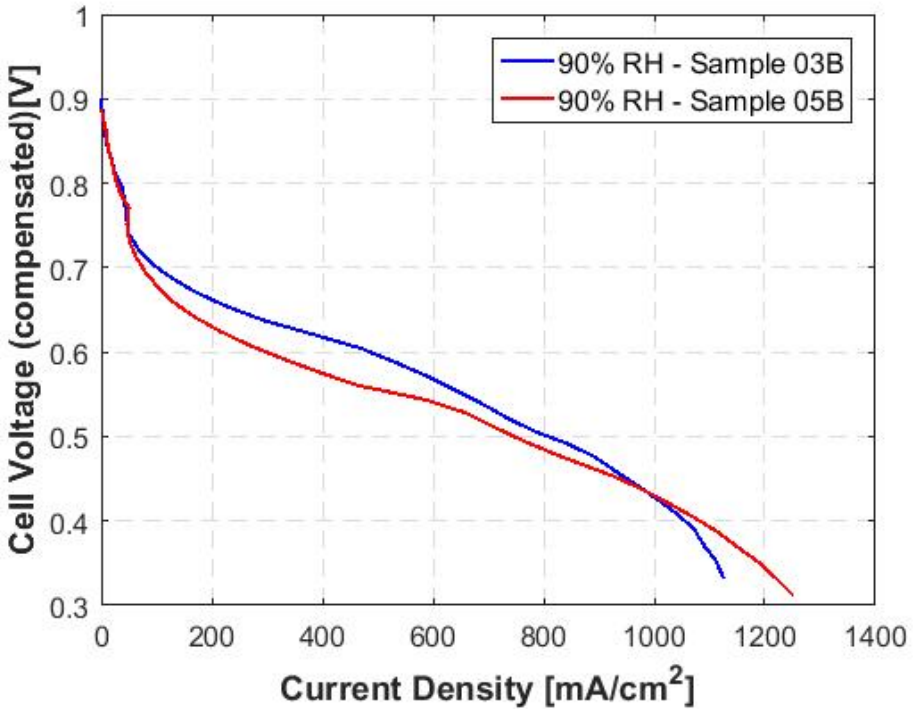

Figure B.48: 0.05 mg_{Pt}/cm^2 Pt loading comparative samples at 90% RH. Cathode side.

Comparative 0,03 mg

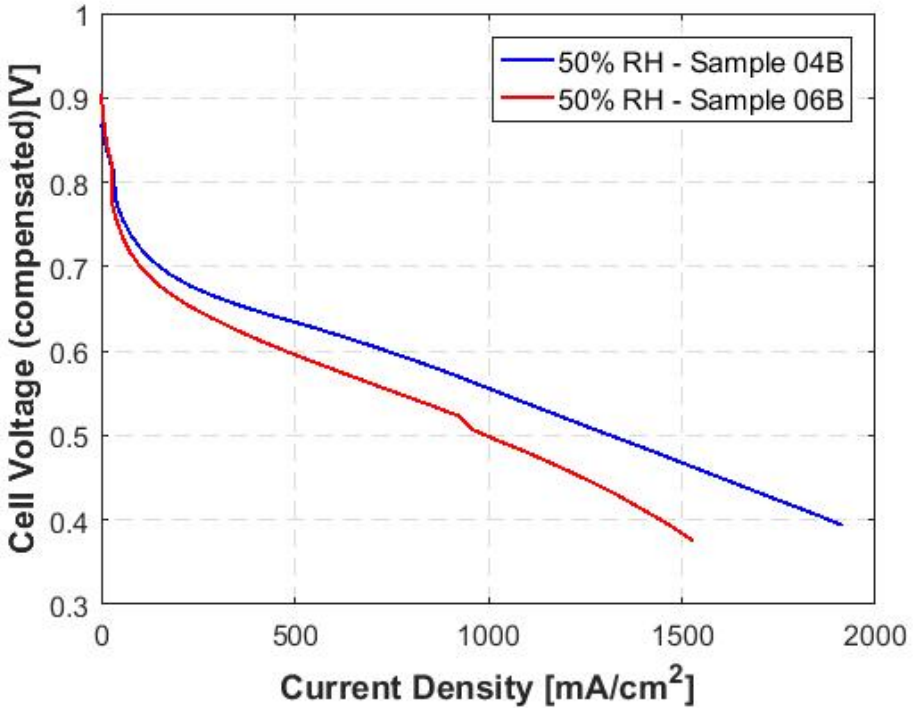

Figure B.49: 0.03 mg_{Pt}/cm^2 Pt loading comparative samples at 50% RH. Cathode side.

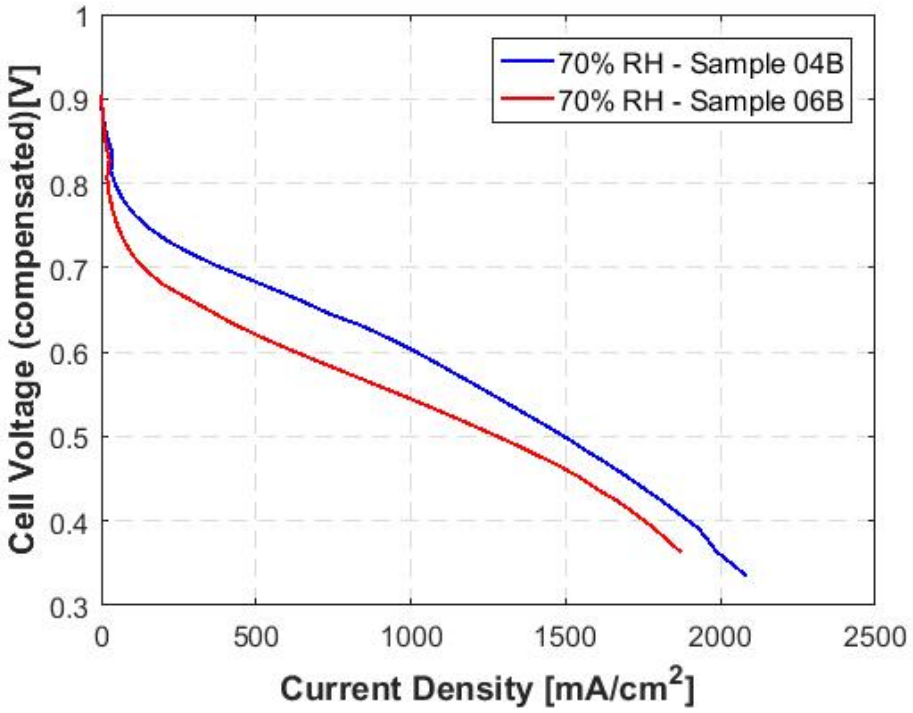

Figure B.50: 0.03 mg_{Pt}/cm^2 Pt loading comparative samples at 70% RH. Cathode side.

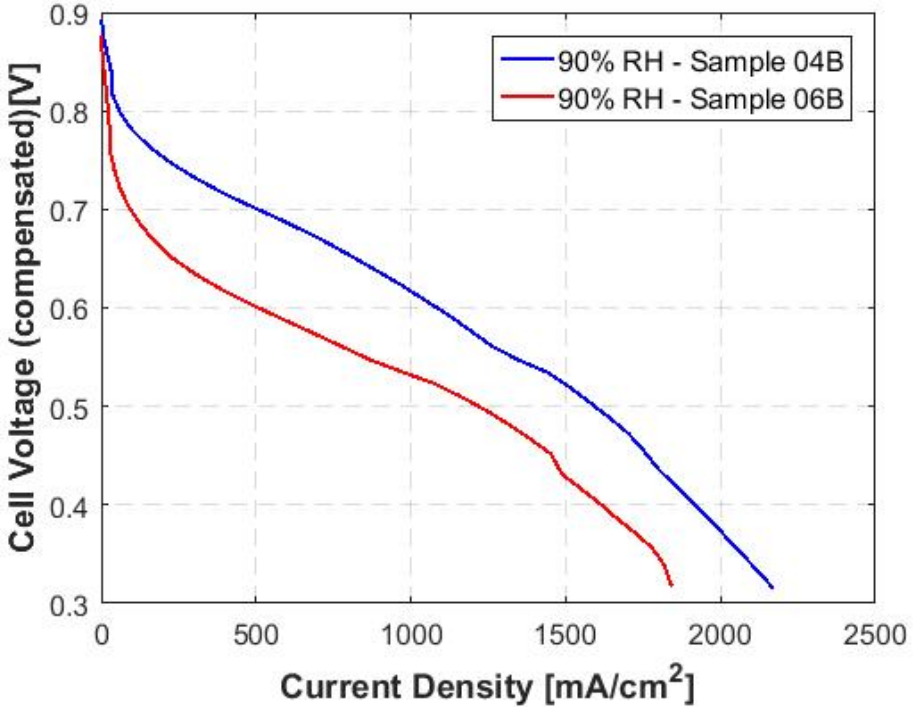

Figure B.51: 0.03 mg_{Pt}/cm^2 Pt loading comparative samples at 90% RH. Cathode side.

Average by relative humidity

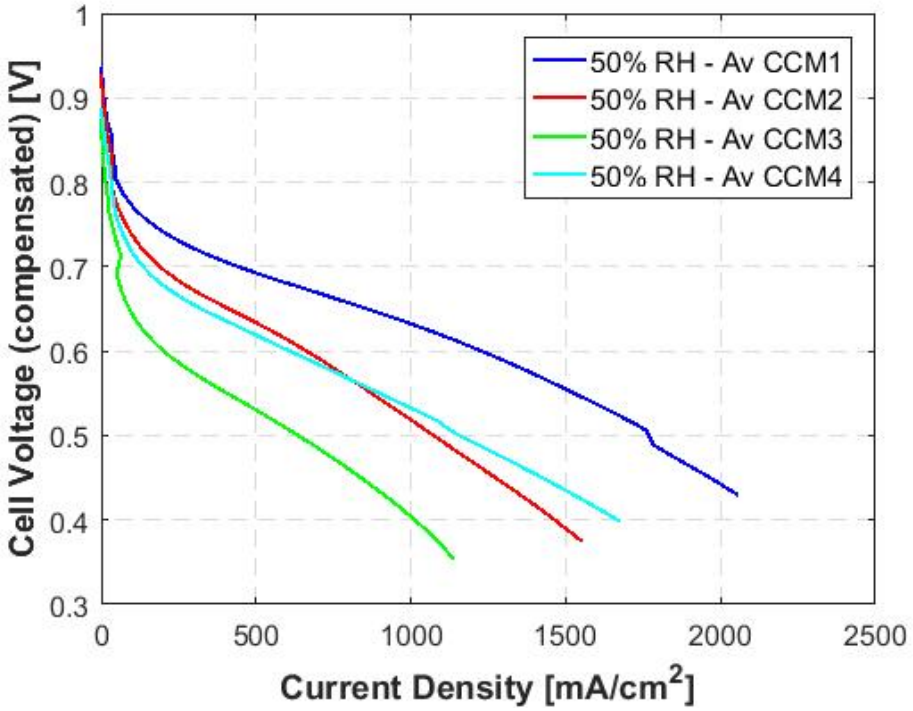

Figure B.52: Pt loading comparative samples at 50% RH. Cathode side.

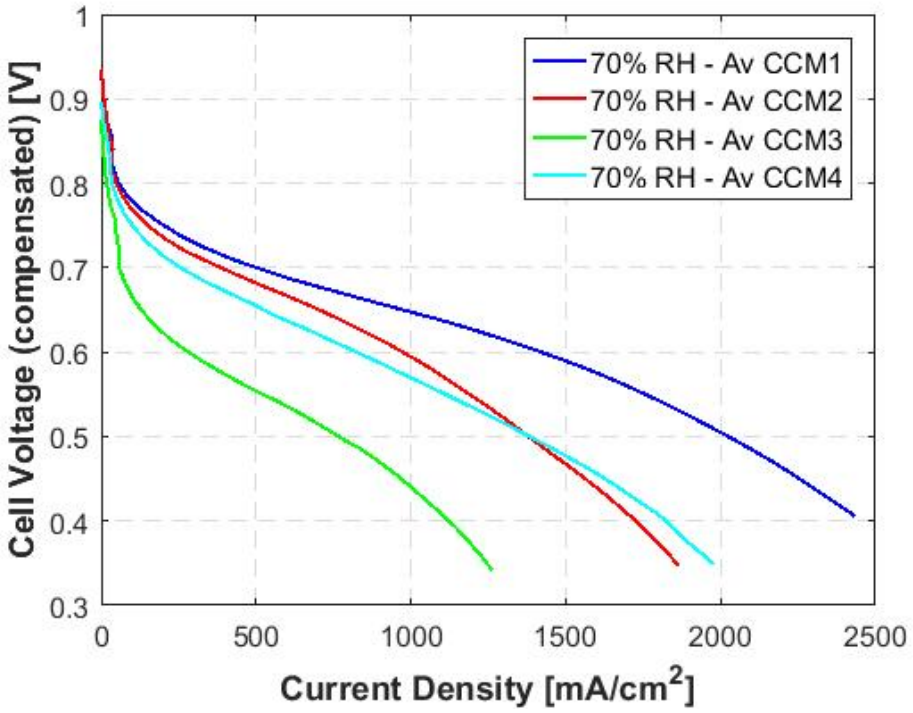

Figure B.53: Pt loading comparative samples at 70% RH. Cathode side.

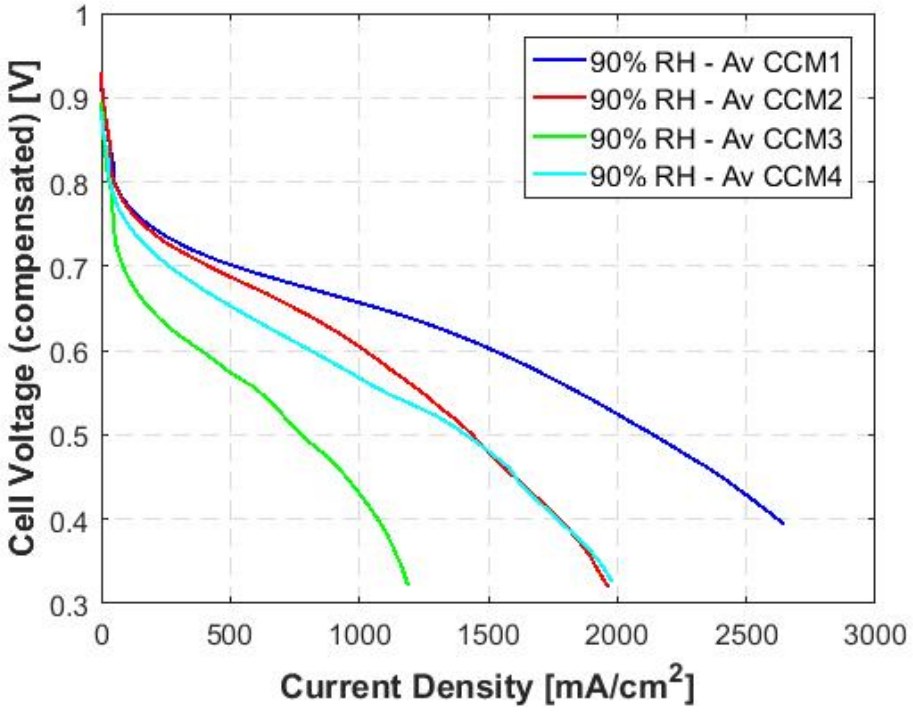

Figure B.54: Pt loading comparative samples at 90% RH. Cathode side.